Supplementary Information

Multidimensional quantitative analysis of mRNA expression within intact vertebrate embryos

Vikas Trivedi[1,2,3,4], Harry M.T. Choi[1], Scott E. Fraser[2,3], and Niles A. Pierce[1,5,6*]

Contents

[1]Division of Biology & Biological Engineering, California Institute of Technology, Pasadena, CA 91125, USA. [2]Translational Imaging Center, University of Southern California, Los Angeles CA 90089, USA. [3]Molecular and Computational Biology, University of Southern California, Los Angeles, CA 90089, USA. [4]Department of Genetics, University of Cambridge, Cambridge, CB2 3EH, UK. [5]Division of Engineering & Applied Science, California Institute of Technology, Pasadena, CA 91125, USA. [6]Weatherall Institute of Molecular Medicine, University of Oxford, Oxford, OX3 9DS, UK. *Email: niles@caltech.edu

List of Figures

List of Tables

S1 Additional materials and methods

S1.1 Probe set and amplifier details

Figures	Organism	Line(s)	Stage	Target	Probes	HCR Amplifier
2, S12–S14	*Danio rerio*	WT	26 hpf	*desma*	8	B1-Alexa546
					7	B3-Alexa647
2, S15–S17	*Danio rerio*	*Gt(desma-citrine)$^{ct122a/+}$*	26 hpf	*citrine*	3	B2-Alexa546
					3	B3-Alexa647
2, S18–S20	*Danio rerio*	WT	26 hpf	*elavl3*	5	B1-Alexa546
					4	B3-Alexa647
2, S21–S23	*Mus musculus*	WT	E9.5	*Acta2*	2	B4-Alexa546
					2	B4-Alexa647
3, S24–S28	*Danio rerio*	hom, het, WT*	26 hpf	*desma*	5	B1-Alexa546
				citrine	5	B2-Alexa647
4, 5, S29–S47	*Danio rerio*	WT	10 hpf	*myod1*	5	B4-Alexa647
				tpm3	2	B1-Alexa488
				her1	5	B3-Alexa514
				her7	5	B2-Alexa546
S1, S2	*Danio rerio*	*Gt(desma-citrine)$^{ct122a/+}$*	26 hpf	*citrine*	5	B2-Alexa647
				ta	9	B1-Alexa546
S3-S7	*Danio rerio*	WT	26 hpf	*tpm3*	2	B1-Alexa647
				desma	7	B3-Alexa546

Table S1. Organisms, target mRNAs, probe sets and amplifiers. *The homozygous vs heterozygous study involves three types of embryos: hom ≡ *Gt(desma-citrine)$^{ct122a/ct122a}$*, het ≡ *Gt(desma-citrine)$^{ct122a/+}$*, and WT.

S1.2 Confocal microscope settings

Figures	Target	Fluorophore	Laser (nm)	Laser Power	Beam Splitter	Filter (nm)	Pixel Size ($x \times y \times z$ μm)	Pixel Time (μs)	Focal Planes	Voxel Size ($x \times y \times z$ μm)
2, S12–S14	*desma*	Alexa546	561	10%	MBS 458/561	563–612	$0.664 \times 0.664 \times 1.5$	3.15	1	$1.99 \times 1.99 \times 1.5$
		Alexa647	633	4.5%	MBS 488/561/633	654–687	$0.664 \times 0.664 \times 1.5$	3.15	1	$1.99 \times 1.99 \times 1.5$
2, S15–S17	*citrine*	Alexa546	561	12%	MBS 458/561	563–612	$0.664 \times 0.664 \times 1.5$	3.15	1	$1.99 \times 1.99 \times 1.5$
		Alexa647	633	12%	MBS 488/561/633	654–687	$0.664 \times 0.664 \times 1.5$	3.15	1	$1.99 \times 1.99 \times 1.5$
2, S18–S20	*elavl3*	Alexa546	561	10%	MBS 458/561	563–612	$0.664 \times 0.664 \times 1.5$	3.15	1	$1.99 \times 1.99 \times 1.5$
		Alexa647	633	6.9%	MBS 488/561/633	654–687	$0.664 \times 0.664 \times 1.5$	3.15	1	$1.99 \times 1.99 \times 1.5$
2, S21–S23	*Acta2*	Alexa546	561	7%	MBS 458/561	563–612	$0.069 \times 0.069 \times 2.0$	6.3	1	$1.86 \times 1.86 \times 2.0$
		Alexa647	633	10%	MBS 488/561/633	654–687	$0.069 \times 0.069 \times 2.0$	6.3	1	$1.86 \times 1.86 \times 2.0$
3, S24–S28	*desma*	Alexa546	561	10%	MBS 458/561	563–612	$0.664 \times 0.664 \times 1.5$	3.15	1	$1.99 \times 1.99 \times 1.5$
	citrine	Alexa647	633	12%	MBS 488/561/633	654–687	$0.664 \times 0.664 \times 1.5$	3.15	1	$1.99 \times 1.99 \times 1.5$
4, 5, S29–S47	*myod1*	Alexa647	633	10%	MBS 488/561/633	654–687	$0.664 \times 0.664 \times 1.24$	3.15	5	$1.99 \times 1.99 \times 6.2$
	tpm3	Alexa488	488	12%	MBS 488/561/633	488–527	$0.664 \times 0.664 \times 1.24$	3.15	5	$1.99 \times 1.99 \times 6.2$
	her1	Alexa514	514	10%	MBS 458/514	537–553	$0.664 \times 0.664 \times 1.24$	3.15	5	$1.99 \times 1.99 \times 6.2$
	her7	Alexa546	561	12%	MBS 458/561	563–612	$0.664 \times 0.664 \times 1.24$	3.15	5	$1.99 \times 1.99 \times 6.2$
S1, S2	*ta*	Alexa546	561	12%	MBS 458/561	563–612	$0.664 \times 0.664 \times 1.5$	3.15	1	$1.99 \times 1.99 \times 1.5$
	citrine	Alexa647	633	10%	MBS 488/561/633	654–687	$0.664 \times 0.664 \times 1.5$	3.15	1	$1.99 \times 1.99 \times 1.5$
S3–S7	*desma*	Alexa546	555	6.5%	MBS 458/555	LP560	$0.625 \times 0.625 \times 1.5$	3.15	1	$1.86 \times 1.86 \times 1.5$
	tpm3	Alexa647	639	6.5%	MBS 488/555/639	LP640	$0.625 \times 0.625 \times 1.5$	3.15	1	$1.86 \times 1.86 \times 1.5$

Table S2. Confocal microscope settings.

S1.3 Image Analysis

S1.3.1 Raw voxel intensities

For each replicate embryo, raw voxel intensities are calculated by averaging neighboring pixel intensities, yielding the voxel sizes listed in Table S2. The total fluorescence within a voxel is a combination of signal and background. Fluorescent background (BACK) arises from three sources in each channel (Choi *et al.*, 2014):

- autofluorescence (AF): fluorescence inherent to the sample,
- non-specific detection (NSD): probes that bind non-specifically in the sample and subsequently lead to HCR signal amplification,
- non-specific amplification (NSA): HCR hairpins that bind non-specifically in the sample.

Fluorescent signal (SIG) in each channel is generated by HCR amplification polymers tethered to probes bound specifically to their cognate target mRNA. For voxel i of replicate embryo n, we denote the background:

$$X_{n,i}^{\mathrm{BACK}} = X_{n,i}^{\mathrm{AF}} + X_{n,i}^{\mathrm{NSD}} + X_{n,i}^{\mathrm{NSA}},$$

the signal:

$$X_{n,i}^{\mathrm{SIG}},$$

and the total fluorescence (SIG+BACK):

$$X_{n,i}^{\mathrm{SIG+BACK}} = X_{n,i}^{\mathrm{SIG}} + X_{n,i}^{\mathrm{BACK}}.$$

S1.3.2 Characterization of signal and background

Signal and background are characterized as described previously (Choi *et al.*, 2014). For each target mRNA, background (BACK) is characterized for voxels in one or more representative rectangular regions of no- or low-expression and the combination of signal and background (SIG+BACK) is characterized for voxels in one or more representative rectangular regions of high expression. The choice of representative regions depends on the type of target mRNA:

- **Transgenic target** (*citrine*): BACK voxel intensities are measured in a region of no expression in WT embryos lacking the target; SIG+BACK voxel intensities are measured in a region of high expression in transgenic embryos containing the target.
- **Endogenous target with local expression** (*elavl2, Acta2, myod1, tpm3, her1, her7*): BACK voxel intensities are measured in a region of no- or low-expression in WT embryos; SIG+BACK voxel intensities are measured in a region of high expression in the same replicate embryos.
- **Endogenous target with global expression** (*desma*): BACK voxel intensities are measured in a region of high expression in WT embryos using the standard in situ protocol but omitting the probes (this yields the partial background estimate BACK $\approx$ AF + NSA); SIG+BACK voxel intensities are measured in a region of high expression in a different set of WT embryo replicates (using the standard in situ protocol including probes).

For the voxels in these regions, we characterize the distribution by plotting a voxel intensity histogram and characterize typical performance by calculating the mean voxel intensity ($\bar{X}_n^{\mathrm{BACK}}$ or $\bar{X}_n^{\mathrm{BACK+SIG}}$ for replicate embryo n). Performance across replicate embryos is characterized by calculating the sample means, $\bar{X}^{\mathrm{BACK}}$ and $\bar{X}^{\mathrm{SIG+BACK}}$, and sample standard deviations, s^{BACK} and $s^{\mathrm{SIG+BACK}}$. The mean signal is then estimated as

$$\bar{X}^{\mathrm{SIG}} = \bar{X}^{\mathrm{SIG+BACK}} - \bar{X}^{\mathrm{BACK}} \tag{S1}$$

with standard deviation estimated via uncertainty propagation as

$$s^{\mathrm{SIG}} \leq \sqrt{(s^{\mathrm{SIG+BACK}})^2 + (s^{\mathrm{BACK}})^2}. \tag{S2}$$

The upper bound on estimated standard deviation holds under the assumption that the correlation between SIG and BACK is non-negative. Estimates for mean signal plus background ($\bar{X}^{\mathrm{SIG+BACK}} \pm s^{\mathrm{SIG+BACK}}$), mean background ($\bar{X}^{\mathrm{BACK}} \pm s^{\mathrm{BACK}}$), and mean signal ($\bar{X}^{\mathrm{SIG}} \pm s^{\mathrm{SIG}}$) are displayed for each target mRNA in Table S3.

S1.3.3 Normalized voxel intensities

To facilitate relative quantitation between subcellular voxels within expression scatter plots, we estimate the normalized HCR signal of voxel i in replicate n as:

$$x_{n,i} \equiv \frac{X_{n,i}^{\mathrm{SIG+BACK}} - \bar{X}^{\mathrm{BACK}}}{X_{\mathrm{max}}^{\mathrm{SIG+BACK}} - \bar{X}^{\mathrm{BACK}}},$$

which translates and rescales the data so that the voxel intensities in each channel fall in the interval [0,1]. Here, $\bar{X}^{\mathrm{BACK}}$ is the mean background across replicates (see Section S1.3.2), and

$$X_{\mathrm{max}}^{\mathrm{SIG+BACK}} \equiv \max_{n,i} X_{n,i}^{\mathrm{SIG+BACK}}$$

is the maximum total fluorescence across replicates (tabulated in Table S3).* This simple and practical normalization approach translates and rescales all voxels identically within a given channel (enabling comparison of slopes in expression scatter plots between replicates), and does not attempt to remove scatter in the normalized signal estimate that is caused by scatter in the background.

S1.3.4 Signal-to-background analysis

The signal-to-background ratio is estimated as (Choi *et al.*, 2014):

$$\bar{X}^{\mathrm{SIG/BACK}} = \bar{X}^{\mathrm{SIG}} / \bar{X}^{\mathrm{BACK}} \tag{S3}$$

with standard deviation estimated via uncertainty propagation as

$$s^{\mathrm{SIG/BACK}} \leq \bar{X}^{\mathrm{SIG/BACK}} \sqrt{\left(\frac{s^{\mathrm{SIG}}}{\bar{X}^{\mathrm{SIG}}}\right)^2 + \left(\frac{s^{\mathrm{BACK}}}{\bar{X}^{\mathrm{BACK}}}\right)^2}. \tag{S4}$$

The upper bound on estimated standard deviation holds under the assumption that the correlation between SIG and BACK is non-negative. The estimated mean signal-to-background ($\bar{X}^{\mathrm{SIG/BACK}} \pm s^{\mathrm{SIG/BACK}}$) is displayed for each target mRNA in Table S3.

*For the homozygous vs heterozygous studies of Figure 3, $X_{\mathrm{max}}^{\mathrm{SIG+BACK}}$ is defined based on the homozygous replicates to enable comparison of slopes between embryo types.

Figures	mRNA	Line	Channel	Signal + Background $\bar{X}^{\mathrm{SIG+BACK}} \pm s^{\mathrm{SIG+BACK}}$	max(Signal + Background) $X^{\mathrm{SIG+BACK}}_{\mathrm{max}}$	Background $\bar{X}^{\mathrm{BACK}} \pm s^{\mathrm{BACK}}$	Signal $\bar{X}^{\mathrm{SIG}} \pm s^{\mathrm{SIG}}$	Signal-to-background $\bar{X}^{\mathrm{SIG/BACK}} \pm s^{\mathrm{SIG/BACK}}$	Replicate embryos (N)
S12, S13	*desma*	WT	Alexa546	1752 ± 235	3886	53 ± 10	1698 ± 236	32 ± 8	6
			Alexa647	1530 ± 234	3452	17 ± 3	1513 ± 235	89 ± 21	6
S15, S16	*citrine*	*Gt(desma-citrine)$^{ct122a/+}$*	Alexa546	1941 ± 130	4011	543 ± 101	1398 ± 165	3 ± 1	6
			Alexa647	1112 ± 89	3194	135 ± 22	977 ± 92	7 ± 1	6
S18, S19	*elavl3*	WT	Alexa546	2332 ± 118	4095	414 ± 59	1918 ± 120	4 ± 1	6
			Alexa647	1939 ± 164	4095	178 ± 18	1761 ± 164	9 ± 1	6
S21, S22	*Acta2*	WT	Alexa546	1428 ± 299	2581	284 ± 17	1142 ± 300	4 ± 1	3
			Alexa647	1336 ± 277	2625	229 ± 27	1107 ± 277	5 ± 1	3
S24, S27	*desma*	*Gt(desma-citrine)$^{ct122a/ct122a}$*	Alexa546	895 ± 114	2386	57 ± 16	838 ± 115	15 ± 5	3
S24, S26	*citrine*		Alexa647	1031 ± 193	3267	44 ± 11	987 ± 194	22 ± 7	3
S25, S27	*desma*	*Gt(desma-citrine)$^{ct122a/+}$*	Alexa546	827 ± 109	2386	57 ± 16	770 ± 110	14 ± 6	3
S25, S26	*citrine*		Alexa647	523 ± 78	3267	44 ± 11	479 ± 79	11 ± 3	3
S29–S32	*myod1*	WT	Alexa647	1073 ± 102	2062	31 ± 14	1042 ± 103	33 ± 15	4
	tpm3		Alexa488	722 ± 256	1943	59 ± 41	663 ± 259	11 ± 9	4
	her1		Alexa514	1075 ± 182	1713	21± 15	1054 ± 183	50 ± 36	4
	her7		Alexa546	856 ± 154	1538	27 ± 16	829 ± 155	31 ± 19	4

Table S3. Characterization of signal and background (mean ± standard deviation, N embryos) for each channel and target mRNA based on the definitions of Sections S1.3.1-S1.3.4 and the depicted regions in the listed figures.

S1.3.5 Signal-to-signal analysis

For the homozygous vs heterozygous study of Figure 3, we estimate signal for two channels (*desma* and *citrine*) in two sample types (hom and het). Using equation (S1), we estimate the mean signal across $N = 3$ homozygous replicate embryos:

$$\bar{X}^{\text{SIG:hom}}_{citrine} = \bar{X}^{\text{SIG+BACK:hom}}_{citrine} - \bar{X}^{\text{BACK}}_{citrine}$$
$$\bar{X}^{\text{SIG:hom}}_{desma} = \bar{X}^{\text{SIG+BACK:hom}}_{desma} - \bar{X}^{\text{BACK}}_{desma}$$

and the mean signal across $N = 3$ heterozygous replicate embryos:

$$\bar{X}^{\text{SIG:het}}_{citrine} = \bar{X}^{\text{SIG+BACK:het}}_{citrine} - \bar{X}^{\text{BACK}}_{citrine}$$
$$\bar{X}^{\text{SIG:het}}_{desma} = \bar{X}^{\text{SIG+BACK:het}}_{desma} - \bar{X}^{\text{BACK}}_{desma}.$$

For each signal estimate, the sample standard deviation is estimated across replicates using equation (S2), yielding $s^{\text{SIG:hom}}_{citrine}, s^{\text{SIG:hom}}_{desma}, s^{\text{SIG:het}}_{citrine}, s^{\text{SIG:het}}_{desma}$. To plot the bar graphs of Figure 3B (mean $\pm$ standard deviation over $N = 3$ replicate embryos), each channel is normalized by the estimated mean signal for the homozygous replicate embryos (i.e., the *citrine* and *desma* bars for the homozygous embryos each have height 1 by definition).

For the bar graph of Figure 3C, we need to estimate the hom/het signal-to-signal ratio for the *citrine* channel. To control for global variation in transcription between the two sample types (hom and het), we normalize the *citrine* signal by the *desma* signal for each sample type, and then use these normalized values to calculate the hom/het ratio for *citrine*.* Using equation (S3), we estimate the signal-to-signal ratio for each sample type as:

$$\bar{X}^{\text{SIG/SIG:hom}}_{citrine/desma} = \bar{X}^{\text{SIG:hom}}_{citrine} / \bar{X}^{\text{SIG:hom}}_{desma}$$

and

$$\bar{X}^{\text{SIG/SIG:het}}_{citrine/desma} = \bar{X}^{\text{SIG:het}}_{citrine} / \bar{X}^{\text{SIG:het}}_{desma}$$

with standard deviations estimated via uncertainty propagation as:

$$s^{\text{SIG/SIG:hom}}_{citrine/desma} \leq \bar{X}^{\text{SIG/SIG:hom}}_{citrine/desma} \sqrt{\left(\frac{s^{\text{SIG:het}}_{citrine}}{\bar{X}^{\text{SIG:hom}}_{citrine}}\right)^2 + \left(\frac{s^{\text{SIG:hom}}_{desma}}{\bar{X}^{\text{SIG:hom}}_{desma}}\right)^2}$$

and

$$s^{\text{SIG/SIG:het}}_{citrine/desma} \leq \bar{X}^{\text{SIG/SIG:het}}_{citrine/desma} \sqrt{\left(\frac{s^{\text{SIG:het}}_{citrine}}{\bar{X}^{\text{SIG:het}}_{citrine}}\right)^2 + \left(\frac{s^{\text{SIG:het}}_{desma}}{\bar{X}^{\text{SIG:het}}_{desma}}\right)^2}.$$

These upper bounds on estimated standard deviations hold under the assumption that the correlation is non-negative between the two quantities whose ratios are being calculated.

Finally, the hom/het signal-to-signal ratio for *citrine* is then:

$$\bar{X}^{\text{SIG/SIG:hom/het}}_{citrine} = \bar{X}^{\text{SIG/SIG:hom}}_{citrine/desma} / \bar{X}^{\text{SIG/SIG:het}}_{citrine/desma}$$

with standard deviation estimated via uncertainty propagation as:

$$s^{\text{SIG/SIG:hom/het}}_{citrine} \leq \bar{X}^{\text{SIG/SIG:hom/het}}_{citrine} \sqrt{\left(\frac{s^{\text{SIG/SIG:hom}}_{citrine/desma}}{\bar{X}^{\text{SIG/SIG:hom}}_{citrine/desma}}\right)^2 + \left(\frac{s^{\text{SIG/SIG:het}}_{citrine/desma}}{\bar{X}^{\text{SIG/SIG:het}}_{citrine/desma}}\right)^2}$$

The upper bound on the estimated standard deviation holds under the assumption that the correlation is non-negative between the two quantities whose ratios are being calculated. The values for the quantities in the above signal-to-signal analysis are summarized in Table S4.

*Note that this approach assumes that the *desma* and *Gt(desma-citrine)* alleles express equally in heterozygous embryos.

Quantity	Value	Figures
$\bar{X}^{\text{SIG:hom}}_{citrine} \pm s^{\text{SIG:hom}}_{citrine}$	987 ± 194	S24, S26
$\bar{X}^{\text{SIG:hom}}_{desma} \pm s^{\text{SIG:hom}}_{desma}$	838 ± 115	S24, S27
$\bar{X}^{\text{SIG:het}}_{citrine} \pm s^{\text{SIG:het}}_{citrine}$	479 ± 79	S25, S26
$\bar{X}^{\text{SIG:het}}_{desma} \pm s^{\text{SIG:het}}_{desma}$	770 ± 110	S25, S27
$\bar{X}^{\text{SIG/SIG:hom}}_{citrine/desma} \pm s^{\text{SIG/SIG:hom}}_{citrine/desma}$	1.2 ± 0.3	
$\bar{X}^{\text{SIG/SIG:het}}_{citrine/desma} \pm s^{\text{SIG/SIG:het}}_{citrine/desma}$	0.6 ± 0.1	
$\bar{X}^{\text{SIG/SIG:hom/het}}_{citrine} \pm s^{\text{SIG/SIG:hom/het}}_{citrine}$	2.0 ± 0.5	

Table S4. Estimated signal-to-signal for the *citrine* channel in homozygous vs heterozygous embryos of Figure 3. Mean $\pm$ standard deviation ($N = 3$ embryos).

S2 Additional data

S2.1 Quantitation control studies

Physically, HCR signal/voxel is a sum of HCR signal/target, which is in turn a sum of HCR signal/polymer. Note that the amplifiers do not first sum the number of targets and then generate a signal proportional to that sum. The proportionality follows from summing the signal generated for individual target molecules, which in turn follows from summing the signal generated by individual amplification polymers. Despite the linearity of this summation process, the signal/voxel could scale nonlinearly with targets/voxel if the signal/polymer varied systematically in space (e.g., a penetration effect) or systematically with target density (e.g., a crowding effect). For example, a systematic penetration effect could potentially cause the signal/polymer to diminish in a depth-dependent fashion. Alternatively, a systematic crowding effect caused by interactions between HCR amplification polymers tethered to different target molecules could potentially cause the signal/polymer to increase or decrease depending on target density. In a 2-channel redundant detection experiment, if a systematic penetration or crowding effect altered the signal for both channels by the same factor, (x_i, y_i) voxel intensity pairs could slide undetected along the line in a scatter plot, undermining the quantitative nature of the signal without undermining the appearance of the scatter plot. Hence, it is important to rule out systematic penetration and crowding effects before using scatter plots to assess quantitative accuracy and precision. In Sections S2.1.1 and S2.1.2 we perform control experiments to test for systematic penetration and crowding effects. These studies suggest the absence of significant effects, supporting the conclusion that scatter plots exhibiting a tight linear distribution with approximately zero intercept indicate that the signal varies approximately linearly with target abundance, thus enabling accurate and precise relative quantitation between voxels within an image.

S2.1.1 Testing probe penetration/hybridization time

In order to perform quantitative analyses at varying depths within thick samples, it is important to ensure that the 132-nt probes have sufficient time to penetrate the sample and hybridize to the target mRNA. Here, we do a 2-channel study to simultaneously measure total fluorescence (signal plus background) for one target that expresses deep within the embryo (*ta*) and one target that expresses near the surface of the embryo (*citrine*). For both targets, a time course of probe penetration/hybridization time (Figure S1) reveals that the mean total fluorescence stabilizes for probe penetration/hybridization times of 8 to 24 hours (Figure S2). For this reason, we perform probe hybridization overnight for all studies.

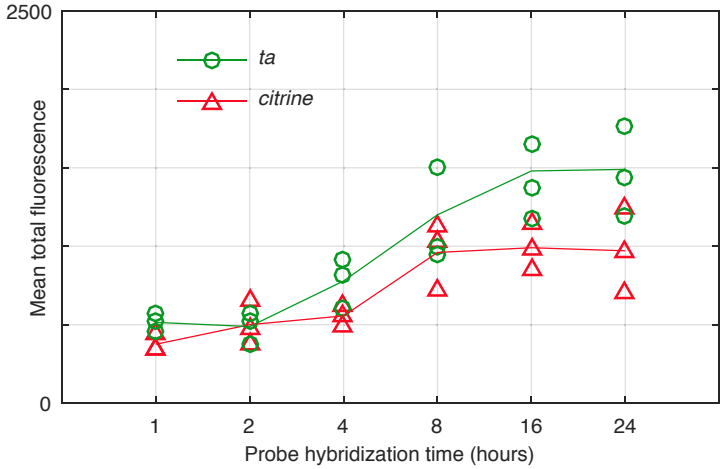

Figure S1. Probe penetration/hybridization time course. Mean total fluorescence (signal plus background) intensity in regions of high expression (rectangles of Figure S2) for each of 3 replicate embryos for each of 6 time points. Whole-mount transgenic *Gt(desma-citrine)*$^{ct122a/+}$ zebrafish embryos fixed 26 hpf.

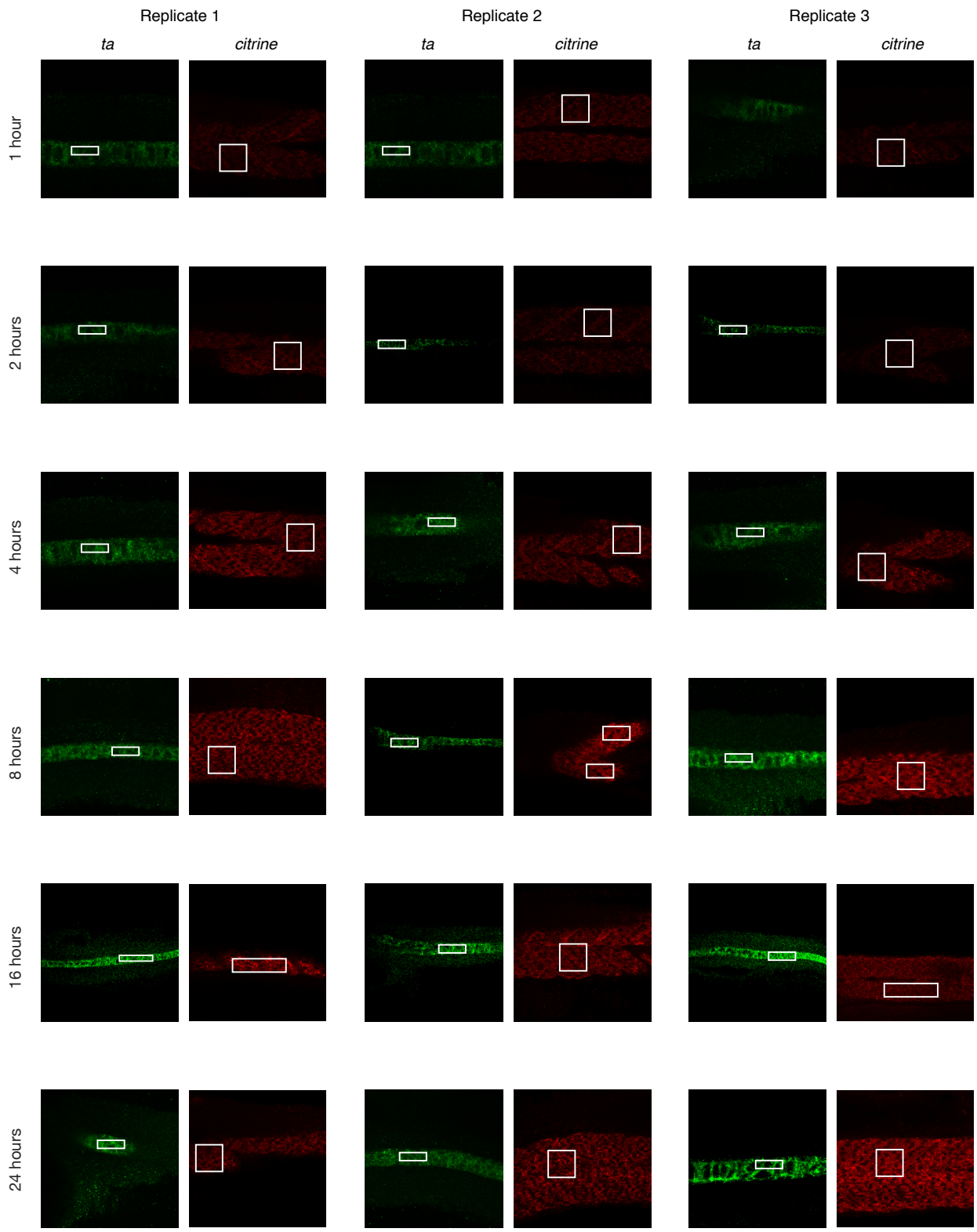

Figure S2. Replicates for probe penetration/hybridization study of Figure S1. For each replicate, both target mRNAs are imaged in the same embryo in different channels (*citrine*: Alexa647, *ta*: Alexa546). Rectangles denote regions used to plot mean total fluorescence (signal plus background) in Figure S1. Whole-mount transgenic *Gt(desma-citrine)*$^{ct122a/+}$ zebrafish embryos fixed 26 hpf.

S2.1.2 Testing for a crowding effect

In order to perform multiplexed quantitative imaging using HCR, it is important that there is not a crowding effect in which amplification polymers tethered to one target molecule affect the signal intensity for a different target molecule. To test for a possible crowding effect, we imaged two target mRNAs that are highly expressed in the same cells (*desma* and *tpm3*) individually (1-target studies) and also simultaneously (2-target studies) within whole-mount zebrafish embryos. Figure S3 compares the signal intensity distributions for 1-target and 2-target studies, revealing similar intensity distributions whether targets were detected alone or together, suggesting that there is not a significant crowding effect (either antagonistic or synergistic).

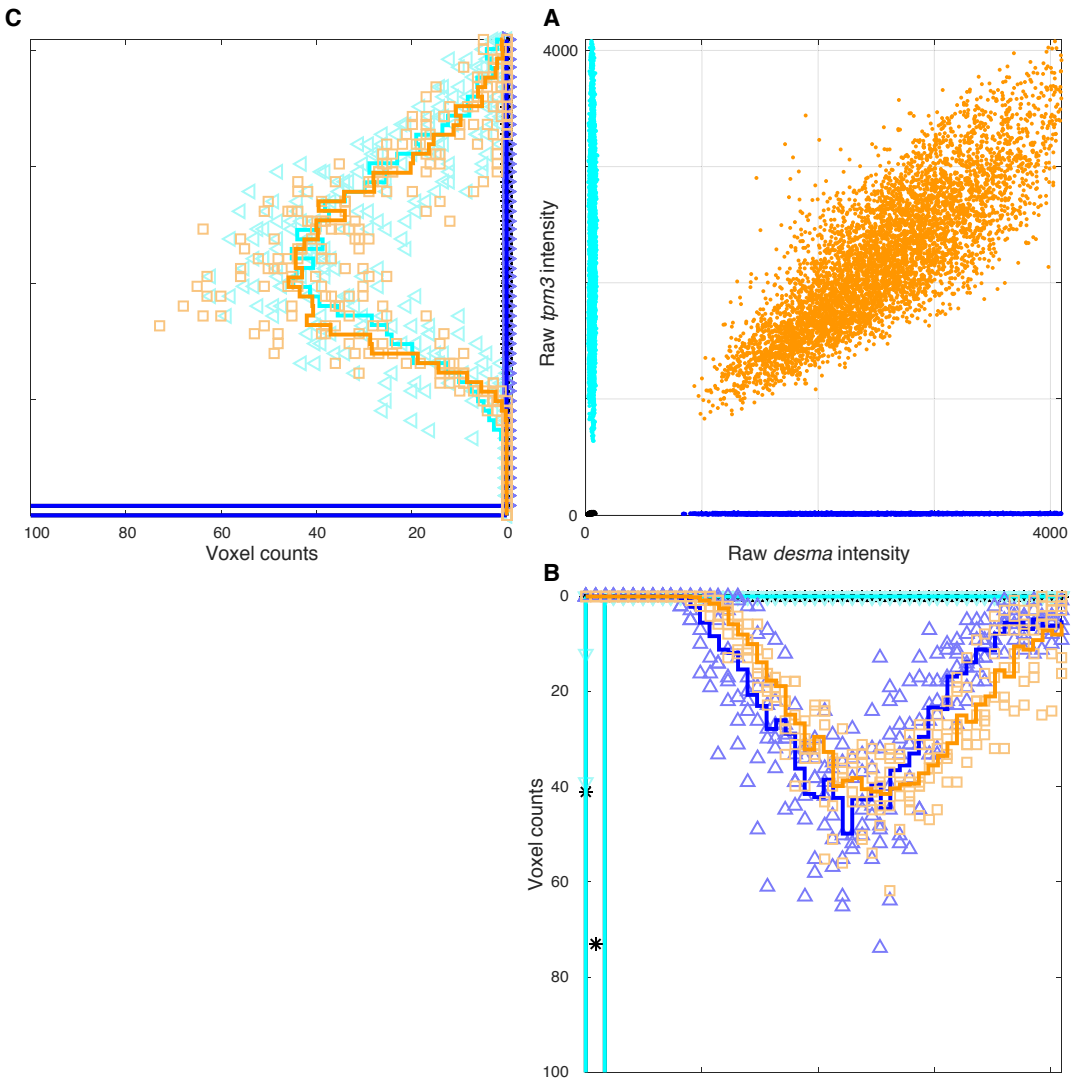

Figure S3. Comparison of signal intensity distributions for individual and simultaneous imaging of *desma* and *tpm3*. (A) Raw voxel intensity scatter plot: *tpm3* channel vs *desma* channel. (B) Raw voxel intensity histogram for *desma* channel. (C) Raw voxel intensity histogram for *tpm3* channel. In panels B and C, solid lines denote average histograms over 6 replicate embryos while symbols denote individual histograms (1 histogram per replicate). Orange data: signal plus background for *desma* and *tpm3* (Figure S4). Blue data: signal plus background for *desma* and background for *tpm3* (Figure S5). Cyan data: background for *desma* and signal plus background for *tpm3* (Figure S6). Black data: background for *desma* and *tpm3* (Figure S7). Voxel size: 2×2 μm.Whole-mount wildtype zebrafish embryos fixed 26 hpf.

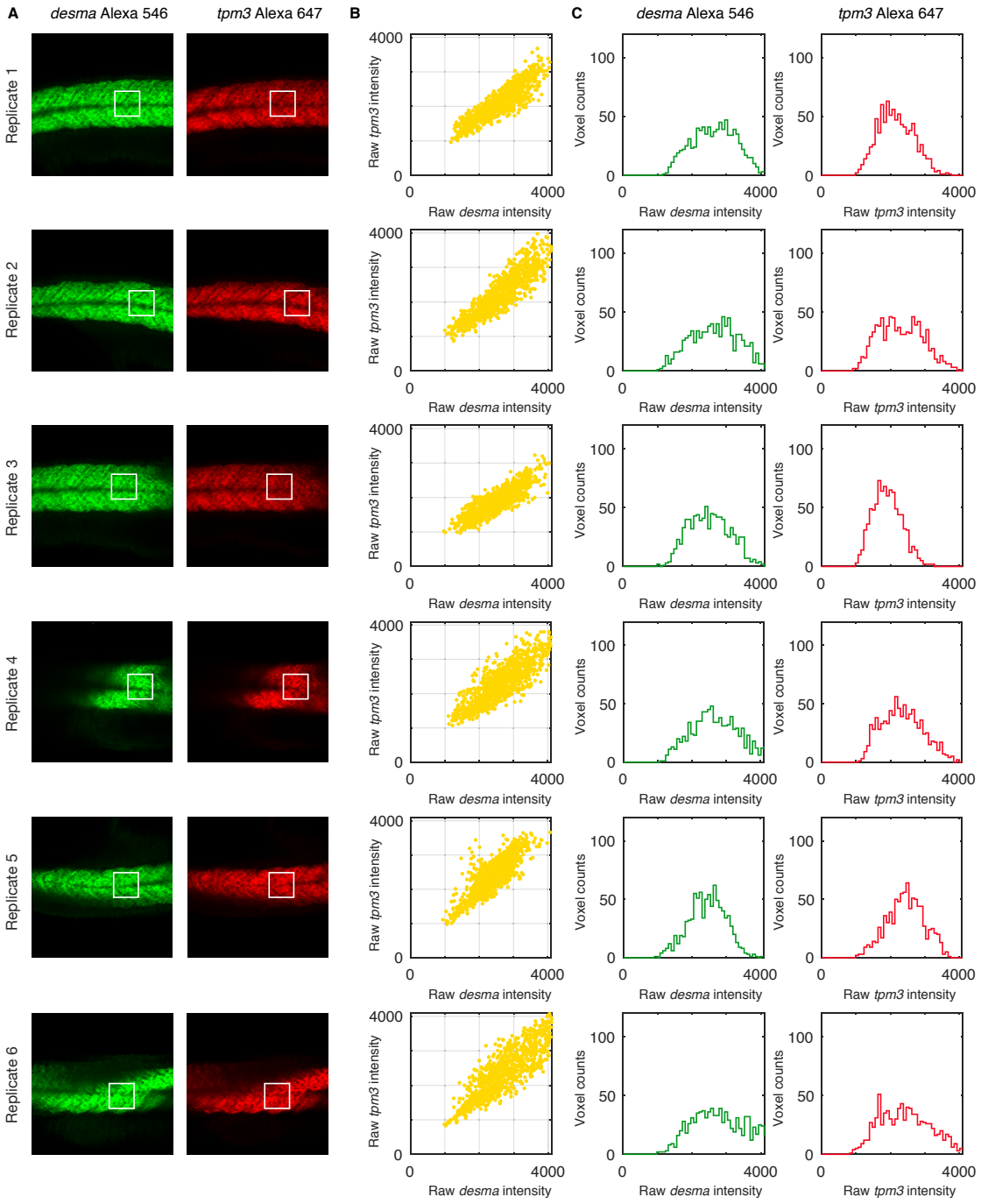

Figure S4. Characterizing signal plus background for *desma* and *tpm3* in a 2-target experiment. (A) Individual channels from 2-channel confocal images depicting regions used to estimate signal plus background. *desma* channel: 7 probes and amplifier B3-Alexa546. *tpm3* channel: 2 probes and amplifier B1-Alexa647. For each of 6 replicate embryos, a representative optical section was selected based on the expression depth of the target mRNAs. Pixel size: 0.6×0.6 μm. (B) Raw voxel intensity scatter plots for the selected regions of panel A representing signal plus background for *desma* and *tpm3*. (C) Raw voxel intensity histograms for the selected regions of panel A representing signal plus background for *desma* and *tpm3*. Same microscope settings used for all replicates in Figures S4–S7. Voxel size: 2×2 μm. Whole-mount wildtype zebrafish embryos fixed 26 hpf.

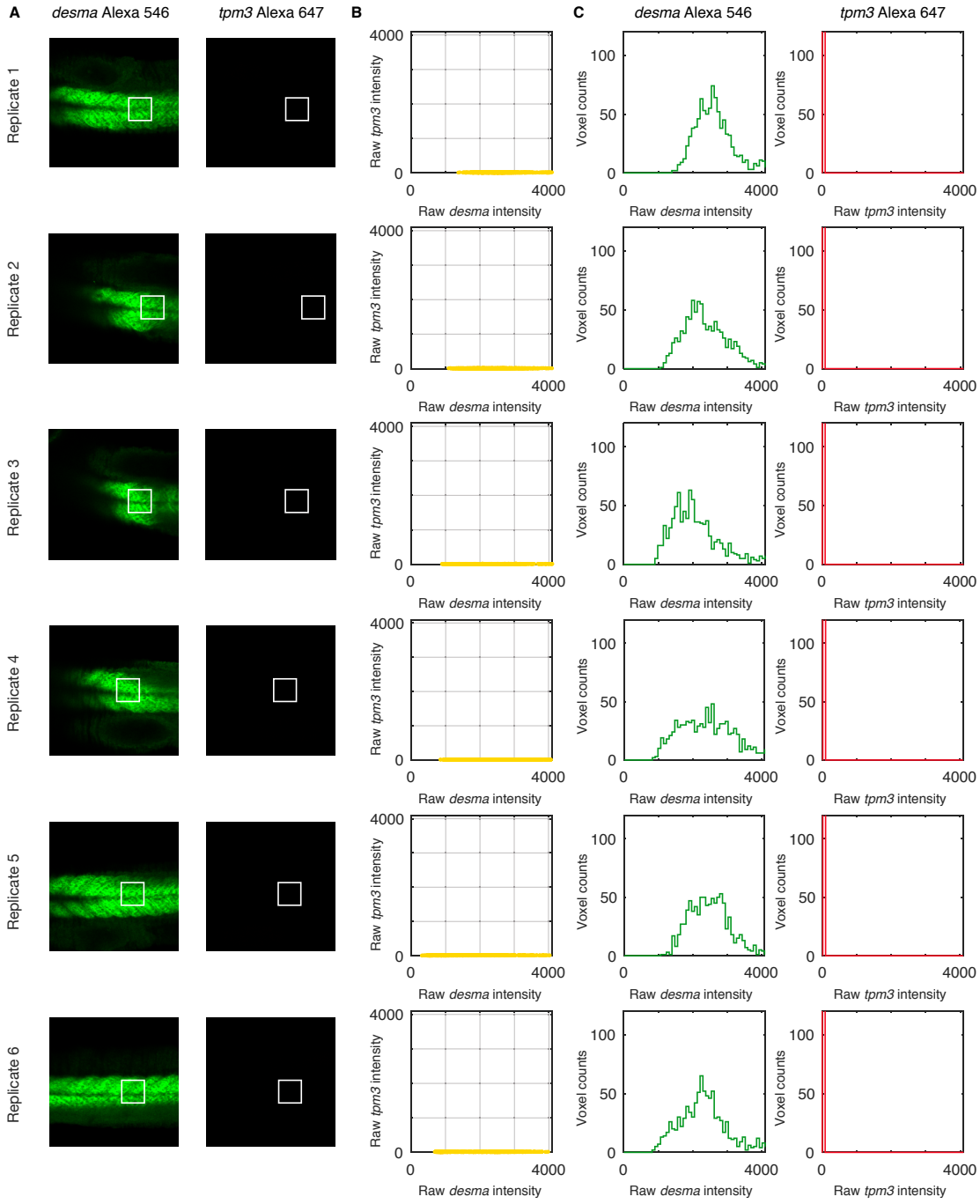

Figure S5. Characterizing signal plus background for *desma* in a 1-target experiment. (A) Individual channels from 2-channel confocal images depicting regions used to estimate signal plus background for *desma* and background for *tpm3*. *desma* channel: 7 probes and amplifier B3-Alexa546. *tpm3* channel: no probes, no amplifier. For each of 6 replicate embryos, a representative optical section was selected based on the expression depth of the target mRNA. Pixel size: 0.6×0.6 μm. (B) Raw voxel intensity scatter plots for the selected regions of panel A representing signal plus background for *desma* and background for *tpm3*. (C) Raw voxel intensity histograms for the selected regions of panel A representing signal plus background for *desma* and background for *tpm3*. Same microscope settings used for all replicates in Figures S4–S7. Voxel size: 2×2 μm. Whole-mount wildtype zebrafish embryos fixed 26 hpf.

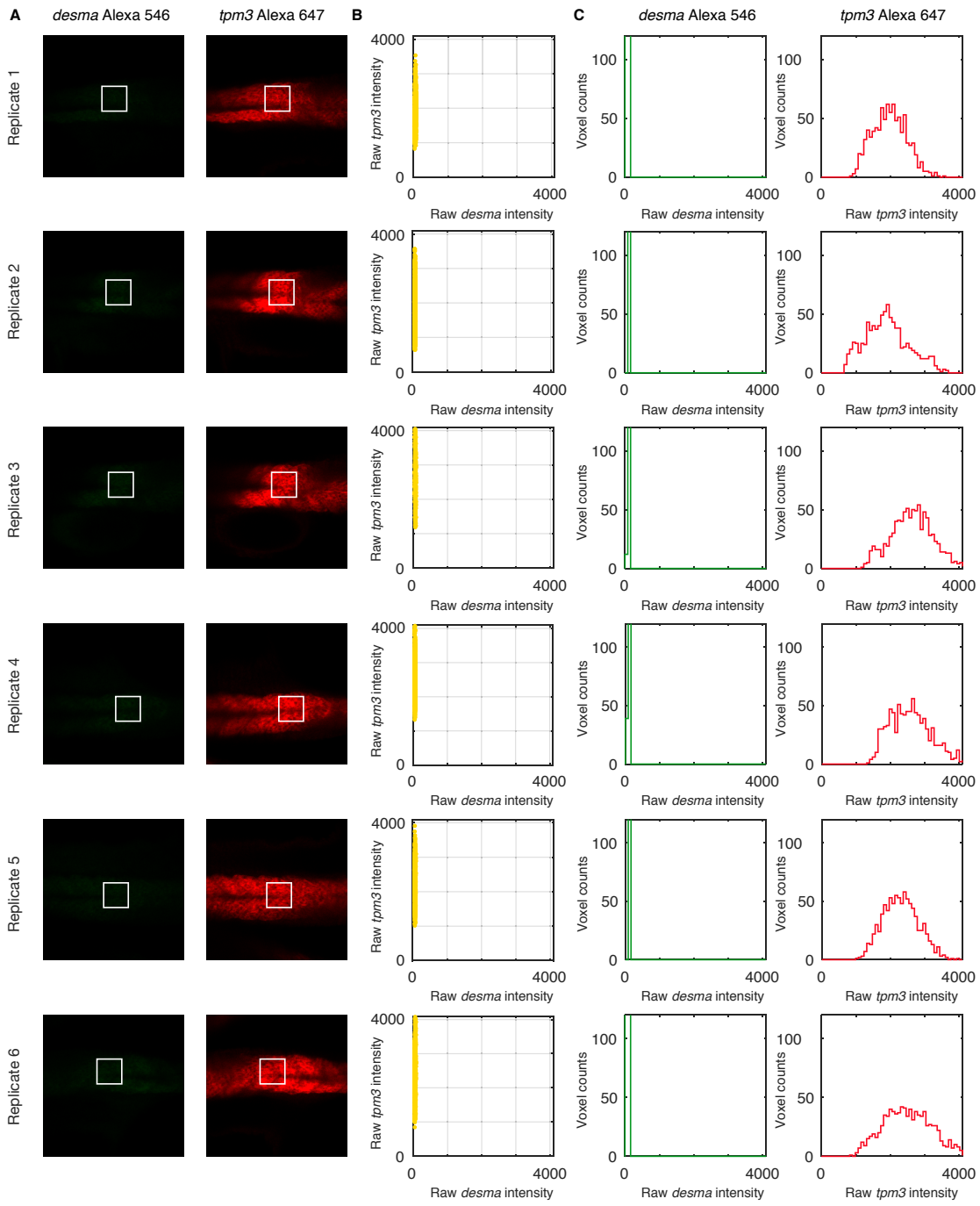

Figure S6. Characterizing signal plus background for *tpm3* in a 1-target experiment. (A) Individual channels from 2-channel confocal images depicting regions used to estimate background for *desma* and signal plus background for *tpm3*. *desma* channel: no probes, no amplifier. *tpm3* channel: 2 probes and amplifier B1-Alexa647. For each of 6 replicate embryos, a representative optical section was selected based on the expression depth of the target mRNA. Pixel size: 0.6×0.6 μm. (B) Raw voxel intensity scatter plots for the selected regions of panel A representing background for *desma* and signal plus background for *tpm3*. (C) Raw voxel intensity histograms for the selected regions of panel A representing background for *desma* and signal plus background for *tpm3*. Same microscope settings used for all replicates in Figures S4–S7. Voxel size: 2×2 μm. Whole-mount wildtype zebrafish embryos fixed 26 hpf.

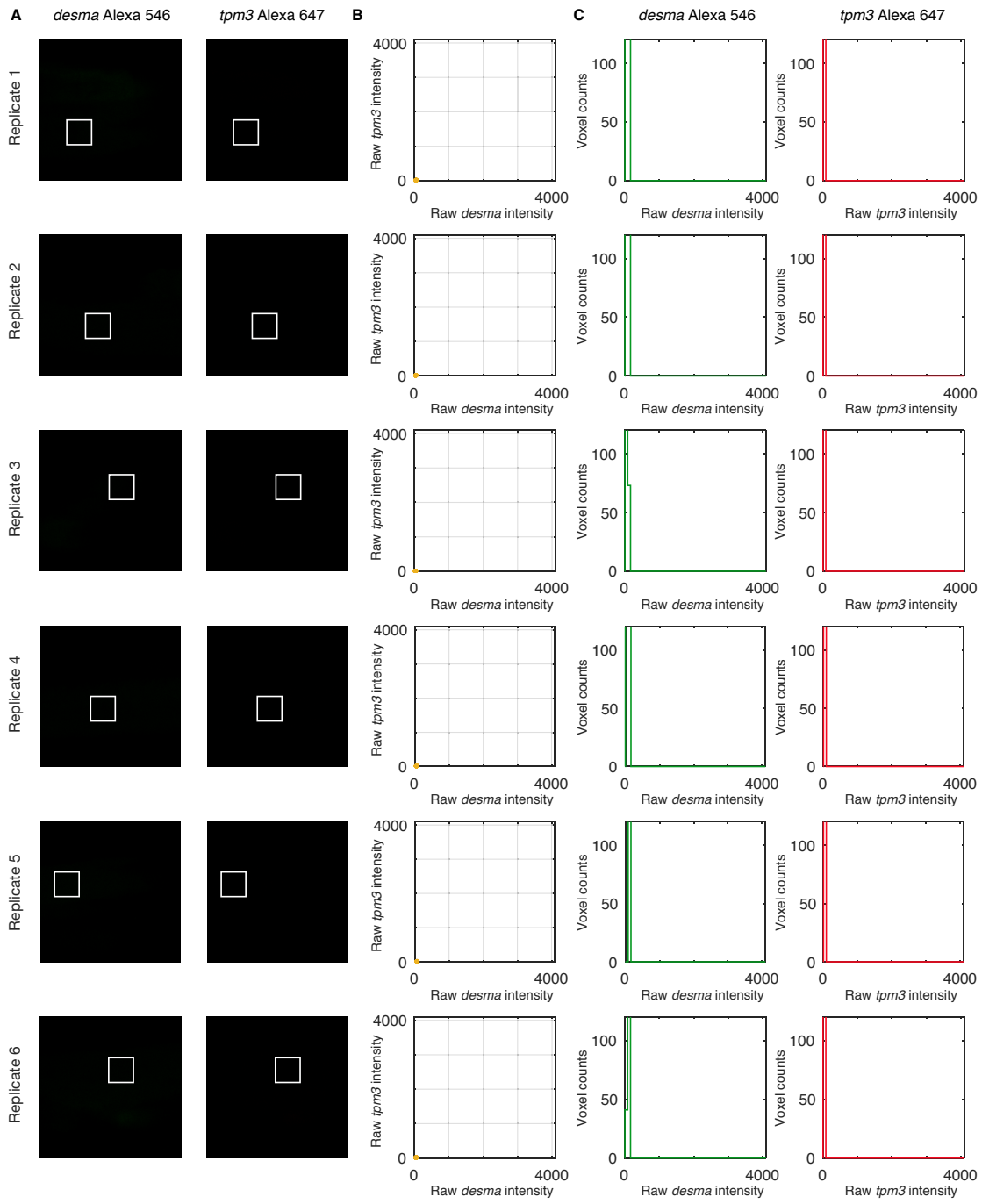

Figure S7. Characterizing background for *desma* and *tpm3*. Individual channels from 2-channel confocal images depicting regions used to estimate background using the standard in situ protocol omitting probes (BACK ≈ AF + NSA; see Section S1.3.2 for definitions). For each of 6 replicate embryos, a representative optical section was selected at approximately the depth where *desma* and *tpm3* are expressed. Same microscope settings used for all replicates in Figures S4–S7. Pixel size: 0.6×0.6 μm. (B) Raw voxel intensity scatter plots for the selected region of panel A. (C) Raw voxel intensity histograms for the scatter plots of panel B. Voxel size: 2×2 μm. Whole-mount wildtype zebrafish embryos fixed 26hpf.

S2.2 Effect of voxel size and probe set size on precision

The precision of expression scatter plots can be improved by averaging over larger voxels or by using a larger probe set. To see this, let us consider a simple model for the signal generated per amplification polymer, and examine the effect on precision as we increase the size of the voxel or the size of the probe set. Suppose each pixel contains one target mRNA that is detected with a single probe that generates a single HCR amplification polymer, and that the signal per amplification polymer is an independent random variable sampled from a normal distribution with mean μ_X and standard deviation σ_X. If we sum M of these independent normally distributed random variables, we obtain a normally distributed random variable with mean $M\mu_X$ and standard deviation $\sqrt{M}\sigma_X$ (Grimmett & Stirzaker, 2004). Now let us consider the effect of increasing the voxel size or the probe set size.

Increasing voxel size. Suppose we average $\sqrt{M} \times \sqrt{M}$ neighboring pixel intensities to create voxels, so each voxel contains M amplification polymers. Then the signal per voxel will be normally distributed with mean μ_X and standard deviation $\sigma_X/\sqrt{M}$. Hence, the scatter around the mean decreases as the voxel size increases, corresponding to an increase in precision, at the cost of a reduction in spatial resolution.

Increasing probe set size. Alternatively, suppose we use the original pixels and increase the probe set size by a factor of M, so each pixel contains M amplification polymers. The signal per target molecule will be normally distributed with mean $M\mu_X$ and standard deviation $\sqrt{M}\sigma_X$. To normalize the signal intensity for comparison to the original image, we divide by a factor of M, so the normalized signal per pixel will be normally distributed with mean μ_X and standard deviation $\sigma_X/\sqrt{M}$. Hence, the scatter around the mean decreases as the probe set size increases, corresponding to an increase in precision. In this case there is no loss in spatial resolution, but there is an increase in the cost of the probe set.

Increasing voxel size and probe set size. The precision benefits of increasing voxel size and probe set size can be exploited simultaneously, as we do in the present work by using probe sets with multiple probes (Table S1) and averaging pixels to obtain subcellular voxels of roughly 2×2 μm (Table S2). Figure S8 illustrates the relationship between precision and voxel size for the four target mRNAs of Figure 2. In these examples, the precision increases with voxel size until the voxel size approaches the length scale of the expression pattern (e.g., for the speckled expression pattern of *elavl3*).

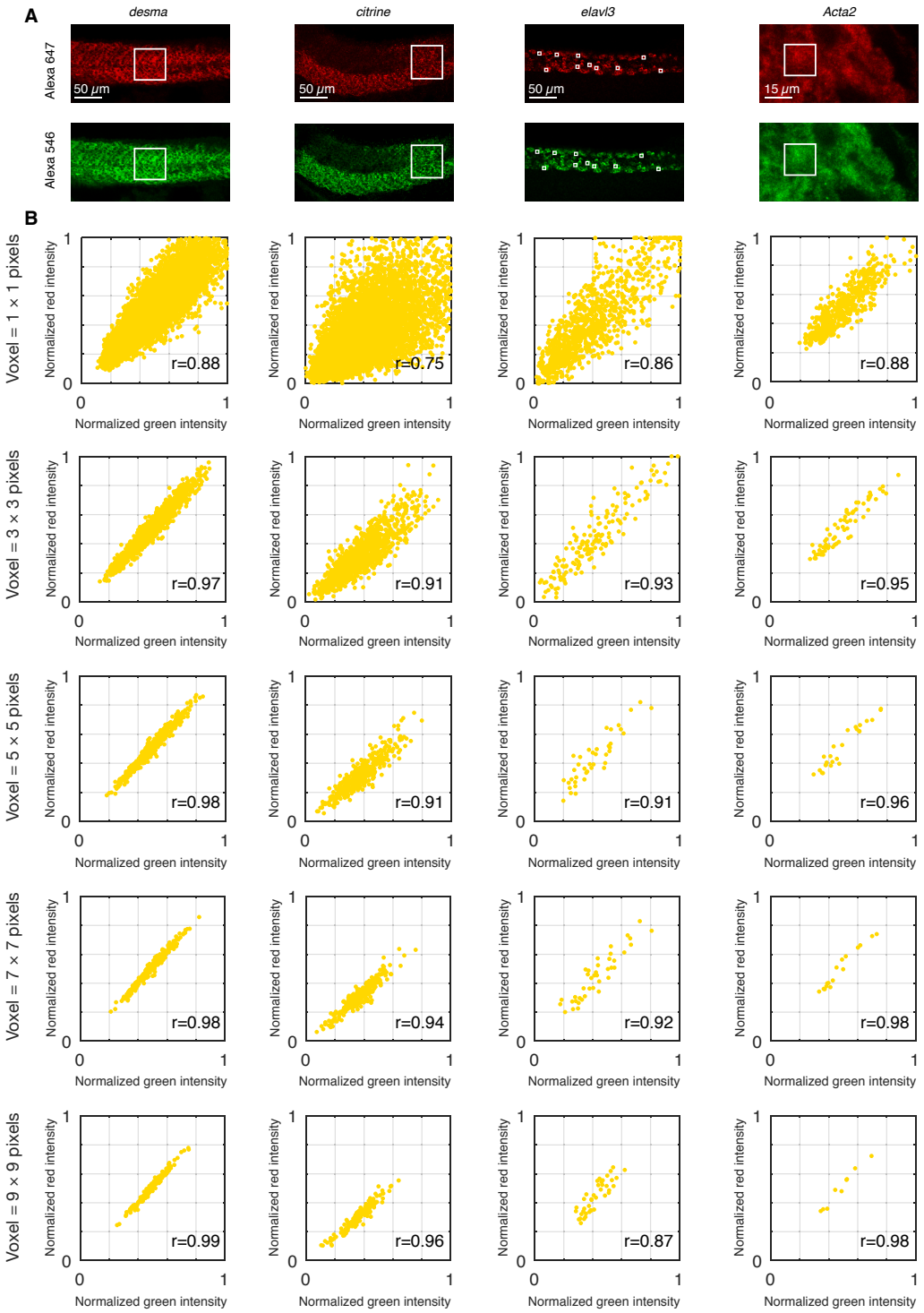

Figure S8. Relationship between precision and voxel size for four target mRNAs (cf. Figure 2CD). The data using 2×2 μm voxels are the same as in Figure 2C. For each target, all voxel intensities are normalized using the approach of Section S1.3.3 and the values in Table S3 (Pearson correlation coefficient, r).

Demonstration of averaging effects with simulated data. To further examine the effects of averaging on quantitative precision, we simulate a 2-channel redundant detection experiment (analogous to Figure 2). With this simulated approach, we can not only examine the precision of the voxel intensity plot that is the output of an experiment (as would be the case with wet lab data), but can also inspect the precision of the intermediates that contribute to that overall precision. For each simulated experiment, we generate raw signal and raw background for each pixel, which are then added to yield the raw signal plus background (total fluorescence) for each pixel. We then estimate the normalized signal using the same procedure as for experimental data (see Section S1.3.3). Note that this estimated signal will have more scatter than the original generated signal because it now includes scatter from the background, which is not removed during the normalization process.

The details of the model used to generate simulated images are as follows:

- Simulated field-of-view: 100×100 pixels (background and signal are simulated for each pixel).
- Target mRNAs per pixel: mean = 0.4, distribution based on 100×100 pixel field-of-view (Figure S9A) from an image used to estimate signal plus background for *citrine* (Alexa 546 channel of Figure S15). With $0.7\times0.7\mu$m pixels and assuming 7×7 μm cell size, this corresponds to a mean of 40 mRNAs per cell. The distribution of mRNAs across pixels is based on an experimental image to ensure that for the simulated image, averaging of neighboring pixels to create voxels will be done over pixels with biologically relevant correlations. For a pixel containing a non-integer number of mRNAs, the signal is scaled proportionally (e.g., for a pixel containing 2.3 target molecules, we simulate signal for 3 target molecules and scale the result: 2.3/3 × (SIG_1 + SIG_2 + SIG_3), representing a simple form of bookkeeping to account for the fact that the signal generated for target molecules can cross pixel boundaries.
- Background per pixel: normally distributed with mean = 492 and standard deviation = 100 (on 0 to 4095 scale of confocal microscope image). These values were calculated based on a 100×100 pixel field-of-view from an image used to estimate background for *citrine* (Alexa 546 channel of Figure S16). For simplicity, the same parameters are used to randomly generate the background independent of the size of the probe set.
- Probe set size: 1, 3, or 9 probes.
- Probe hybridization yield: 0.5 (one sample from Bernoulli distribution per probe to determine if target is detected by probe).
- HCR polymers per probe: 2 (one HCR initiator at each end).
- HCR polymer length: normally distributed with mean = 200 monomers (Choi *et al.*, 2014) and standard deviation = 40 monomers (one sample per HCR initiator).
- Fluorophores per HCR monomer: 1 (each HCR hairpin carries one fluorophore).
- Fluorescence units per fluorophore: 6.39 (on 0 to 4095 scale of confocal microscope image; this value is chosen so that simulated mean total fluorescence per voxel (signal plus background) matches the experimental value of 2025 for the field-of-view of Figure S9A).
- Voxel size: 1×1, 3×3, or 9×9 pixels per voxel (pixel values averaged to obtain voxel value).

For the baseline case using a probe set with 3 probes and 1×1 pixels per voxel (to match the conditions used in the original experiment of Figure S15), the expected value for the signal per voxel is:

$$
\begin{aligned}
\text{mean signal per voxel} \;=\;& 0.4 \text{ targets per pixel} \\
&\times 3 \text{ probes in set} \\
&\times 0.5 \text{ probe hybridization yield} \\
&\times 2 \text{ polymers per probe} \\
&\times 200 \text{ monomers per polymer} \\
&\times 1 \text{ fluorophore per monomer} \\
&\times 6.39 \text{ fluorescence units per fluorophore} \\
=\;& 1533.6 \text{ fluorescence units (on 0 to 4095 scale of confocal microscope image).}
\end{aligned}
$$

The expected value of the background per voxel is 492 fluorescence units, the expected value of the mean total

fluorescence (signal plus background) is 2025.6 = 1533.6 + 492 fluorescence units, and the expected value for the signal-to-background is 3.1. For simplicity, these same parameters are used to independently randomly generate the background and signal for both channels in the simulated redundant detection experiment.

Figure S9B depicts the 100×100 pixel simulated image (signal plus background) based on the experimental image of Figure S9A. Figures S10 and S11 illustrate with simulated data the beneficial effect on precision of increasing either the voxel size, the probe set size, or both.

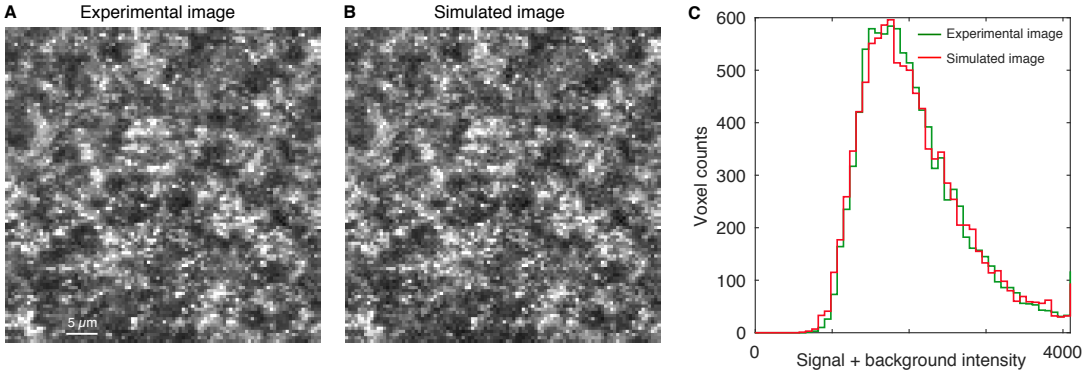

Figure S9. Experimental and simulated images used to examine effects of voxel size and probe set size on precision in Figures S10 and S11. (A) Experimental image. (B) Simulated image. (C) Pixel intensity histograms for experimental and simulated images.

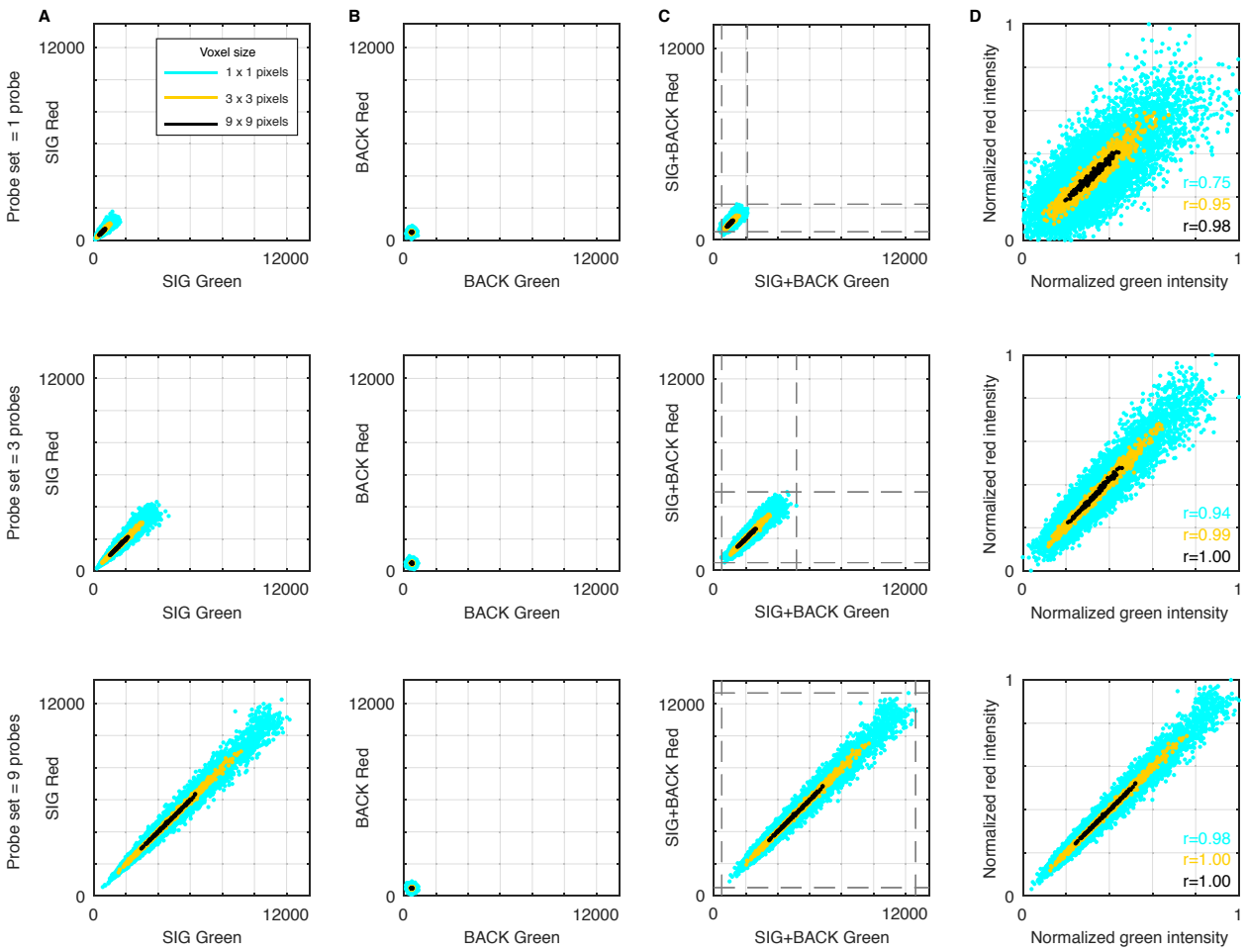

Figure S10. Simulations to study the effect of averaging on precision. Rows represent different probe set sizes: 1, 3, or 9 probes per set. Colors denote different voxel sizes: 1×1, 3×3, or 9×9 pixels per voxel. (A) Simulated signal. (B) Simulated background. (C) Simulated signal plus background. (D) Estimated normalized signal calculated using the approach of Section S1.3.3 and the values denoted by dashed lines in panel C (Pearson correlation coefficient, r). The same normalization is performed for all voxels within a row.

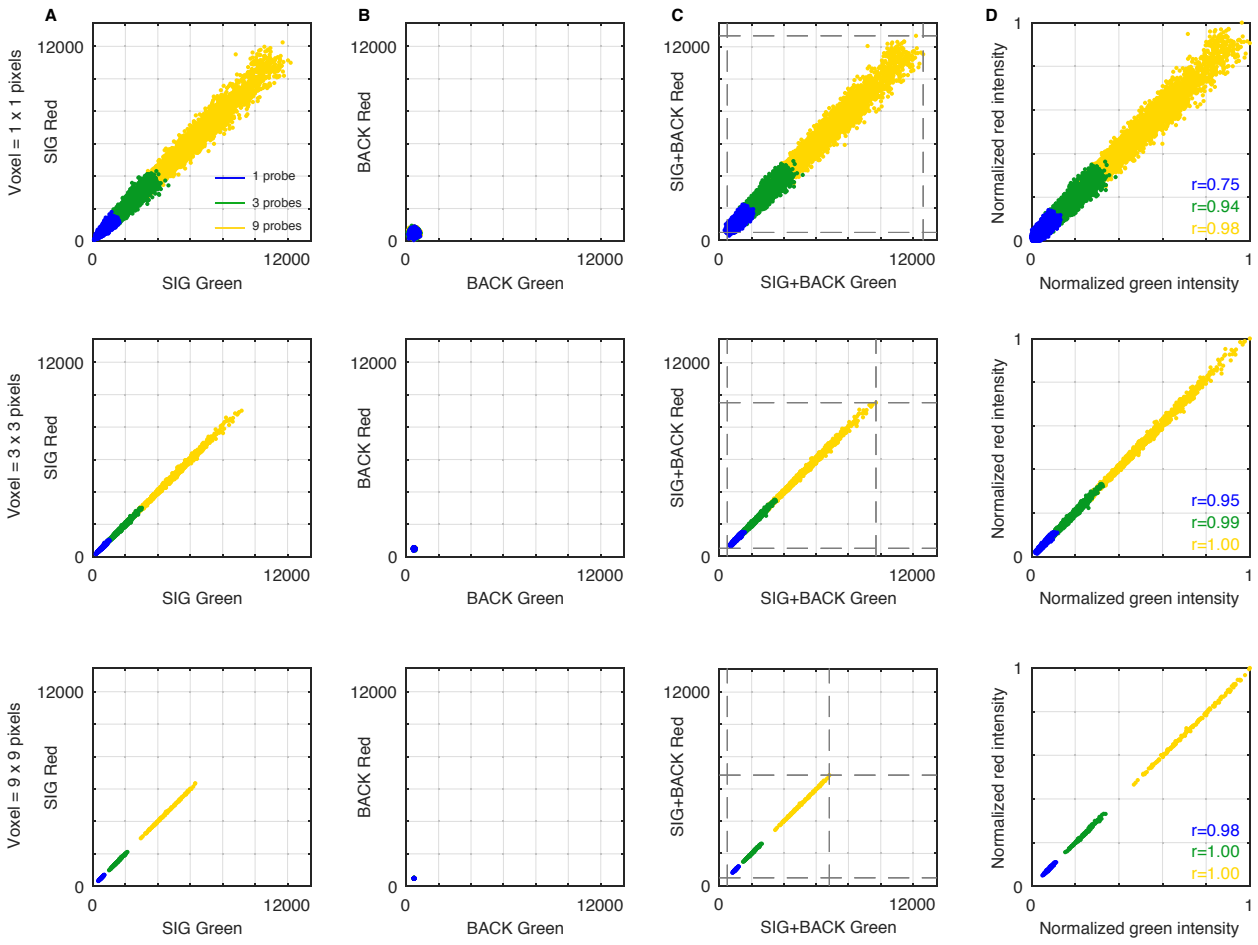

Figure S11. Simulations to study the effect of averaging on precision. Rows represent different voxel sizes: 1×1, 3×3, or 9×9 pixels per voxel. Colors denote different probe set sizes: 1, 3, or 9 probes per set. (A) Simulated signal. (B) Simulated background. (C) Simulated signal plus background. Dashed lines denote values used for normalization. (D) Estimated normalized signal calculated using the approach of Section S1.3.3 and the values denoted by dashed lines in panel C (Pearson correlation coefficient, r). The same normalization is performed for all voxels within a row.

S2.3 Replicates and additional redundant mapping data (cf. Figure 2)

This section provides replicates for the redundant mapping studies of Figure 2, including characterization of signal and background for each channel and target mRNA. The following types of data are presented for each of four targets:

- Raw 2-channel images depicting regions used to estimate signal plus background or background for each channel (see Section S1.3.2 for a description of the different approaches used for different types of target mRNAs).
- Raw voxel intensity scatter plots representing signal plus background or background (see Section S1.3.1 for definitions).
- Normalized voxel intensity scatter plots representing estimated normalized signal (see Section S1.3.3 for definitions). For a given channel and target mRNA, the normalization process translates and rescales all voxel intensities identically across replicates, enabling comparison of amplitudes and slopes within expression scatter plots for different embryos.
- Raw voxel intensity histograms representing signal plus background or background for each channel.

S2.3.1 *desma* in whole-mount zebrafish embryos

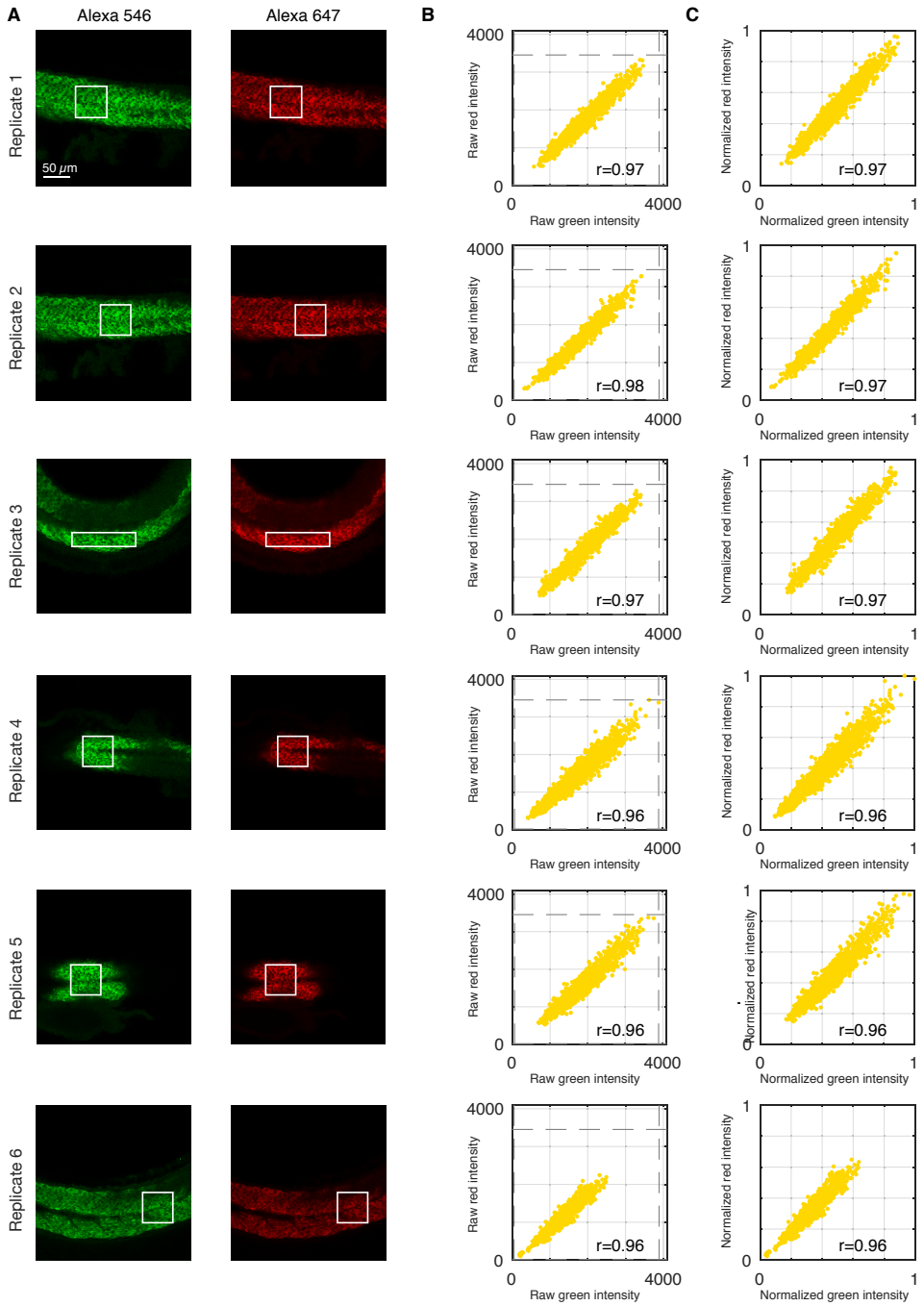

Figure S12. Characterizing signal plus background for redundant detection of *desma* (cf. Figure 2). (A) Individual channels from 2-channel confocal images depicting regions used to estimate signal plus background. For each of six replicate embryos, a representative optical section was selected based on the expression depth of the target mRNA. Pixel size: 0.7×0.7 μm. (B) Raw voxel intensity scatter plots representing signal plus background for the selected regions of panel A (Pearson correlation coefficient, r). Dashed lines denote values tabulated in Table S3 that are used for voxel intensity normalization via the method of Section S1.3.3. Voxel size: 2×2 μm. (C) Normalized voxel intensity scatter plots representing estimated normalized signal. Whole-mount wildtype zebrafish embryos fixed 26 hpf.

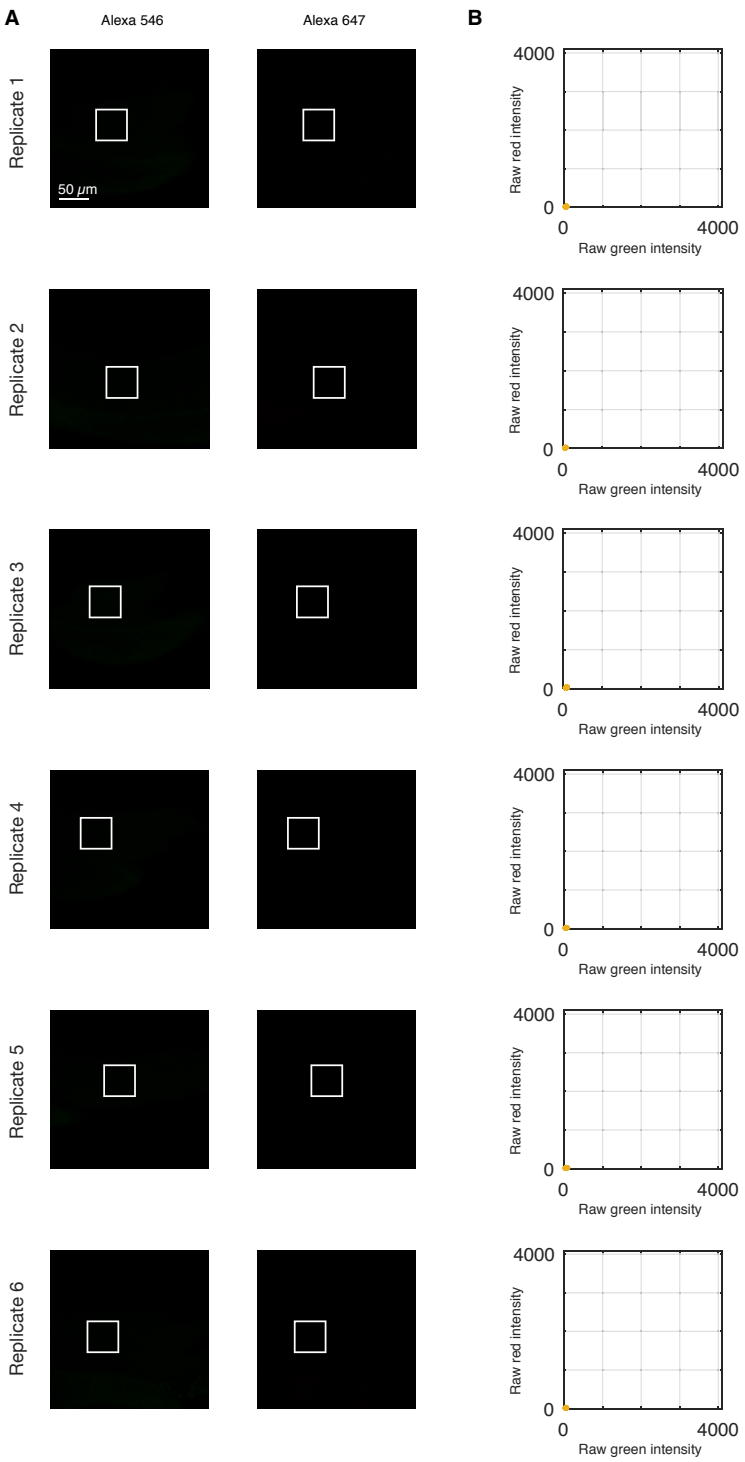

Figure S13. Characterizing background for redundant detection of *desma* (cf. Figure 2). (A) Individual channels from 2-channel confocal images depicting regions used to estimate background using the standard in situ protocol omitting probes (BACK ≈ AF + NSA; see Section S1.3.2 for definitions). For each of six replicate embryos, a representative optical section was selected at approximately the depth where *desma* is expressed. Same microscope settings as for Figure S12. Pixel size: 0.7×0.7 μm. (B) Raw voxel intensity scatter plots representing background for the selected regions of panel A. Voxel size: 2×2 μm. Whole-mount wildtype zebrafish embryos fixed 26 hpf.

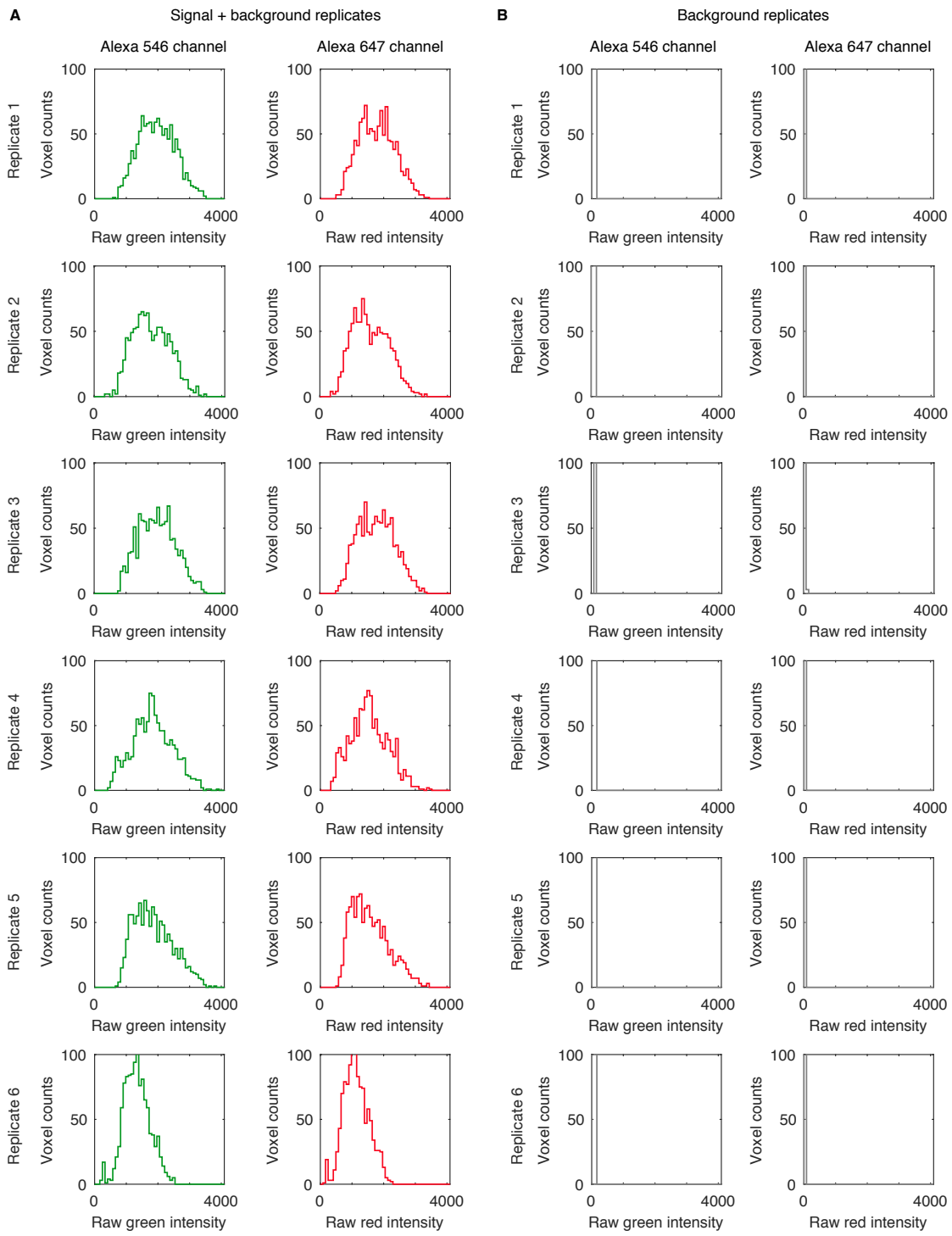

Figure S14. Raw voxel intensity histograms for redundant detection of *desma* (cf. Figure 2). (A) Signal plus background for each channel (voxels in selected regions of Figure S12). (B) Background for each channel (voxels in selected regions of Figure S13). The same microscope settings are used for all replicates. The total number of voxels is the same for each histogram.

S2.3.2 *citrine* in whole-mount zebrafish embryos

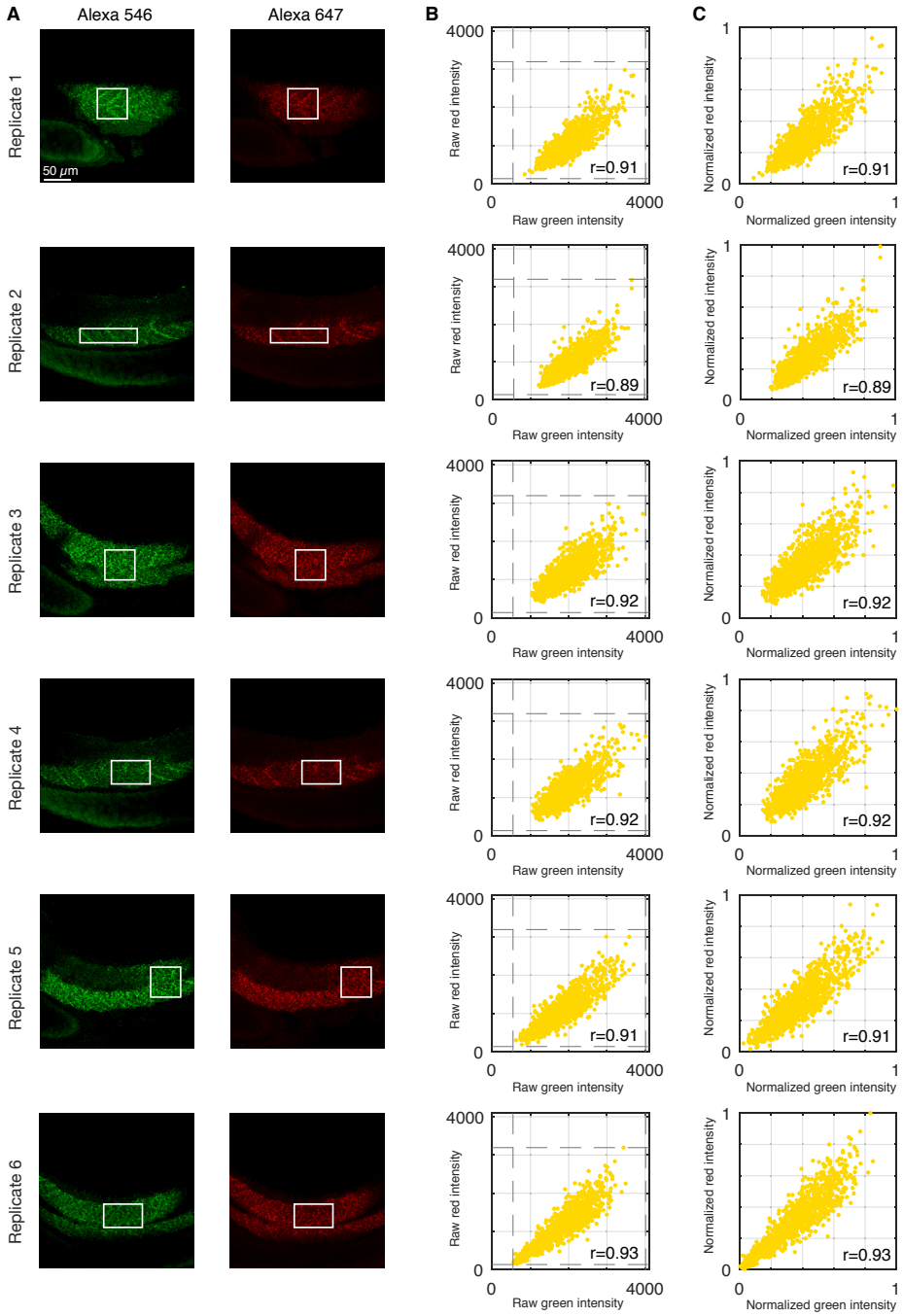

Figure S15. Characterizing signal plus background for redundant detection of *citrine* (cf. Figure 2). (A) Individual channels from 2-channel confocal images depicting regions used to estimate signal plus background. For each of six replicate embryos, a representative optical section was selected for each channel based on the expression depth of the target mRNA. Pixel size: 0.7×0.7 μm. (B) Raw voxel intensity scatter plots representing signal plus background for the selected regions of panel A (Pearson correlation coefficient, r). Dashed lines denote values tabulated in Table S3 that are used for voxel intensity normalization via the method of Section S1.3.3. Voxel size: 2×2 μm. (C) Normalized voxel intensity scatter plots representing estimated normalized signal. Whole-mount transgenic *Gt(desma-citrine)*$^{ct122a/+}$ zebrafish embryos fixed 26 hpf.

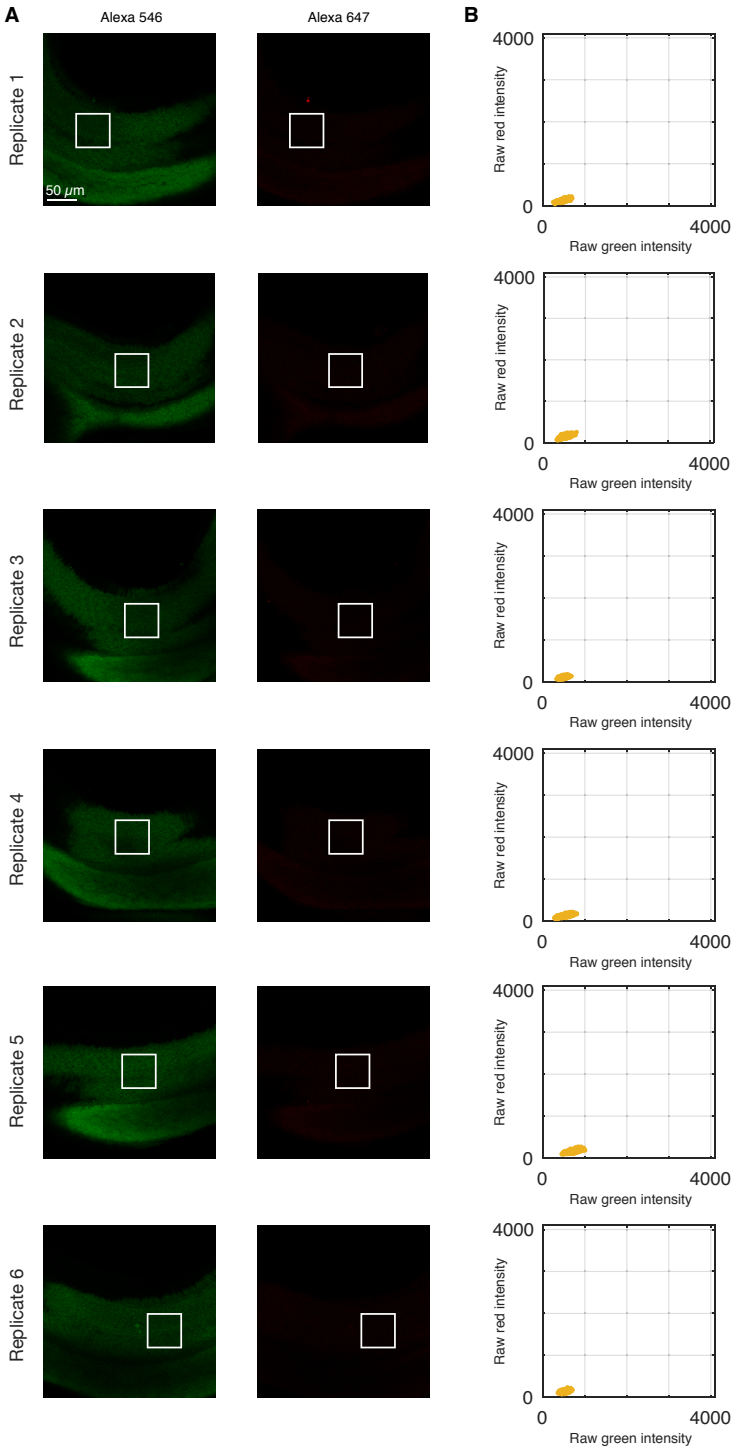

Figure S16. Characterizing background for redundant detection of *citrine* (cf. Figure 2). (A) Individual channels from 2-channel confocal images used to estimate background in wildtype embryos lacking the target (BACK = AF + NSA + NSD; see Section S1.3.2). For each of six replicate embryos, a representative optical section was selected at approximately the depth where *citrine* is expressed in transgenic embryos. Same microscope settings as for Figure S15. Pixel size: 0.7×0.7 μm. (B) Raw voxel intensity scatter plots representing background for the selected regions of panel A. Voxel size: 2×2 μm. Whole-mount wildtype zebrafish embryos fixed 26 hpf.

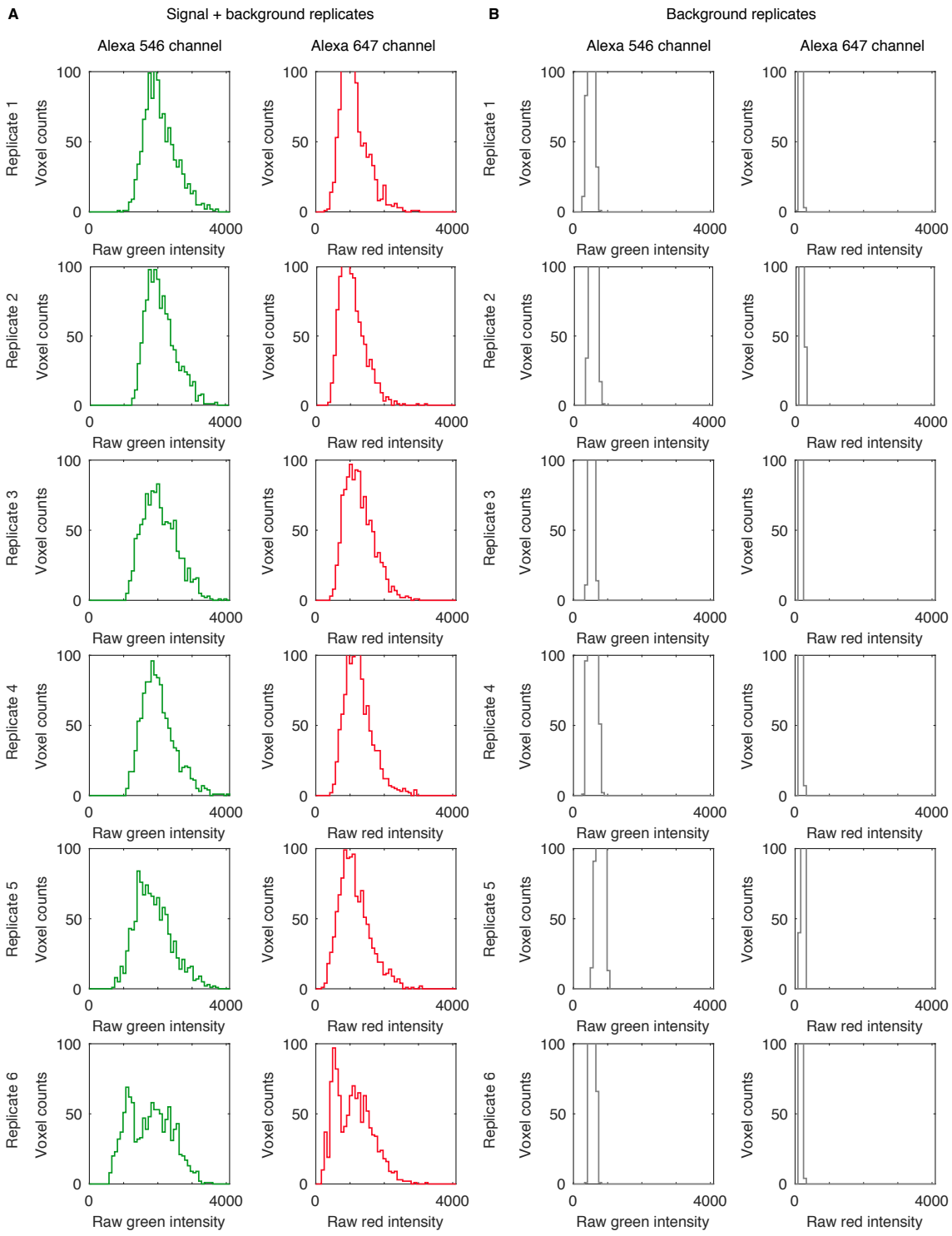

Figure S17. Raw voxel intensity histograms for redundant detection of *citrine* (cf. Figure 2). (A) Signal plus background for each channel (voxels in selected regions of Figure S15). (B) Background for each channel (voxels in selected regions of Figure S16). The same microscope settings are used for all replicates. The total number of voxels is the same for each histogram.

S2.3.3 *elavl3* in whole-mount zebrafish embryos

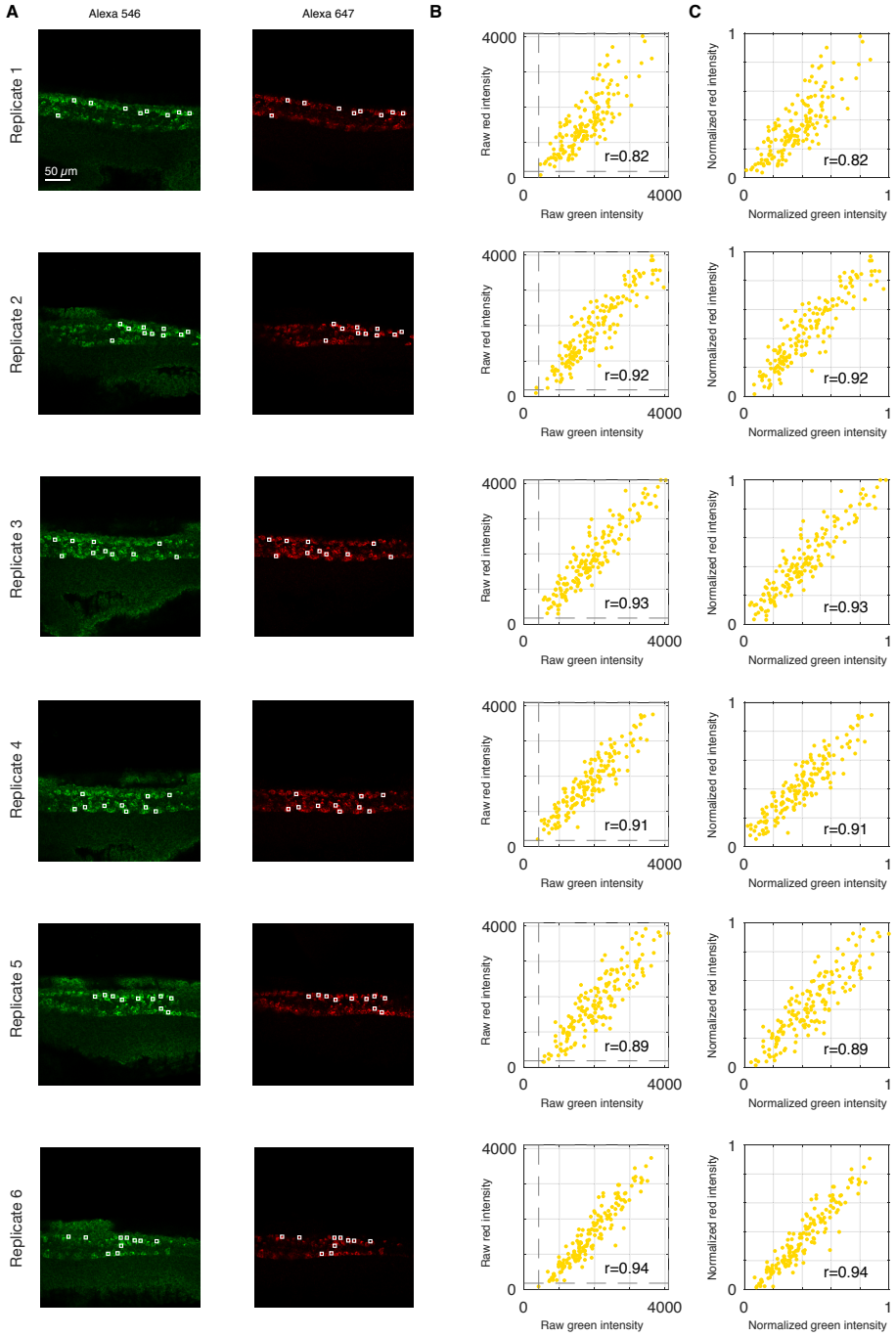

Figure S18. Characterizing signal plus background for redundant detection of *elavl3* (cf. Figure 2). (A) Individual channels from 2-channel confocal images depicting regions used to estimate signal plus background. For each of six replicate embryos, a representative optical section was selected based on the expression depth of the target mRNA. Pixel size: 0.7×0.7 μm. (B) Raw voxel intensity scatter plots representing signal plus background for the selected regions of panel A (Pearson correlation coefficient, r). Dashed lines denote values tabulated in Table S3 that are used for voxel intensity normalization via the method of Section S1.3.3. Voxel size: 2×2 μ m. (C) Normalized voxel intensity scatter plots representing estimated normalized signal. Whole-mount wildtype zebrafish embryos fixed 26 hpf.

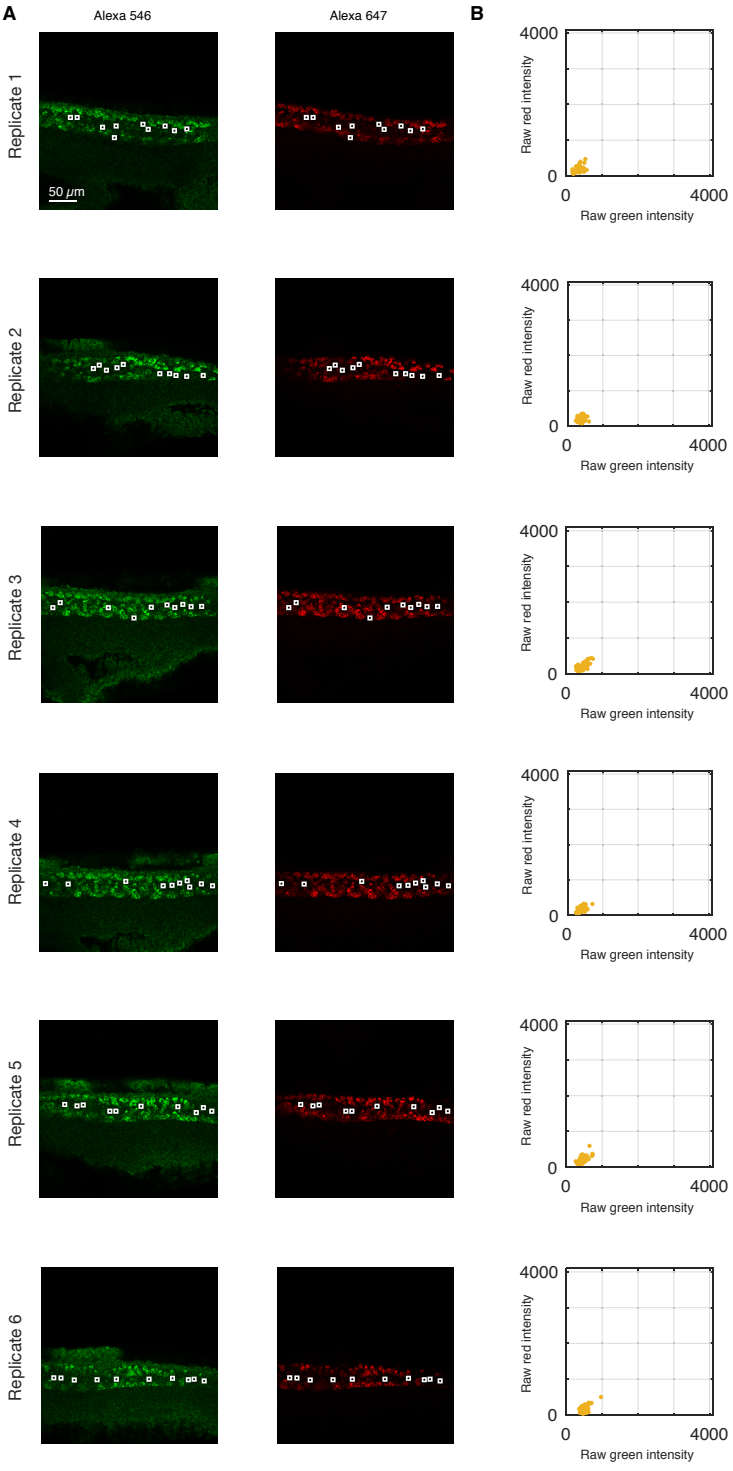

Figure S19. Characterizing background for redundant detection of *elavl3* (cf. Figure 2). (A) Individual channels from 2-channel confocal images depicting regions used to estimate background (BACK = AF + NSA + NSD; see Section S1.3.2); different regions of these same images used to estimate signal plus background in Figure S18. Pixel size: 0.7×0.7 μm. (B) Raw voxel intensity scatter plots representing background for the selected regions of panel A. Voxel size: 2×2 μm. Whole-mount wildtype zebrafish embryos fixed 26 hpf.

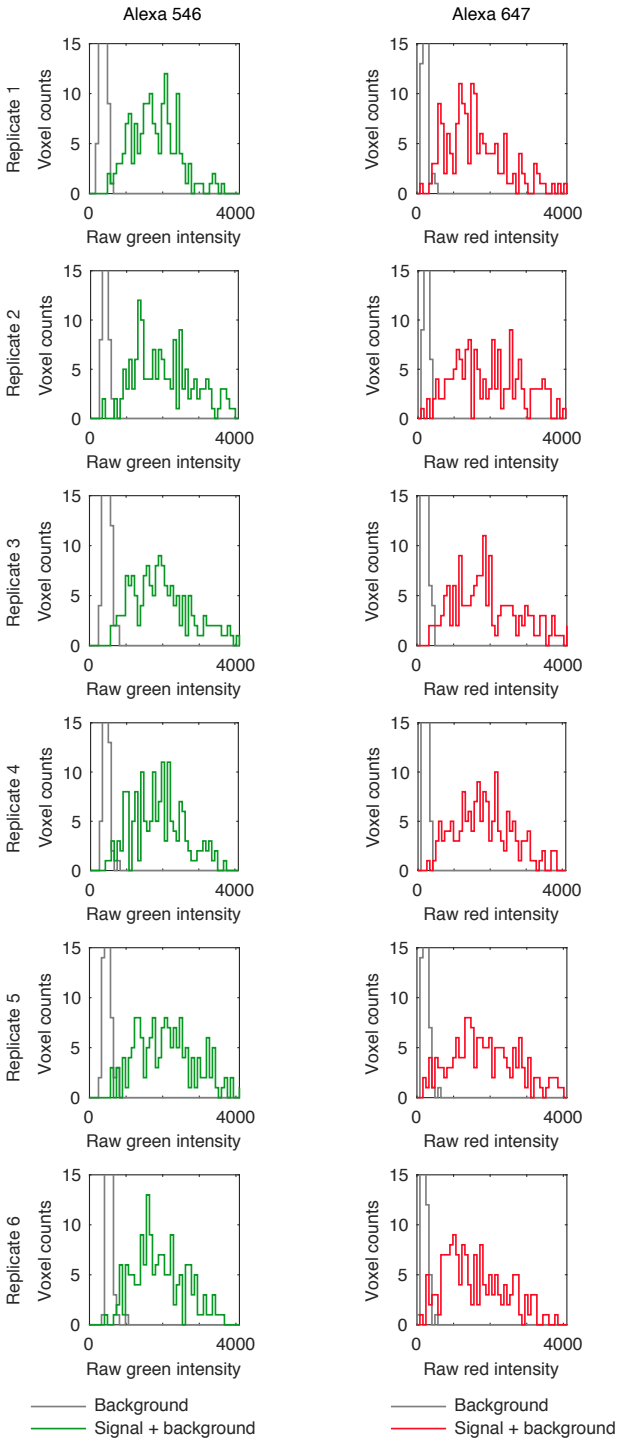

Figure S20. Raw voxel intensity histograms for redundant detection of *elavl3* (cf. Figure 2). Signal plus background for each channel (voxels in selected regions of Figure S18) and background for each channel (voxels in selected regions of Figure S19). Signal plus background and background are characterized in different regions of the same image for each replicate embryo. The total number of voxels is the same for each histogram.

S2.3.4 *Acta2* in whole-mount mouse embryos

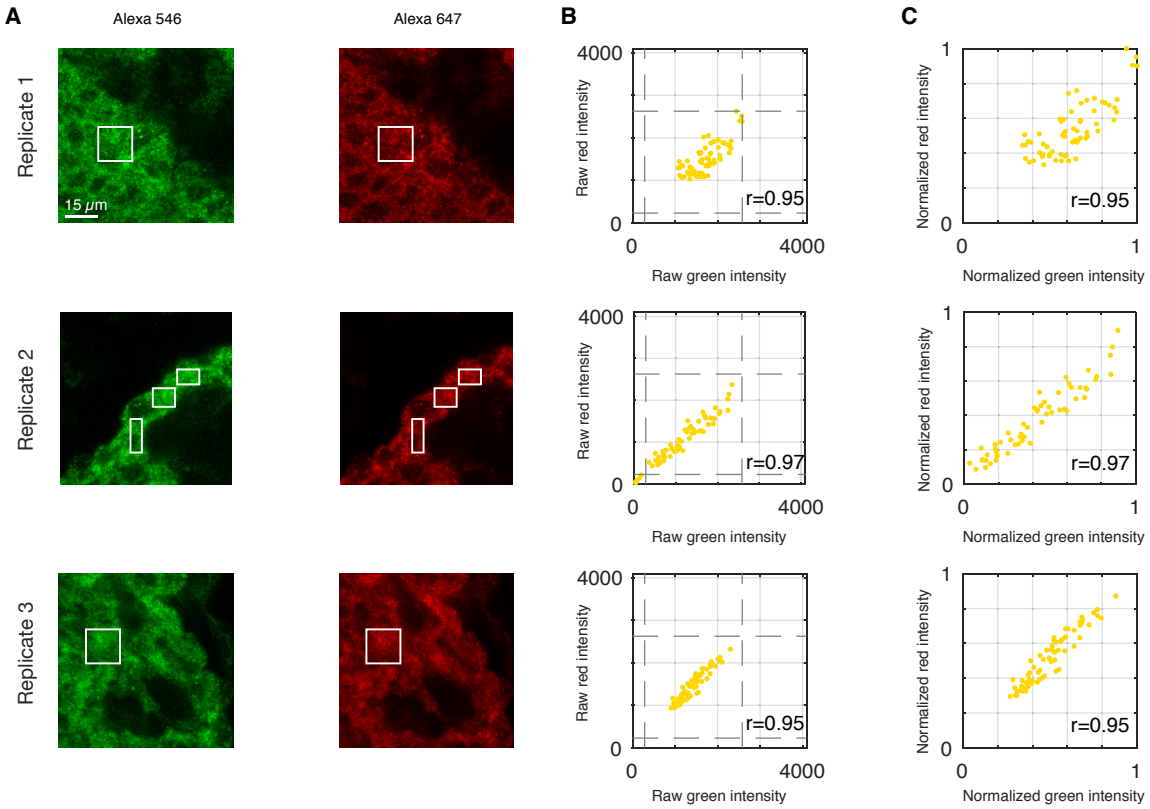

Figure S21. Characterizing signal plus background for redundant detection of *Acta2* (cf. Figure 2). (A) Individual channels from 2-channel confocal images depicting regions used to estimate signal plus background. For each of three replicate embryos, a representative optical section was selected based on the expression depth of the target mRNA. Pixel size: 0.07×0.07 μm. (B) Raw voxel intensity scatter plots representing signal plus background for the selected regions of panel A (Pearson correlation coefficient, r). Dashed lines denote values tabulated in Table S3 that are used for voxel intensity normalization via the method of Section S1.3.3. Voxel size: $2\times2\mu$m. (C) Normalized voxel intensity scatter plots representing estimated normalized signal. Whole-mount wildtype mouse embryos fixed E9.5.

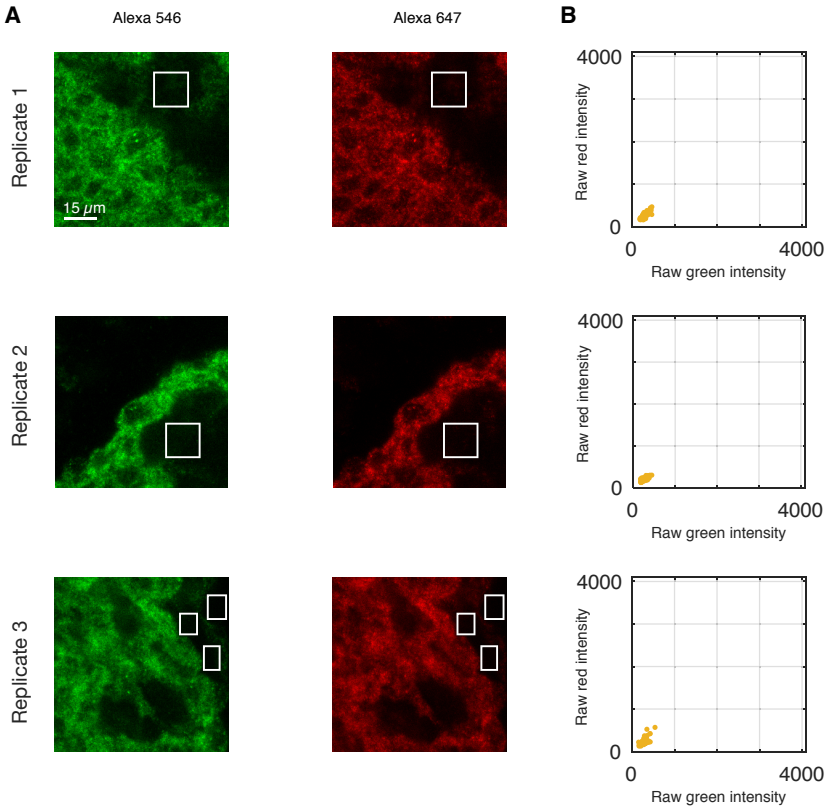

Figure S22. Characterizing background for redundant detection of *Acta2* (cf. Figure 2). (A) Individual channels from 2-channel confocal images depicting regions used to estimate background (BACK = AF + NSA + NSD; see Section S1.3.2); different regions of these same images used to estimate signal plus background in Figure S21. Pixel size: 0.07×0.07 μm. (B) Raw voxel intensity scatter plots representing background for the selected regions of panel A. Voxel size: 2×2 μm. Whole-mount wildtype mouse embryos fixed E9.5.

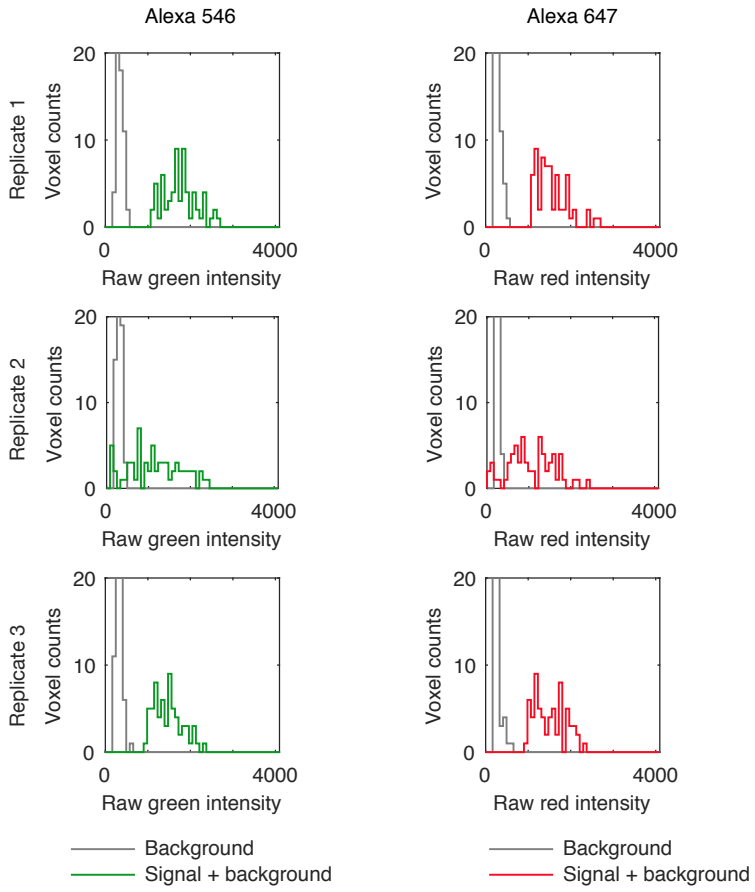

Figure S23. Raw voxel intensity histograms for redundant detection of *Acta2* (cf. Figure 2). Signal plus background for each channel (voxels in selected regions of Figure S21) and background for each channel (voxels in selected regions of Figure S22). Signal plus background and background are characterized in different regions of the same image for each replicate embryo. The total number of voxels is the same for each histogram.

S2.4 Replicates and additional homozyogous vs heterozygous data (cf. Figure 3)

This section provides replicates for the homozygous vs heterozygous study of Figure 3, including characterization of signal and background as follows:

- For transgenic target *citrine*, signal plus background is characterized in homozygous embryos (Figure S24) and heterozygous embryos (Figure S25) containing the target. Background is characterized in wildtype embryos lacking the target (Figure S26).
- For endogenous target *desma*, signal is characterized in homozygous embryos (Figure S24) and heterozygous embryos (Figure S25) containing the target. Background is characterized in wildtype embryos containing the target using the standard in situ protocol omitting probes (Figure S27).

For each target, the identical normalization is used for both homozygous and heterozygous embryos (based on the maximum voxel intensity in the homozygous replicates), enabling comparison of amplitudes and slopes between embryo types. Raw voxel intensity histograms for signal plus background and background are shown for both targets in Figure S28.

S2.4.1 Homozygous embryos

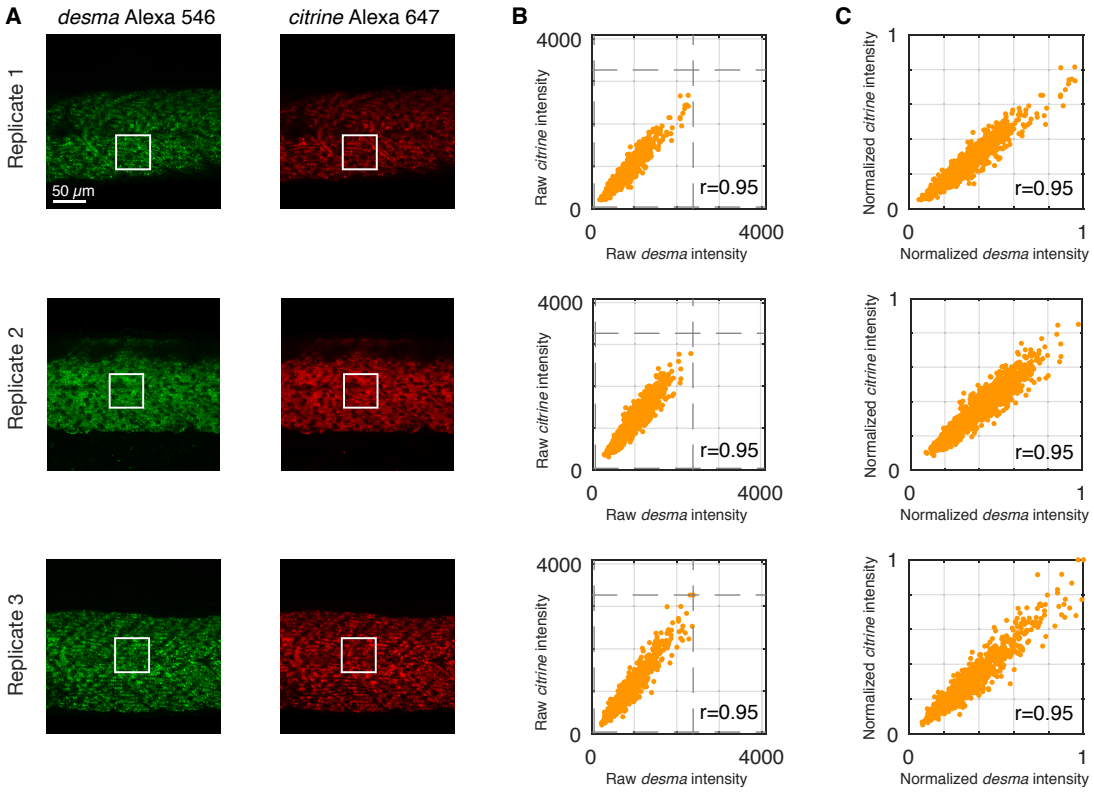

Figure S24. Characterizing signal plus background for *citrine* and *desma* in homozygous embryos (cf. Figure 3). (A) Individual channels from 2-channel confocal images depicting regions used to estimate signal plus background. For each of 3 replicate embryos, a representative optical section was selected based on the expression depth of the target mRNAs. Pixel size: 0.7×0.7 μm. (B) Raw voxel intensity scatter plots representing signal plus background for the selected regions of panel A (Pearson correlation coefficient, r). Dashed lines denote values tabulated in Table S3 that are used for voxel intensity normalization via the method of Section S1.3.3. Voxel size: 2×2 μm. (C) Normalized voxel intensity scatter plots representing estimated normalized signal. Whole-mount homozygous *Gt(desma-citrine)*$^{ct122a/ct122a}$ zebrafish embryos fixed 26 hpf.

S2.4.2 Heterozygous embryos

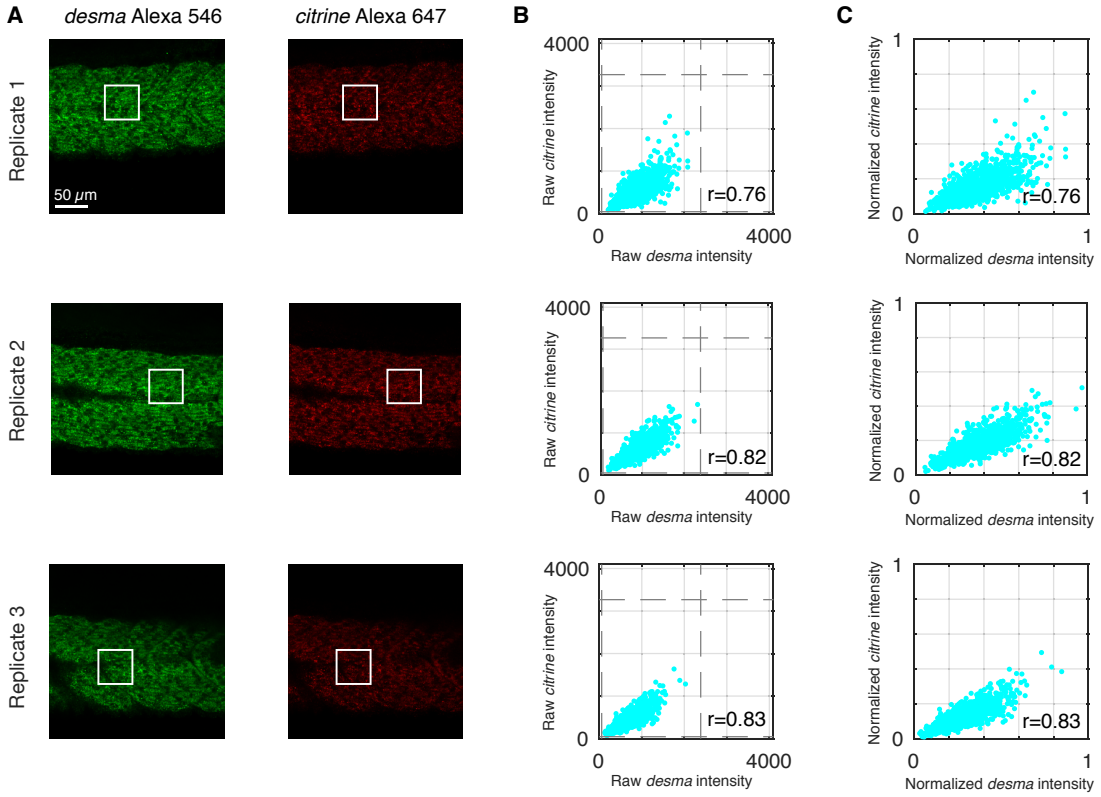

Figure S25. Characterizing signal plus background for *citrine* and *desma* in heterozygous embryos (cf. Figure 3). (A) Individual channels from 2-channel confocal images depicting regions used to estimate signal plus background. For each of 3 replicate embryos, a representative optical section was selected based on the expression depth of the target mRNAs. Same microscope settings as for Figure S24. Pixel size: 0.7×0.7 μm. (B) Raw voxel intensity scatter plots representing signal plus background for the selected regions of panel A (Pearson correlation coefficient, r). Dashed lines denote values tabulated in Table S3 that are used for voxel intensity normalization via the method of Section S1.3.3. Voxel size: 2×2 μm. (C) Normalized voxel intensity scatter plots representing estimated normalized signal. Whole-mount heterozygous *Gt(desma-citrine)*$^{ct122a/+}$ zebrafish embryos fixed 26 hpf.

S2.4.3 Wildtype embryos

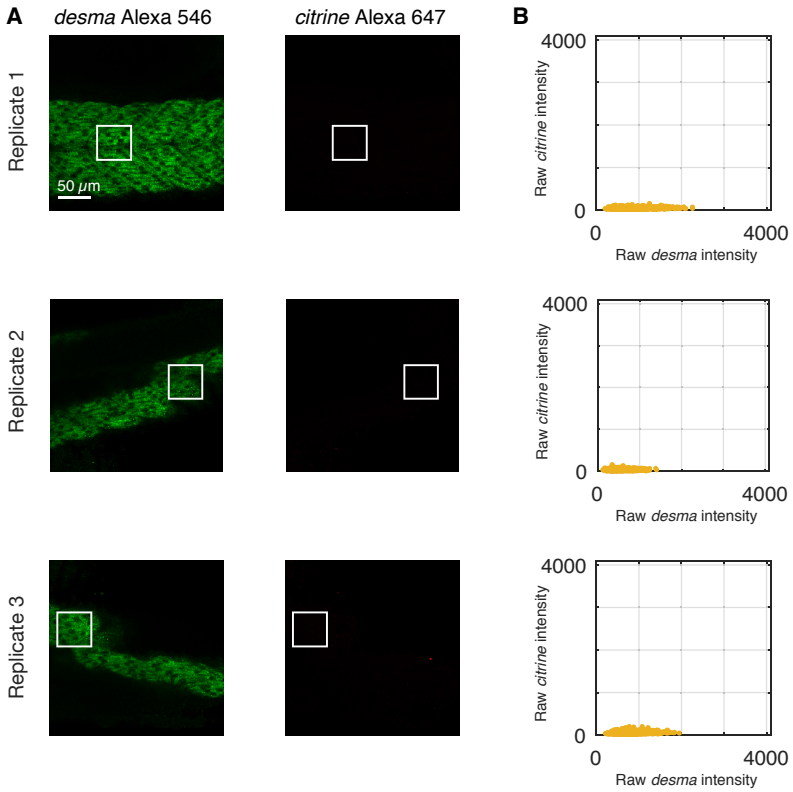

Figure S26. Characterizing background for *citrine* in wildtype embryos (cf. Figure 3). (A) Individual channels from 2-channel confocal images used to estimate background in wildtype embryos lacking the target (BACK = AF + NSA + NSD; see Section S1.3.2). For each of 3 replicate embryos, a representative optical section was selected at the depth where *desma* is expressed. Same microscope settings as for Figure S24. Pixel size: 0.7×0.7 μm. (B) Raw voxel intensity scatter plots representing *citrine* background and *desma* signal plus background for the selected regions of panel A. Voxel size: 2×2 μm. Whole-mount wildtype zebrafish embryos fixed 26 hpf.

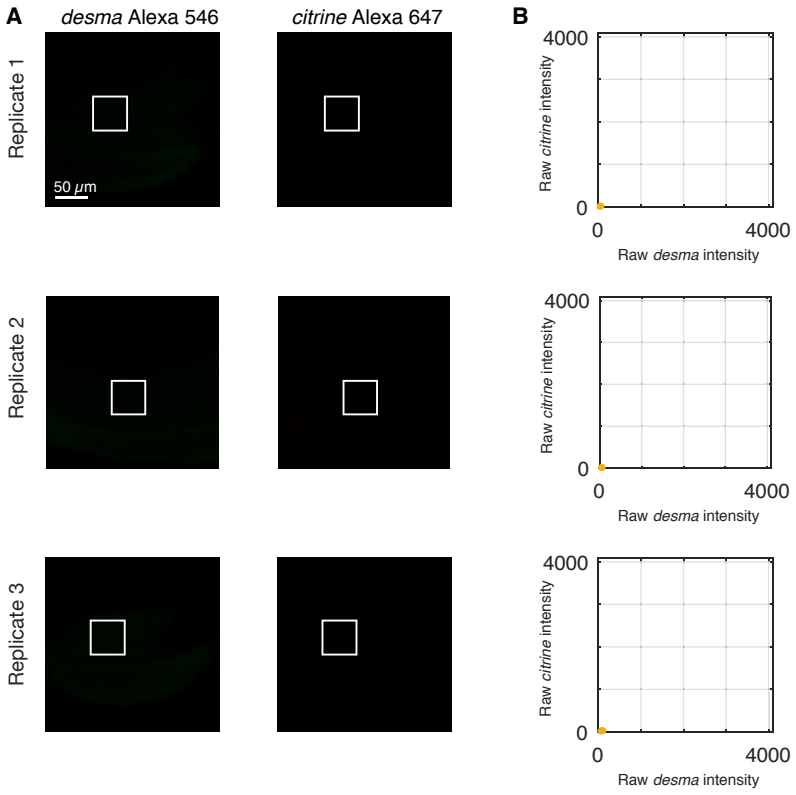

Figure S27. Characterizing background for *desma* in wildtype embryos (cf. Figure 3). (A) Individual channels from 2-channel confocal images depicting regions used to estimate background using the standard in situ protocol omitting probes (BACK ≈ AF + NSA ; see Section S1.3.2 for definitions). For each of 3 replicate embryos, a representative optical section was selected at approximately the depth where *desma* is expressed. Same microscope settings as for Figure S24. Pixel size: 0.7×0.7 μm. (B) Raw voxel intensity scatter plots representing *citrine* and *desma* background for the selected regions of panel A. Voxel size: 2×2 μm. Whole-mount wildtype zebrafish embryos fixed 26 hpf.

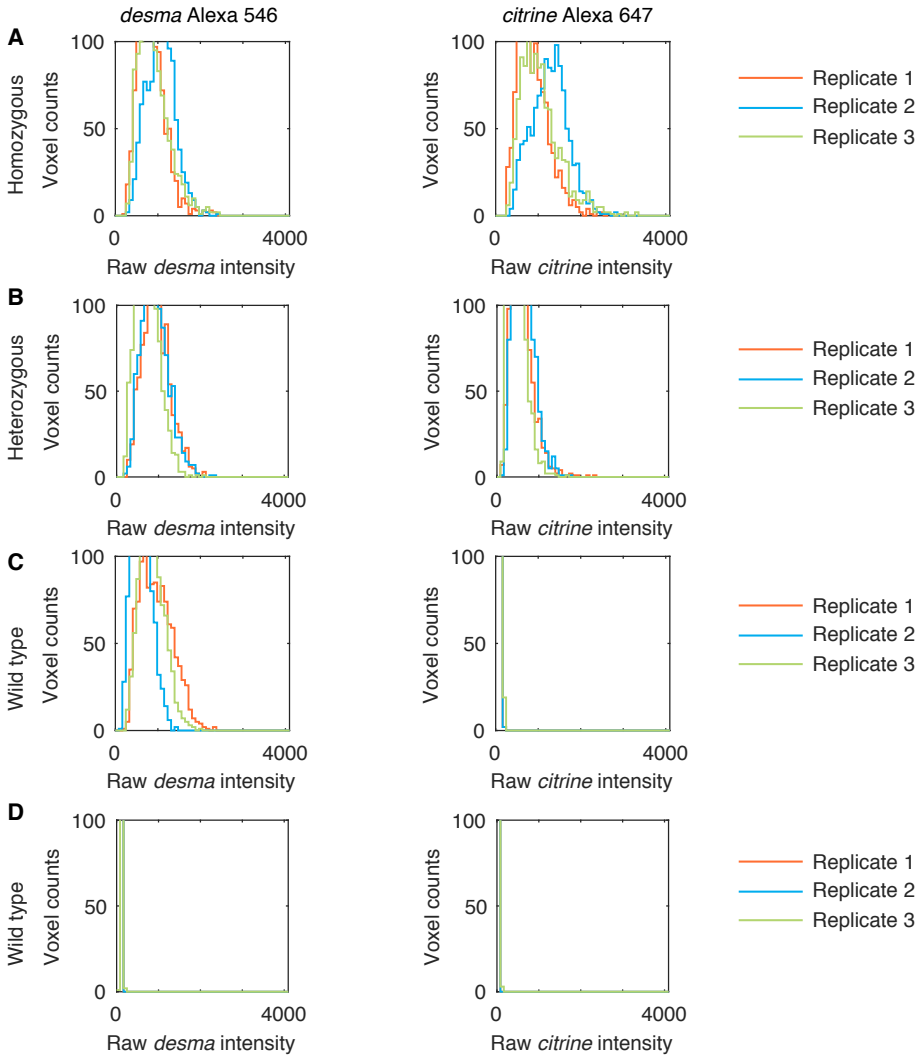

Figure S28. Raw voxel intensity histograms for *citrine* and *desma* (cf. Figure 3). (A) Signal plus background in homozygous embryos (voxels in selected regions of Figure S24). (B) Signal plus background in heterozygous embryos (voxels in selected regions of Figure S25). (C) Background for *citrine* in wildtype embryos (voxels in selected regions of Figure S26). (D) Background for *desma* in wildtype embryos (voxels in selected regions of Figure S27). The same microscope settings are used for all replicates. The total number of voxels is the same for each histogram.

S2.5 Replicates and additional read-out/read-in data (cf. Figure 4)

4-channel mean intensity images are used to display expression for 4 target mRNAs. For each channel, a stack of five optical sections was selected based on the expression depth of the corresponding mRNA. Different regions of the same mean intensity images are analyzed for Figures 4, 5, and S29–S47. Expression scatter plots are presented using normalized voxel intensities for each channel (see Section S1.3.3 for definitions). For a given channel, the normalization process translates and rescales all voxel intensities identically across replicates, enabling comparison of amplitudes and slopes within expression scatter plots for different embryos. The following studies are presented:

- Section S2.5.1 characterizes signal and background using the definitions and methods of Section S1.3 for each of 4 target mRNAs. Mean signal, background, and signal-to-background estimates are summarized in Table S3.
- Section S2.5.2 presents the raw voxel intensity scatter plots used for the read-out/read-in studies of Figures 4 and S34–S40.
- Sections S2.5.3–S2.5.6 present additional read-out/read-in examples for four embryos. Cluster shading is propagated between the quadrants in the expression scatter plots, which is akin to projecting the voxel intensities onto 4 axes, but without the difficulty of 4-dimensional visualization. This approach can be extended to N-dimensional expression data simply by using $\binom{N}{2}$ pairwise scatter plots (for compactness we display only 4 of the 6 possible pairwise plots for $N = 4$ targets).

S2.5.1 Characterizing signal and background for *myod1, tpm3, her1, her7*

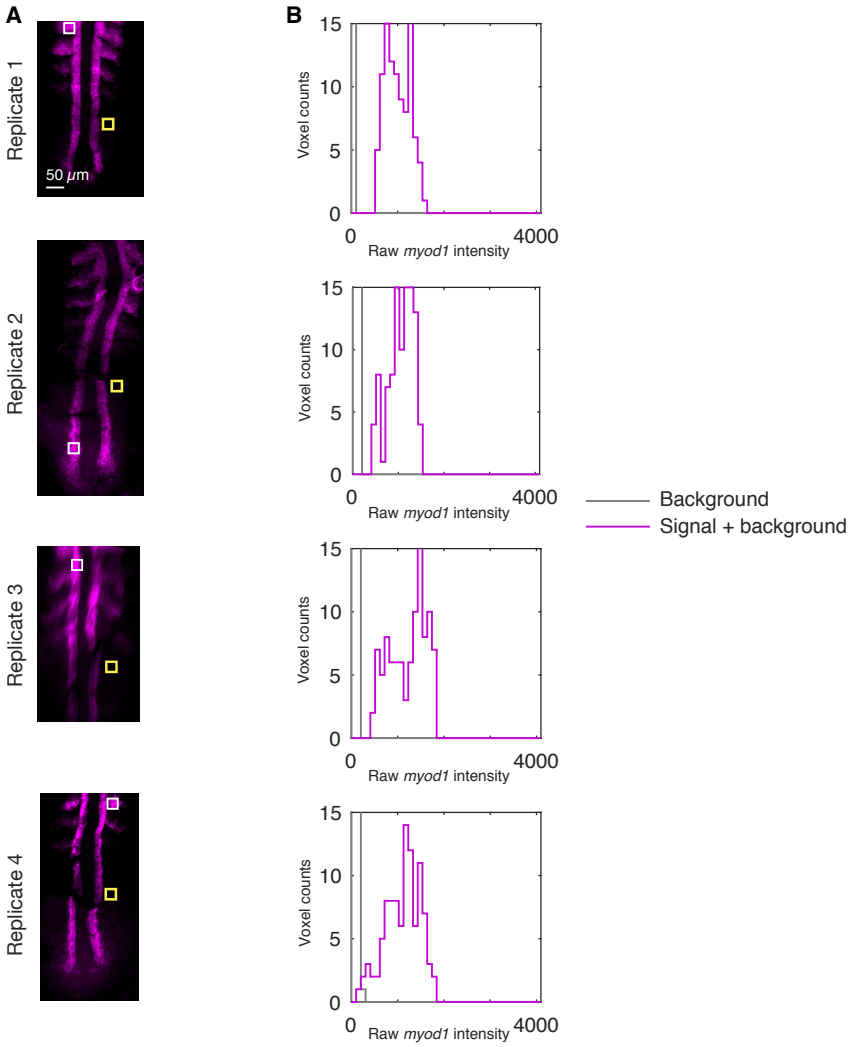

Figure S29. Characterizing signal and background for *myod1* (cf. Figures 4 and 5). (A) Mean intensity images from 4-channel confocal images depicting regions used to estimate signal plus background (white boundary) and background (yellow boundary). For each of four replicate embryos, a stack of five optical sections was selected based on the expression depth of *myod1*. Pixel size: 0.7×0.7 μm. (B) Raw voxel intensity histograms for signal plus background (voxels within white boundary of panel A) and background (voxels within yellow boundary). Voxel size: 2×2 μm. The total number of voxels is the same for each histogram. Whole-mount wildtype zebrafish embryos fixed 10 hpf.

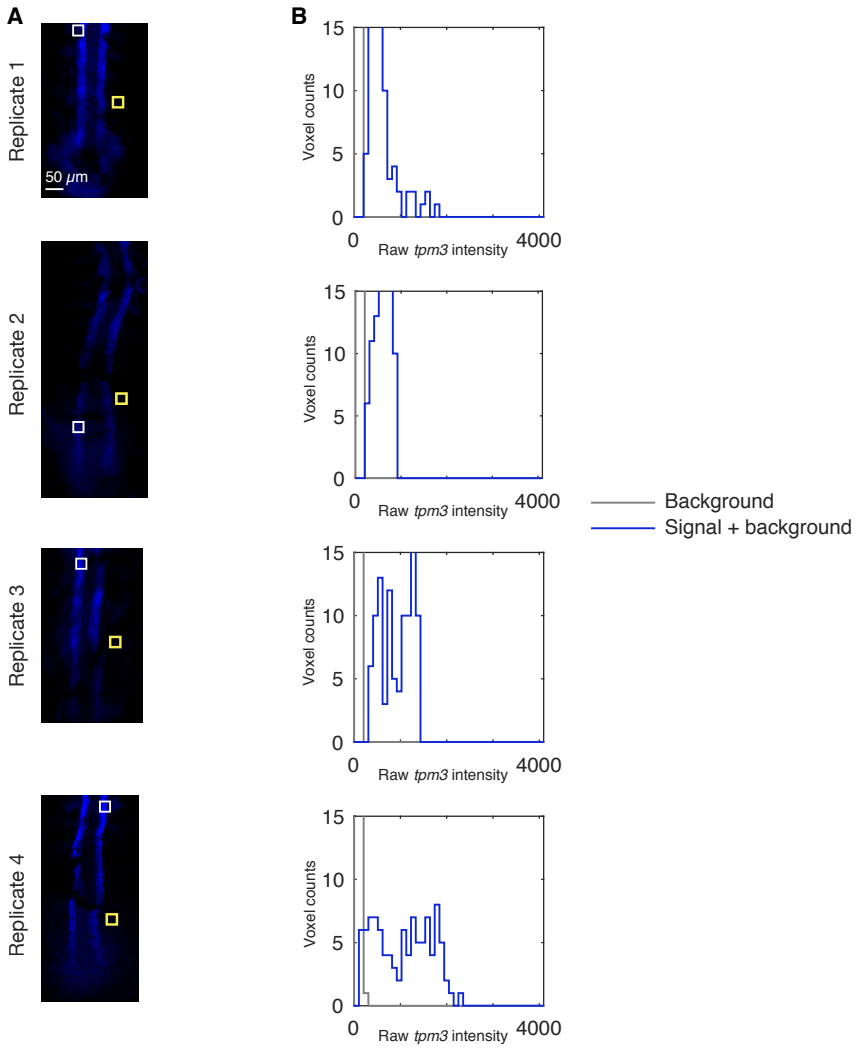

Figure S30. Characterizing signal and background for *tpm3* (cf. Figures 4 and 5). (A) Mean intensity images from 4-channel confocal images depicting regions used to estimate signal plus background (white boundary) and background (yellow boundary). For each of four replicate embryos, a stack of five optical sections was selected based on the expression depth of *tpm3*. Pixel size: 0.7×0.7 μm. (B) Raw voxel intensity histograms for signal plus background (voxels within white boundary of panel A) and background (voxels within yellow boundary). Voxel size: 2×2 μm. The total number of voxels is the same for each histogram. Whole-mount wildtype zebrafish embryos fixed 10 hpf.

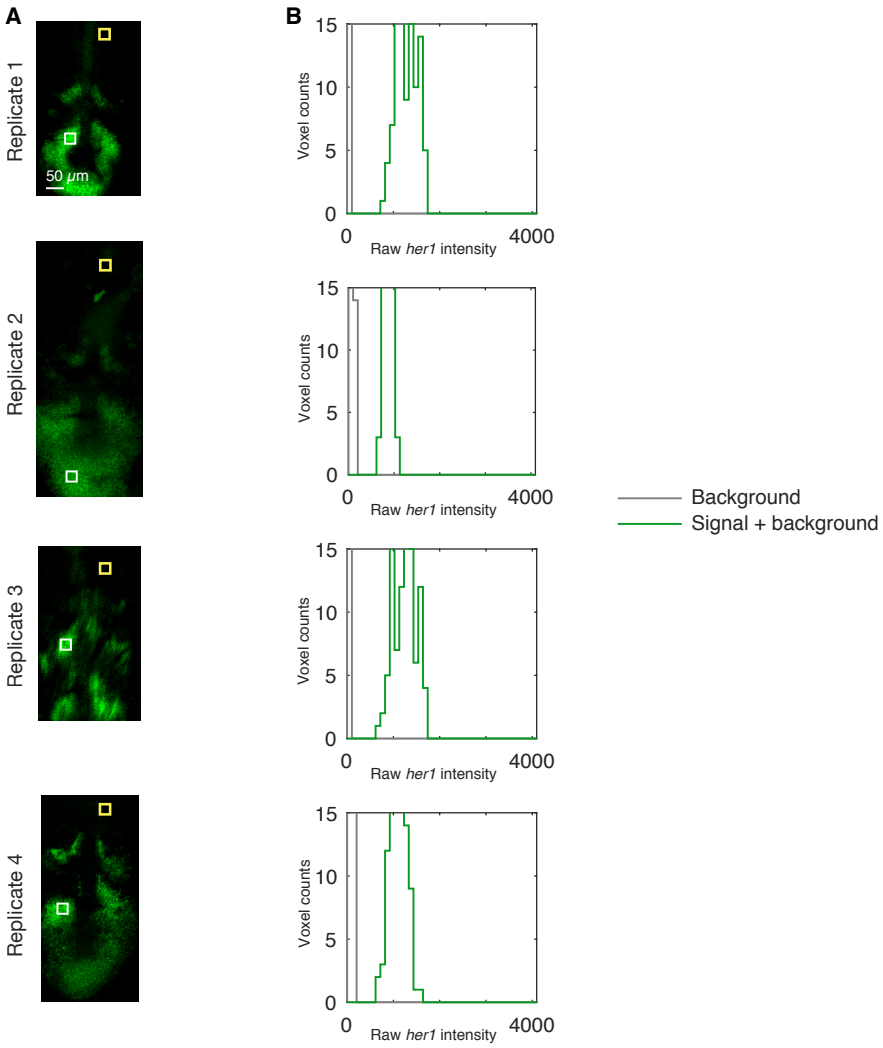

Figure S31. Characterizing signal and background for *her1* (cf. Figures 4 and 5). (A) Mean intensity images from 4-channel confocal images depicting regions used to estimate signal plus background (white boundary) and background (yellow boundary). For each of four replicate embryos, a stack of five optical sections was selected based on the expression depth of *her1*. Pixel size: 0.7×0.7 μm. (B) Raw voxel intensity histograms for signal plus background (voxels within white boundary of panel A) and background (voxels within yellow boundary). Voxel size: 2×2 μm. The total number of voxels is the same for each histogram. Whole-mount wildtype zebrafish embryos fixed 10 hpf.

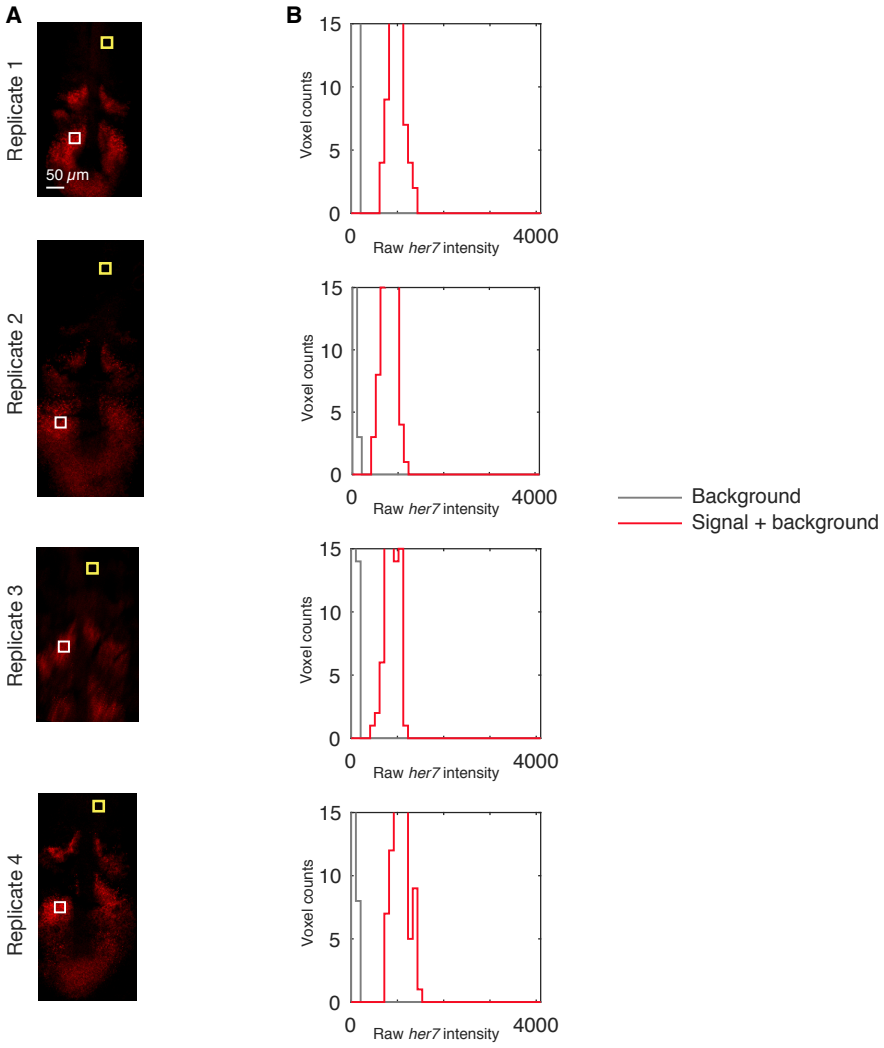

Figure S32. Characterizing signal and background for *her7* (cf. Figures 4 and 5). (A) Mean intensity images from 4-channel confocal images depicting regions used to estimate signal plus background (white boundary) and background (yellow boundary). For each of four replicate embryos, a stack of five optical sections was selected based on the expression depth of *her7*. Pixel size: 0.7×0.7 μm. (B) Raw voxel intensity histograms for signal plus background (voxels within white boundary of panel A) and background (voxels within yellow boundary). Voxel size: 2×2 μm. The total number of voxels is the same for each histogram. Whole-mount wildtype zebrafish embryos fixed 10 hpf.

S2.5.2 Raw data for read-out/read-in studies

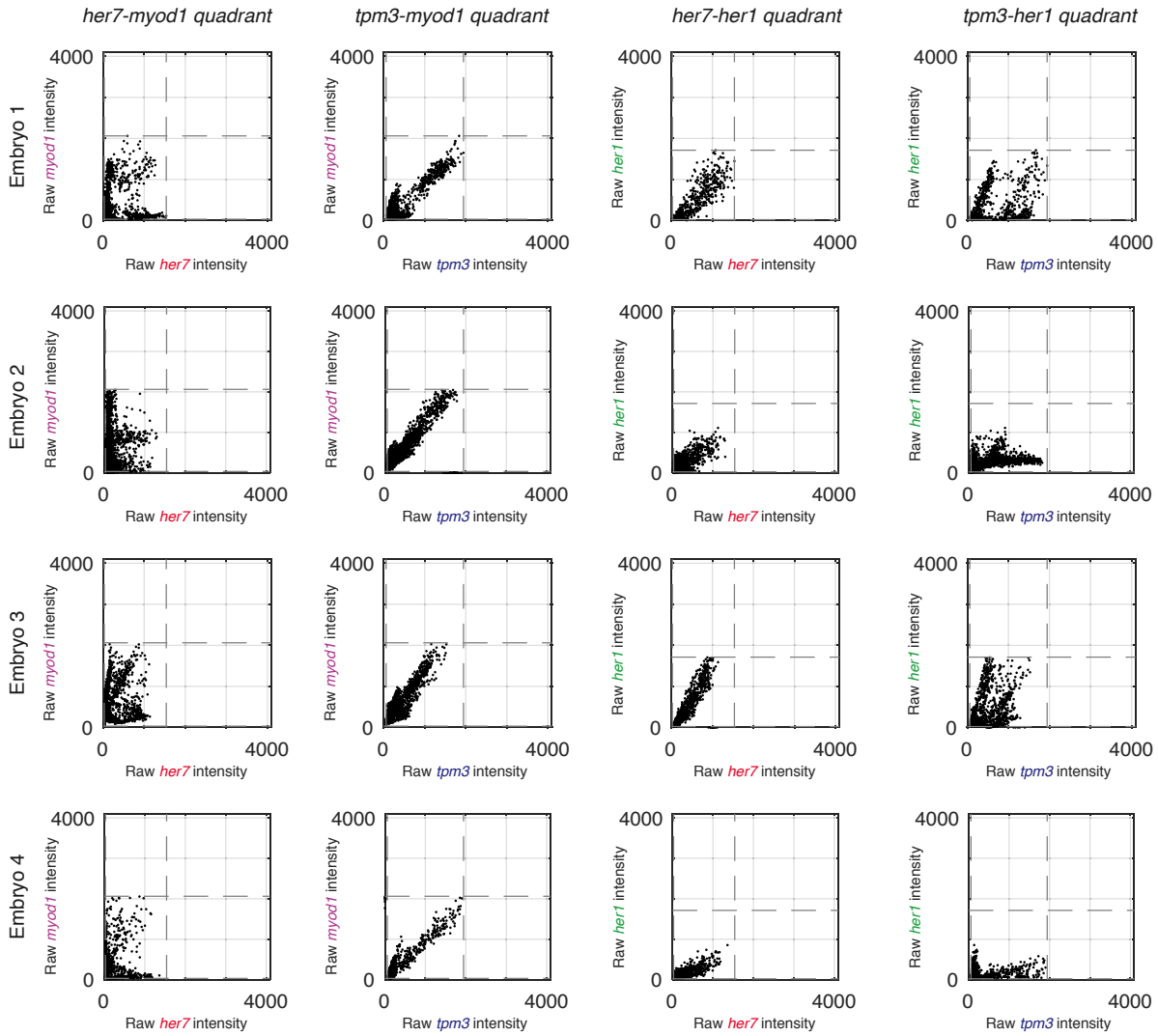

Figure S33. Raw data for read-out and read-in for all embryos (cf. Figures 4 and S34–S40). Raw voxel intensity scatter plots representing signal plus background for the selected regions used for read-out/read-in for Embryos 1–4. Dashed lines denote values tabulated in Table S3 that are used for voxel intensity normalization via the method of Section S1.3.3. Voxel size: $2\times2\times6$ μm.

S2.5.3 Read-out/read-in examples for Embryo 1

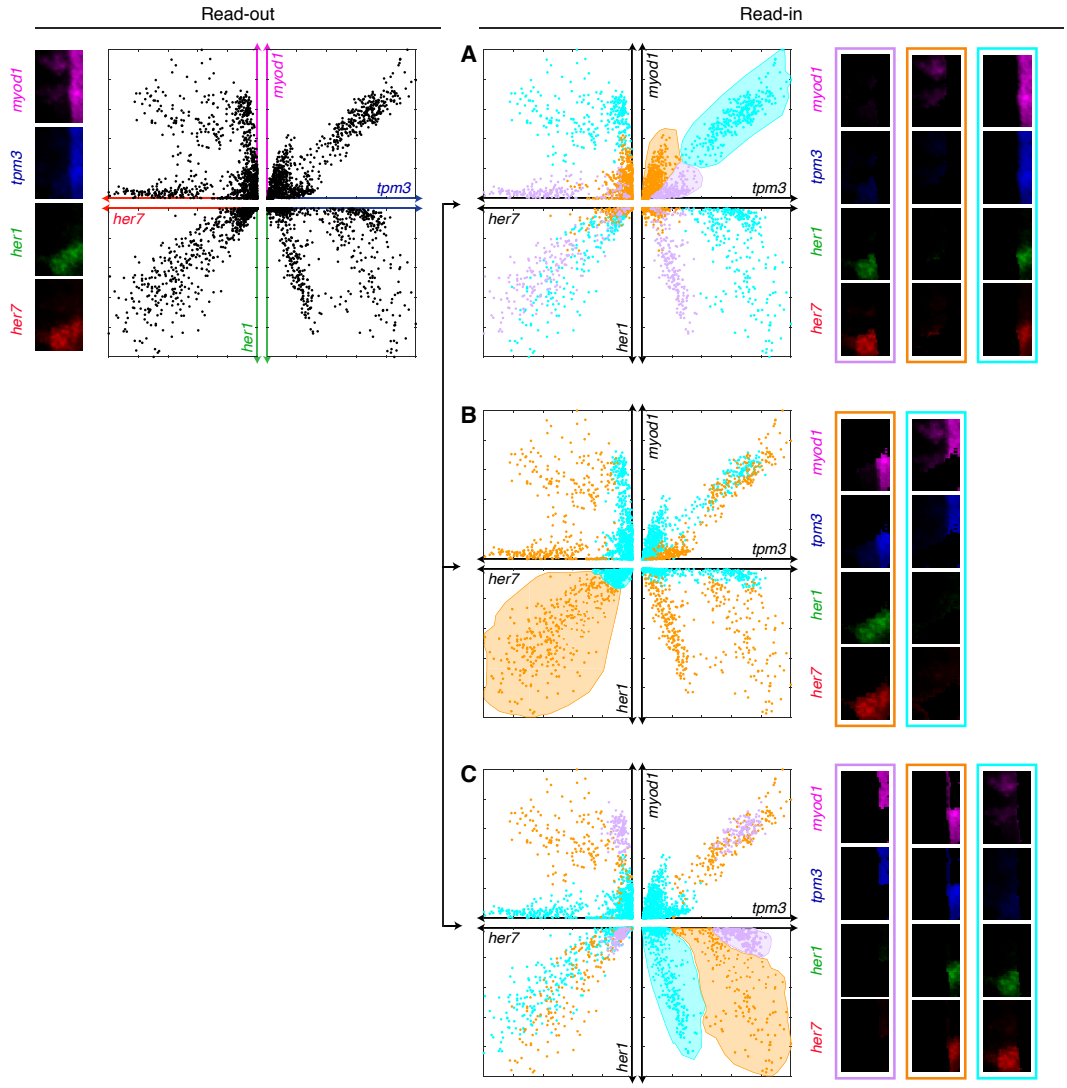

Figure S34. Additional quantitative read-out and read-in examples for Embryo 1 (cf. Figure 4). In contrast to Figure 4CD, where quantitative read-out is followed by selection of expression clusters of interest in the *her7-myod1* quadrant, here expression clusters are selected in either the (A) *tpm3-myod1* quadrant, (B) *her7-her1* quadrant, or (C) *tpm3-her1* quadrant. Quantitative read-in then automatically segments the 4-channel image to reveal the corresponding anatomical loci within the embryo.

S2.5.4 Read-out/read-in examples for Embryo 2

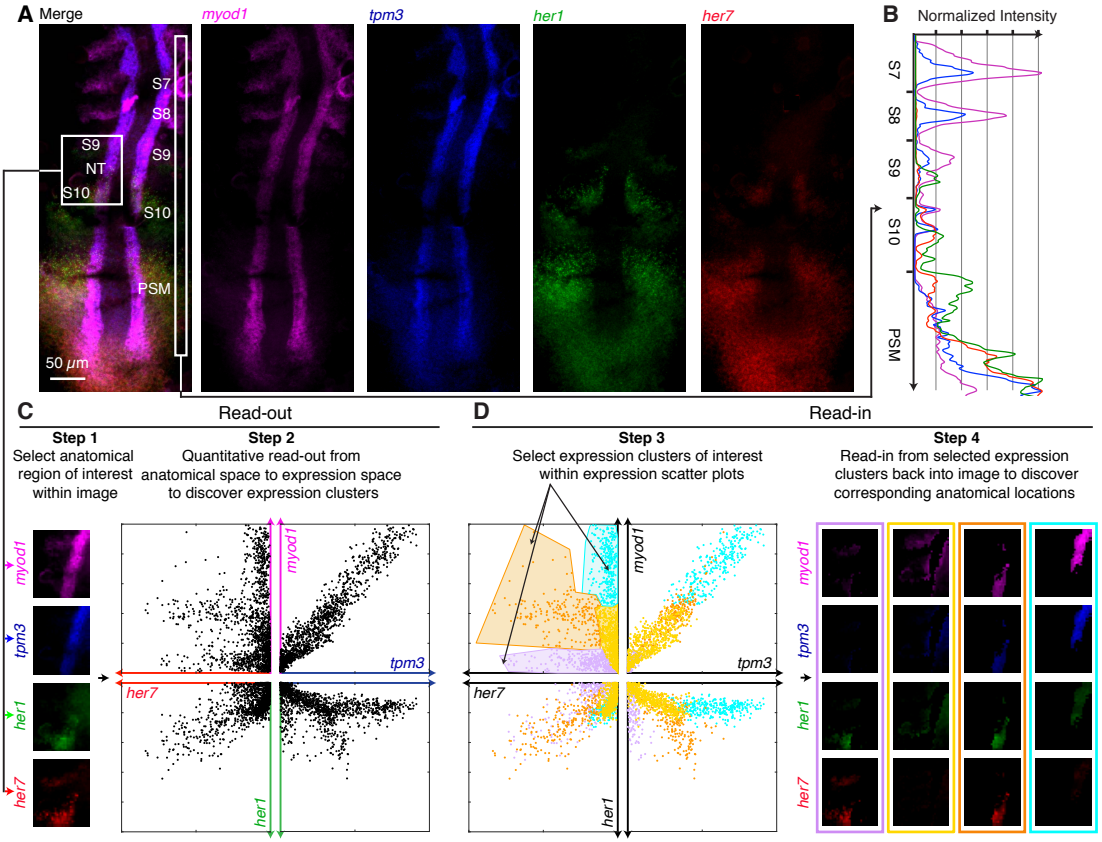

Figure S35. Quantitative read-out and read-in for Embryo 2 (cf. Figure 4). (A) Four-channel quantitative expression map for four target mRNAs in a whole-mount zebrafish embryo. For each channel, a mean intensity image is shown for a stack of five optical sections selected based on the expression depth of the corresponding target mRNA. Confocal microscopy. Embryo fixed 10 hpf. Pixel size: 0.7×0.7 μm. (B) Normalized expression profiles for four target mRNAs along a strip of interest (see panel A) crossing four somites (S7, S8, S9, S10) and the presomitic mesoderm (PSM). (C) Read-out from a region of interest (see panel A) within a 4-channel image (left) to pairwise expression scatter plots (right), revealing distinct expression clusters with different slopes and amplitudes. Each point within an expression scatter plot represents normalized voxel intensities for a pair of target mRNAs. Voxel size: 2×2×6 μm. (D) Read-in from expression clusters selected in the *her7-myod1* quadrant (left) back into the embryo (right), automatically segmenting the 4-channel image to reveal the corresponding anatomical loci. Lavender, yellow, orange, and cyan cluster shading is propagated into the other three quadrants.

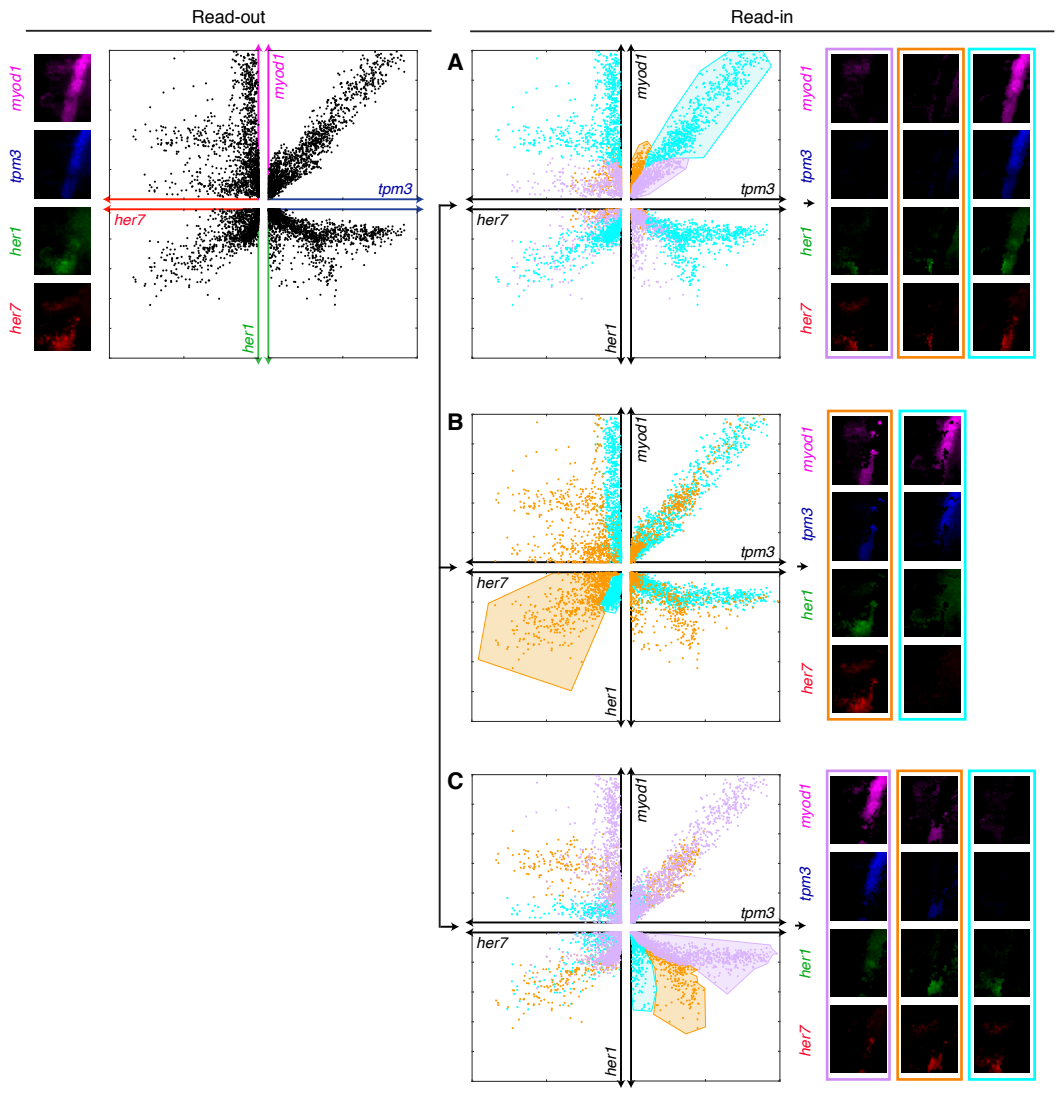

Figure S36. Additional quantitative read-out and read-in examples for Embryo 2 (cf. Figure S35). In contrast to Figure S35CD, where quantitative read-out is followed by selection of expression clusters of interest in the *her7-myod1* quadrant, here expression clusters are selected in either the (A) *tpm3-myod1* quadrant, (B) *her7-her1* quadrant, or (C) *tpm3-her1* quadrant. Quantitative read-in then automatically segments the 4-channel image to reveal the corresponding anatomical loci within the embryo. Voxel intensities are re-normalized within each segmented image to emphasize local expression features within each segmentation.

S2.5.5 Read-out/read-in examples for Embryo 3

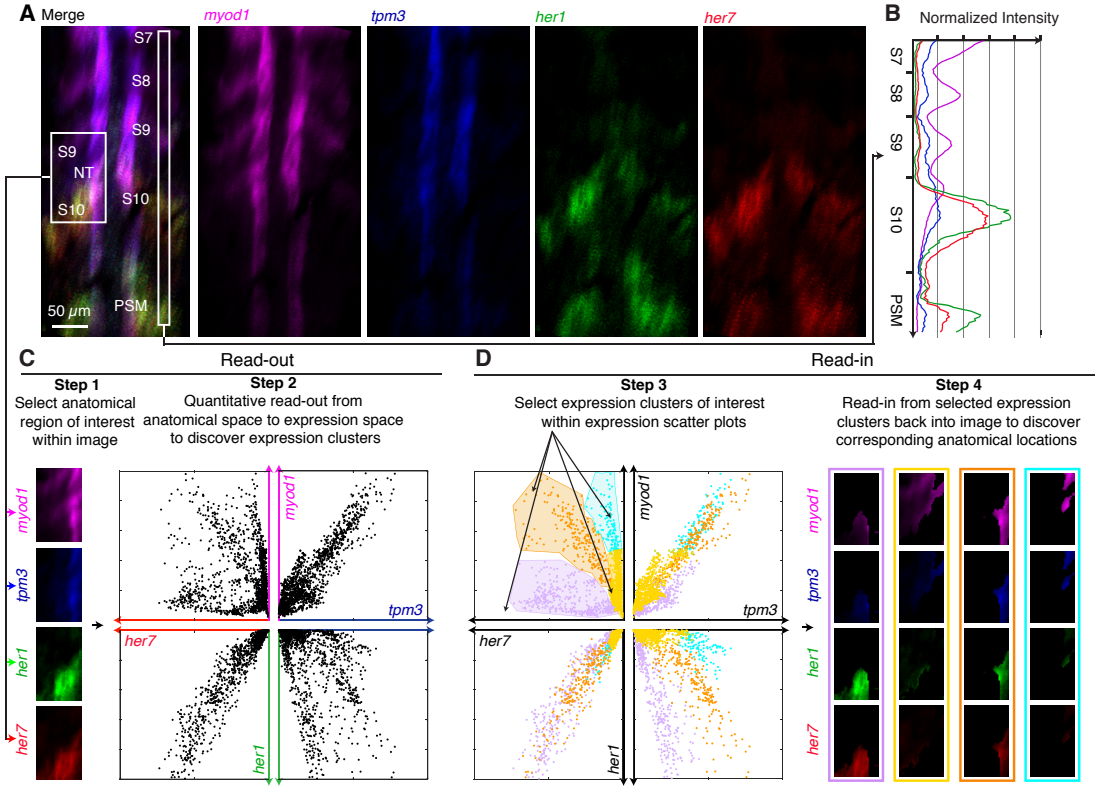

Figure S37. Quantitative read-out and read-in for Embryo 3 (cf. Figure 4). (A) Four-channel quantitative expression map for four target mRNAs in a whole-mount zebrafish embryo. For each channel, a mean intensity image is shown for a stack of five optical sections selected based on the expression depth of the corresponding target mRNA. Confocal microscopy. Embryo fixed 10 hpf. Pixel size: 0.7×0.7 μm. (B) Normalized expression profiles for four target mRNAs along a strip of interest (see panel A) crossing four somites (S7, S8, S9, S10) and the presomitic mesoderm (PSM). (C) Read-out from a region of interest (see panel A) within a 4-channel image (left) to pairwise expression scatter plots (right), revealing distinct expression clusters with different slopes and amplitudes. Each point within an expression scatter plot represents normalized voxel intensities for a pair of target mRNAs. Voxel size: 2×2×6 μm. (D) Read-in from expression clusters selected in the *her7-myod1* quadrant (left) back into the embryo (right), automatically segmenting the 4-channel image to reveal the corresponding anatomical loci. Lavender, yellow, orange, and cyan cluster shading is propagated into the other three quadrants.Voxel intensities are re-normalized within each segmented image to emphasize local expression features within each segmentation.

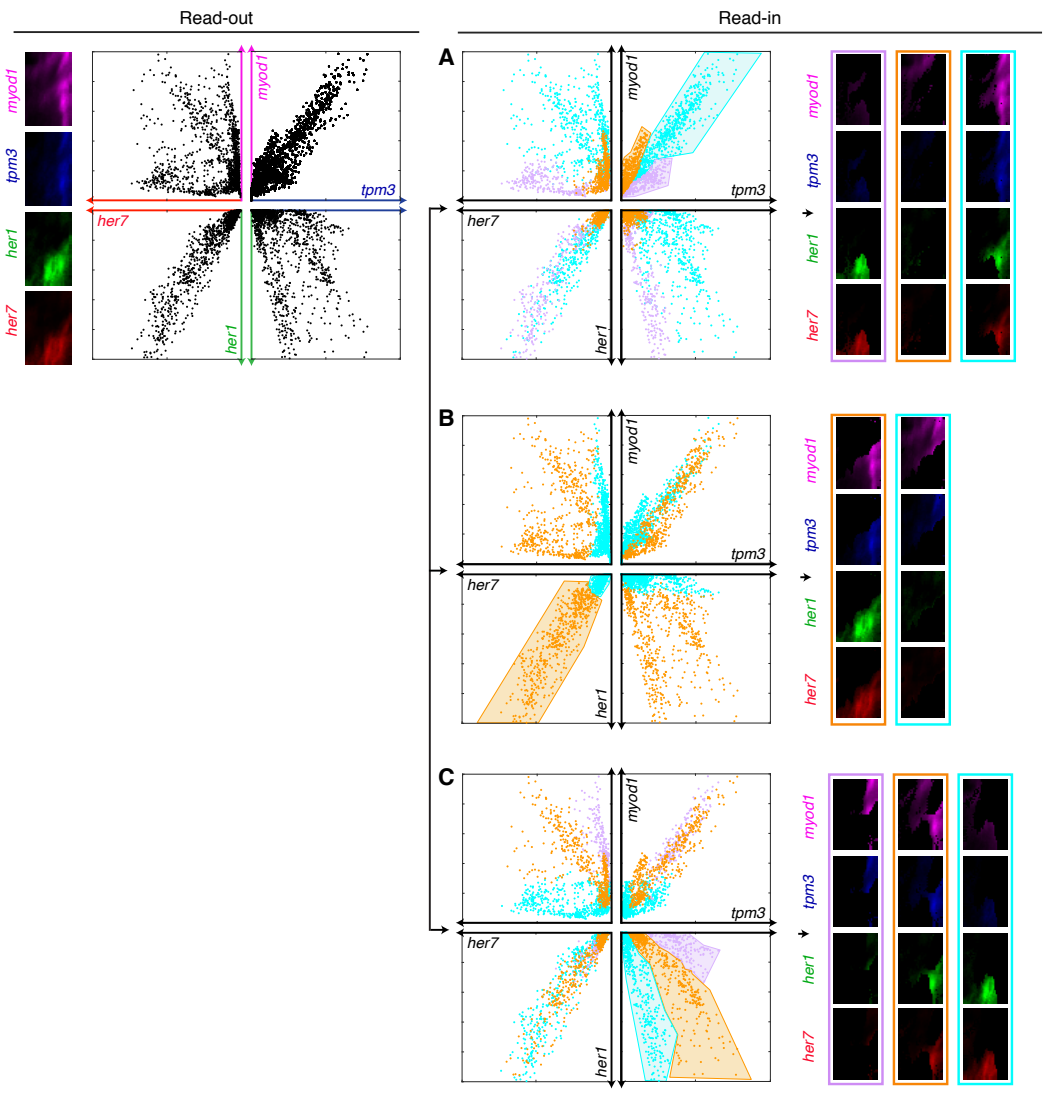

Figure S38. Additional quantitative read-out and read-in examples for Embryo 3 (cf. Figure S37). In contrast to Figure S37CD, where quantitative read-out is followed by selection of expression clusters of interest in the *her7-myod1* quadrant, here expression clusters are selected in either the (A) *tpm3-myod1* quadrant, (B) *her7-her1* quadrant, or (C) *tpm3-her1* quadrant. Quantitative read-in then automatically segments the 4-channel image to reveal the corresponding anatomical loci within the embryo.

S2.5.6 Read-out/read-in examples for Embryo 4

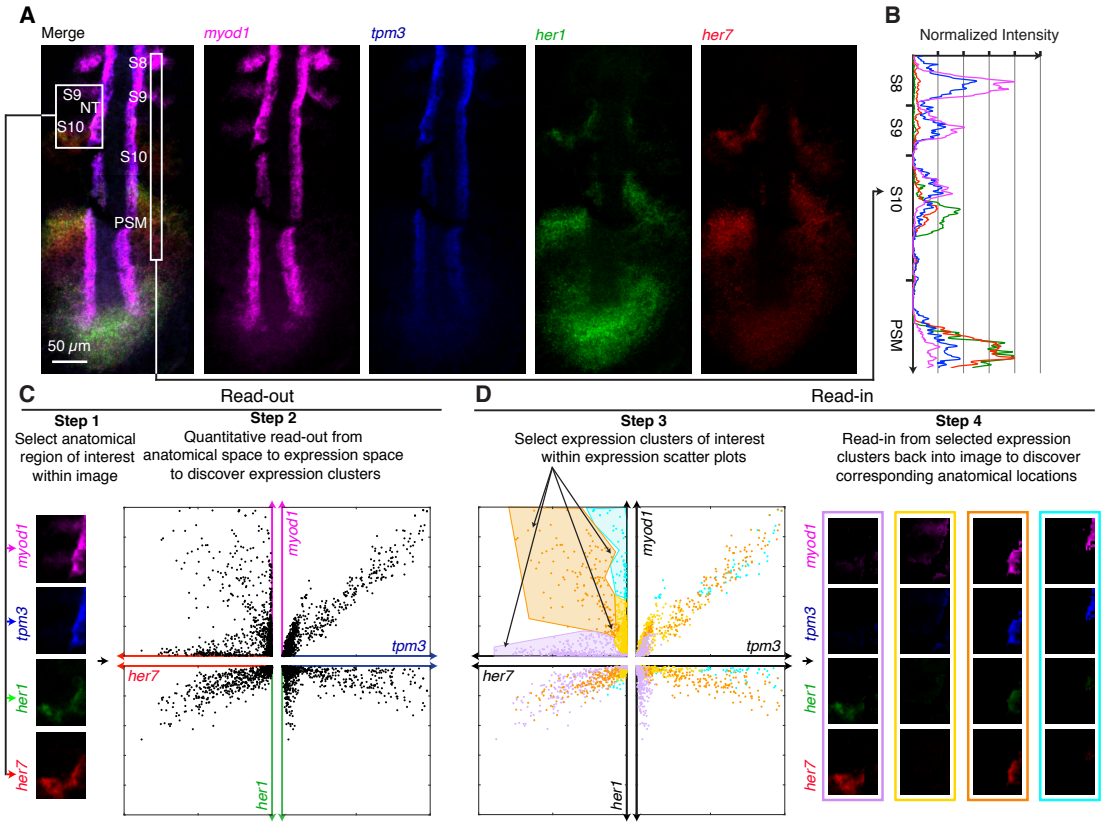

Figure S39. Quantitative read-out and read-in for Embryo 4 (cf. Figure 4). (A) Four-channel quantitative expression map for four target mRNAs in a whole-mount zebrafish embryo. For each channel, a mean intensity image is shown for a stack of five optical sections selected based on the expression depth of the corresponding target mRNA. Confocal microscopy. Embryo fixed 10 hpf. Pixel size: 0.7×0.7 μm. (B) Normalized expression profiles for four target mRNAs along a strip of interest (see panel A) crossing three somites (S8, S9, S10) and the presomitic mesoderm (PSM). (C) Read-out from a region of interest (see panel A) within a 4-channel image (left) to pairwise expression scatter plots (right), revealing distinct expression clusters with different slopes and amplitudes. Each point within an expression scatter plot represents normalized voxel intensities for a pair of target mRNAs. Voxel size: 2×2×6 μm. (D) Read-in from expression clusters selected in the *her7-myod1* quadrant (left) back into the embryo (right), automatically segmenting the 4-channel image to reveal the corresponding anatomical loci. Lavender, yellow, orange, and cyan cluster shading is propagated into the other three quadrants.Voxel intensities are re-normalized within each segmented image to emphasize local expression features within each segmentation.

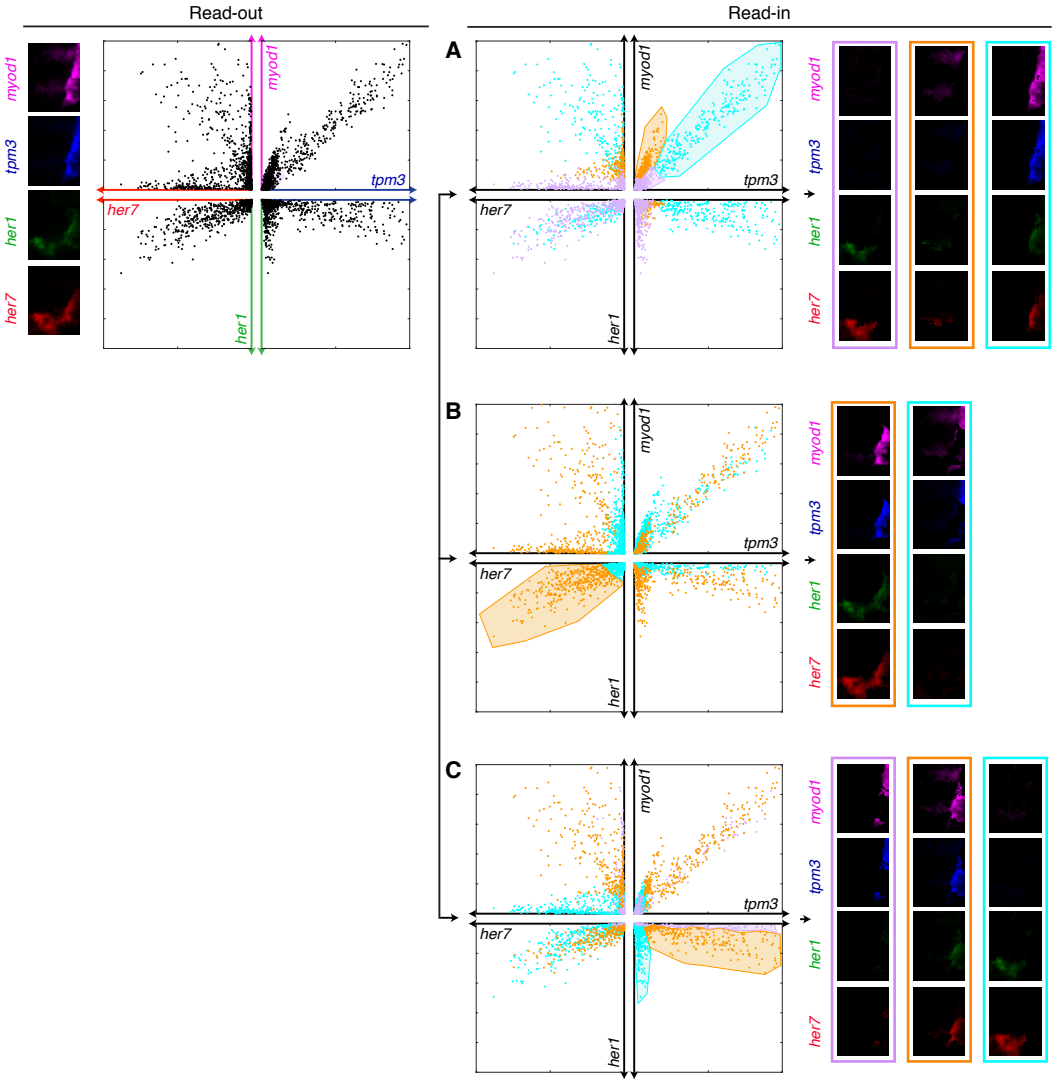

Figure S40. Additional quantitative read-out and read-in examples for Embryo 4 (cf. Figure S39). In contrast to Figure S39CD, where quantitative read-out is followed by selection of expression clusters of interest in the *her7-myod1* quadrant, here expression clusters are selected in either the (A) *tpm3-myod1* quadrant, (B) *her7-her1* quadrant, or (C) *tpm3-her1* quadrant. Quantitative read-in then automatically segments the 4-channel image to reveal the corresponding anatomical loci within the embryo.

S2.6 Replicates and additional somitogenesis data (cf. Figure 5)

4-channel mean intensity images are used to display expression for 4 target mRNAs. For each channel, a stack of five optical sections was selected based on the expression depth of the corresponding mRNA. Different regions of the same mean intensity images are analyzed for Figures 4, 5, and S29–S47. Expression scatter plots are presented using normalized voxel intensities for each channel (see Section S1.3.3 for definitions). For a given channel, the normalization process translates and rescales all voxel intensities identically across replicates, enabling comparison of amplitudes and slopes within expression scatter plots for different embryos. The following studies are presented:

- Section S2.6.1 presents the raw voxel intensity scatter plots used for the somitogenesis studies of Figures 5 and S42–S47.
- Section S2.6.2 compares expression scatter plots for left and right somites for each of four replicate embryos. Assuming that somitogenesis is symmetrical and that comparable regions are analyzed in the left and right somites, the resulting left and right scatter plots serve as technical replicates within each embryo.
- Sections S2.6.3–S2.6.6 present detailed expression scatter plots (all 6 pairwise combinations of 4 target mRNAs) for left and right somites in four embryos.
- Section S2.6.7 presents subcircuit scatter plots for left and right somites in four embryos.

S2.6.1 Raw data for somitogenesis studies

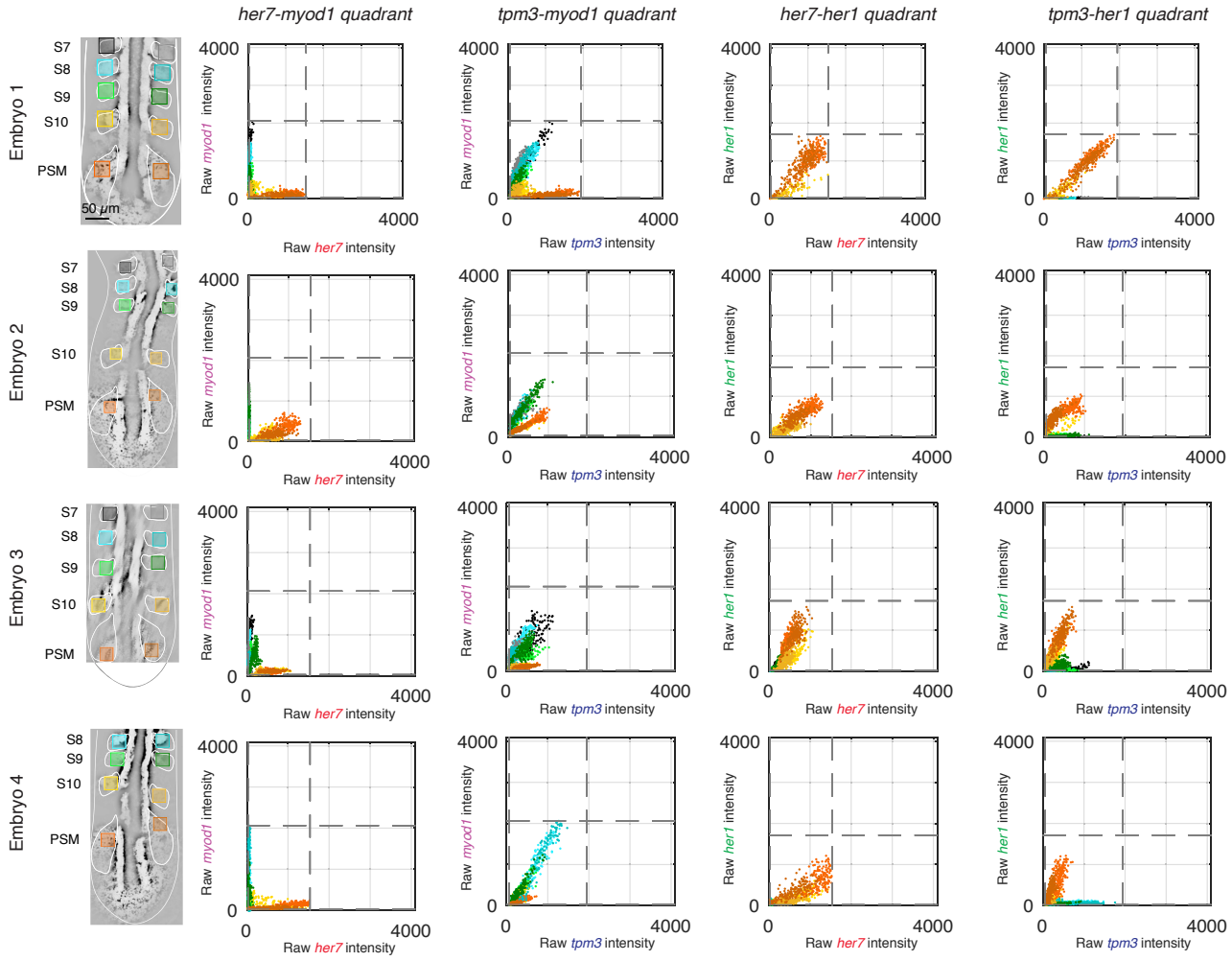

Figure S41. Raw data for somitogenesis for all embryos (cf. Figure 5). Raw voxel intensity scatter plots representing signal plus background for the selected regions of the image used for somitogenesis study in each embryo. Dashed lines denote values tabulated in Table S3 that are used for voxel intensity normalization via the method of Section S1.3.3. Voxel size: $2\times2\times6$ μm.

S2.6.2 Expression scatter plots for left and right somites for Embryos 1–4

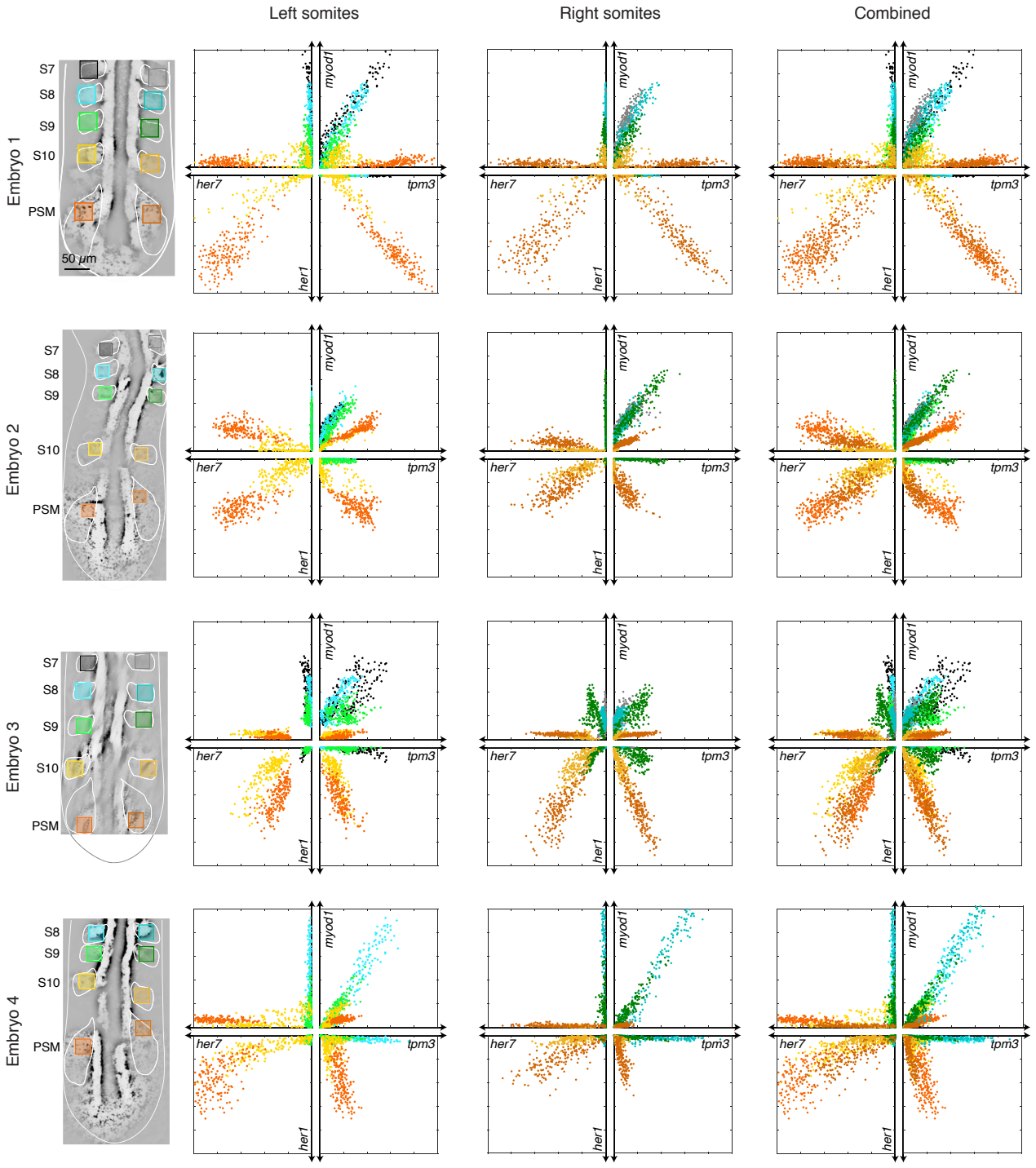

Figure S42. Expression scatter plots for left and right somites for Embryos 1–4 (cf. Figure 5B). Expression clusters are shaded based on regulatory locus within the embryo (grayscale merge of four channels depicting left or right somites S7, S8, S9, S10 and left or right presomitic mesoderm (PSM); Embryo 4 does not include S7). Confocal microscopy. Mean intensity image. Voxel size: 2×2×6 μm. Embryo fixed 10 hpf.

S2.6.3 Detailed expression scatter plots for Embryo 1

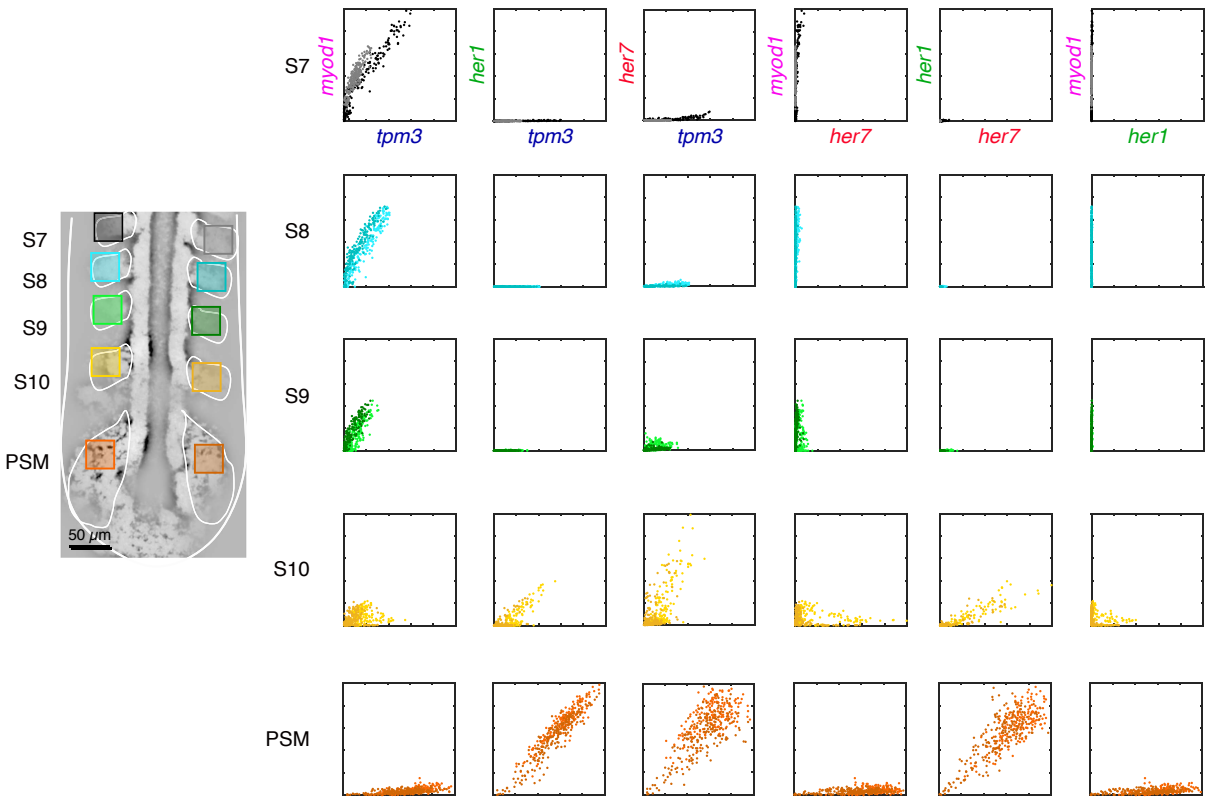

Figure S43. Detailed expression scatter plots for four target mRNAs for Embryo 1 (cf. Figure 5B): all six pairwise combinations for four target mRNAs for left and right somites. Expression clusters are shaded based on regulatory locus within the embryo, revealing different slopes and amplitudes for somites S7, S8, S9, S10, and the presomitic mesoderm (PSM). Confocal microscopy. Mean intensity image. Voxel size: $2\times2\times6$ μm. Embryo fixed 10 hpf.

S2.6.4 Detailed expression scatter plots for Embryo 2

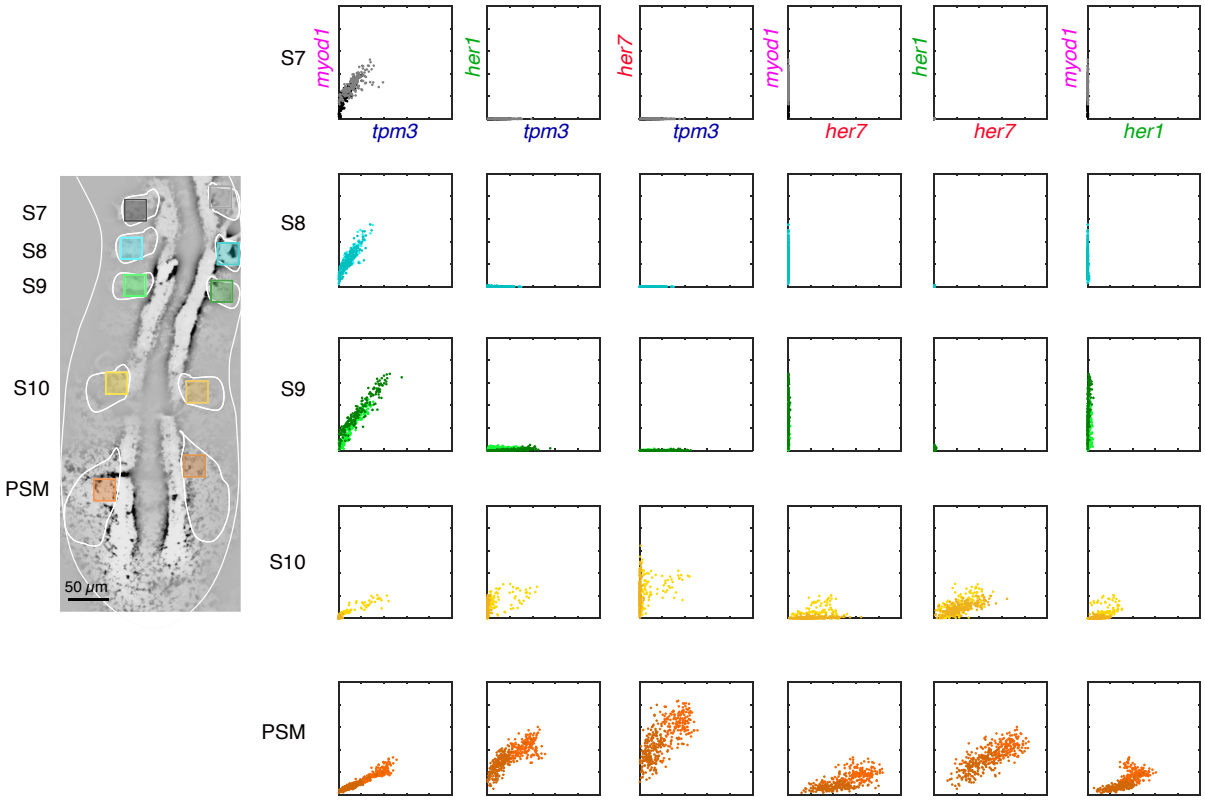

Figure S44. Detailed expression scatter plots for four target mRNAs for Embryo 2 (cf. Figure 5B): all six pairwise combinations for four target mRNAs for left and right somites. Expression clusters are shaded based on regulatory locus within the embryo, revealing different slopes and amplitudes for somites S7, S8, S9, S10, and the presomitic mesoderm (PSM). Confocal microscopy. Mean intensity image. Voxel size: $2\times2\times6$ μm. Embryo fixed 10 hpf.

S2.6.5 Detailed expression scatter plots for Embryo 3

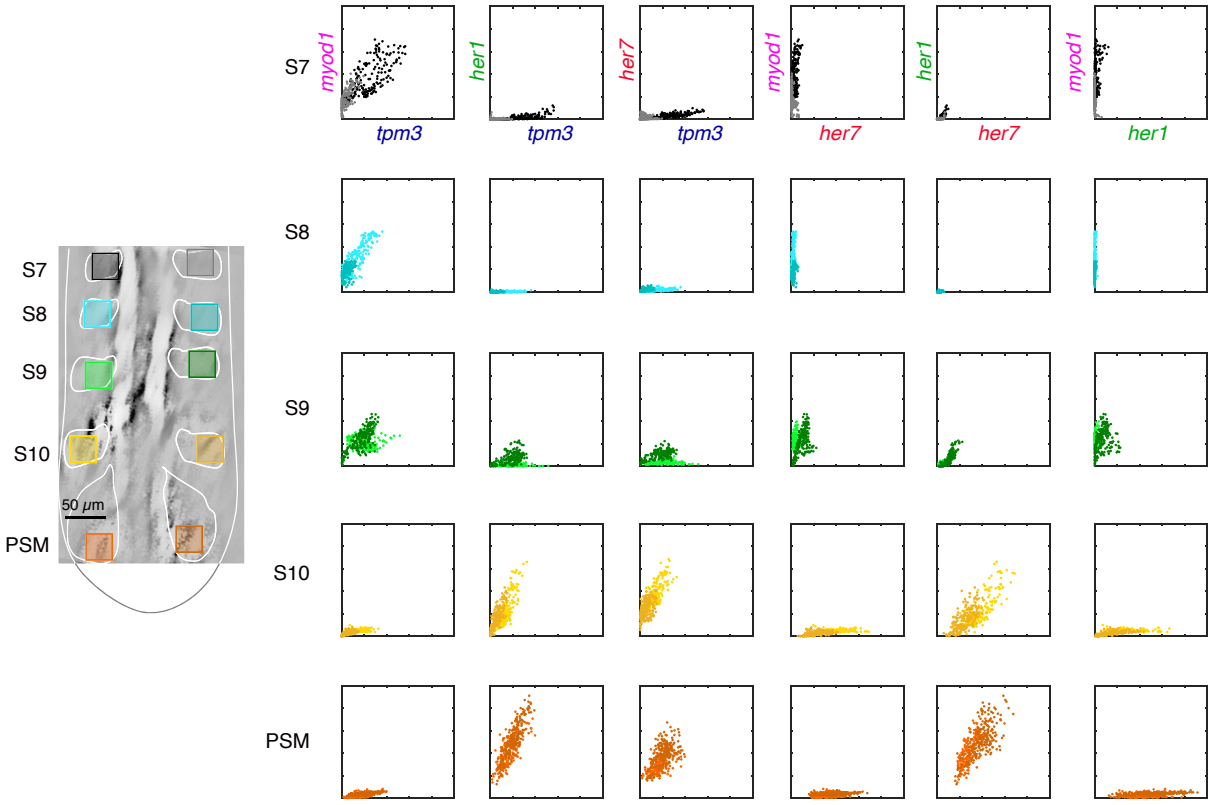

Figure S45. Detailed expression scatter plots for four target mRNAs for Embryo 3 (cf. Figure 5B): all six pairwise combinations for four target mRNAs for left and right somites. Expression clusters are shaded based on regulatory locus within the embryo, revealing different slopes and amplitudes for somites S7, S8, S9, S10, and the presomitic mesoderm (PSM). Confocal microscopy. Mean intensity image. Voxel size: $2\times2\times6$ μm. Embryo fixed 10 hpf.

S2.6.6 Detailed expression scatter plots for Embryo 4

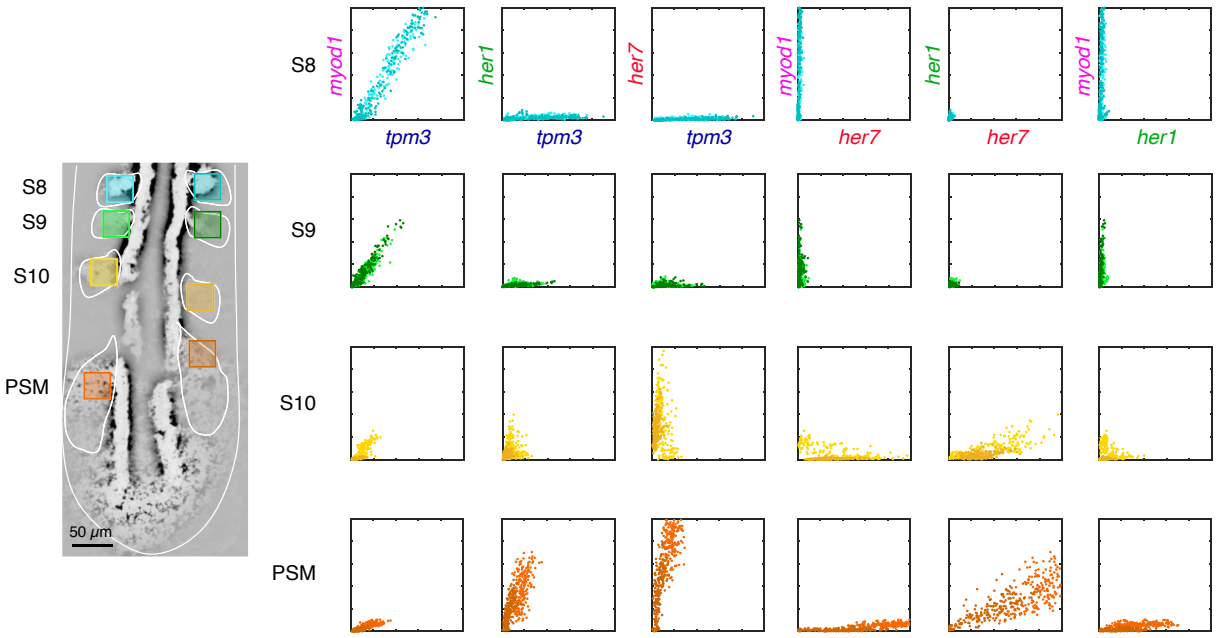

Figure S46. Detailed expression scatter plots for four target mRNAs for Embryo 4 (cf. Figure 5B): all six pairwise combinations for four target mRNAs for left and right somites. Expression clusters are shaded based on regulatory locus within the embryo, revealing different slopes and amplitudes for somites S8, S9, S10, and the presomitic mesoderm (PSM). Confocal microscopy. Mean intensity image. Voxel size: $2\times2\times6$ μm. Embryo fixed 10 hpf.

S2.6.7 Subcircuit scatter plots for left and right somites for Embryos 1–4

For voxel i of replicate embryo n, the amplitude of the *her1-her7* subcircuit is defined by

$$\sqrt{\left[(x_{n,i}^{her1})^2 + (x_{n,i}^{her7})^2\right]/2} \in [0,1],$$

and the amplitude of the *myod1-tpm3* subcircuit is defined by

$$\sqrt{\left[(x_{n,i}^{myod1})^2 + (x_{n,i}^{tpm3})^2\right]/2} \in [0,1].$$

Here, $x_{n,i}^{her1}$ represents the estimated normalized signal for voxel i of replicate n (see Section S1.3.3 for definitions).

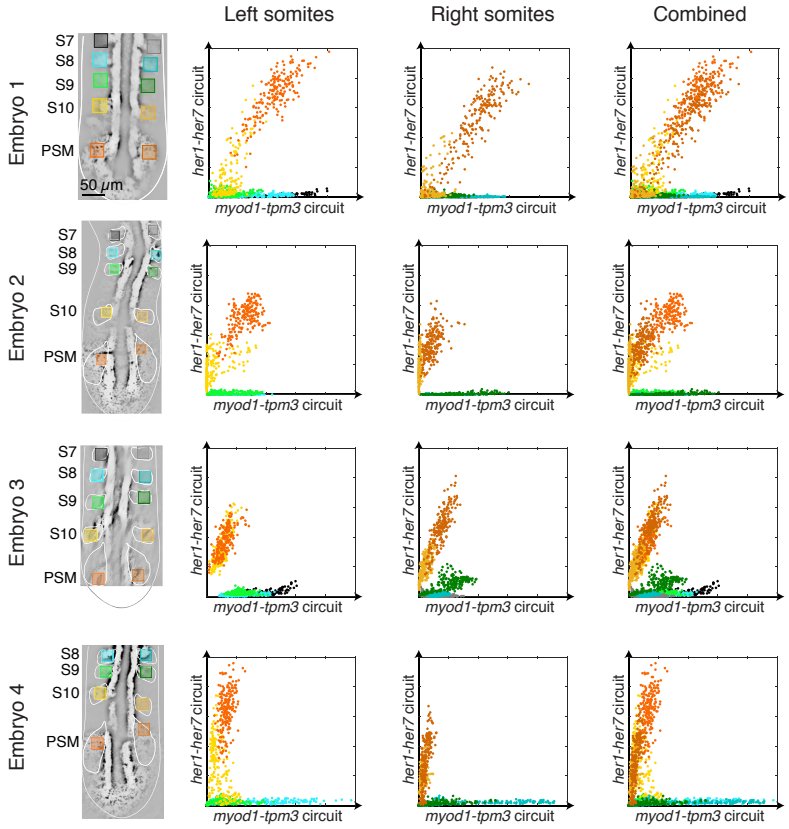

Figure S47. Subcircuit scatter plots for left and right somites for Embryos 1–4 (cf. Figure 5C). Amplitude of *her1-her7* subcircuit vs amplitude of the *myod1-tpm3* subcircuit. Voxels are shaded based on regulatory locus within the embryo (left or right somites S7, S8, S9, S10 and left or right presomitic mesoderm (PSM); Embryo 4 does not include S7). Confocal microscopy. Mean intensity image. Voxel size: 2×2×6 μm. Embryo fixed 10 hpf.

S3 Probe sequences

Each target mRNA is detected using a probe set containing between 2 and 9 DNA probes, each addressing a 50-nt subsequence of the target mRNA. Within a given probe set, each DNA probe carries two initiators for the same DNA HCR amplifier (36 nt initiator + 5 nt spacer + 50 nt mRNA recognition sequence + 5 nt spacer + 36 nt initiator = 132 nt total). Sequences are listed $5'$ to $3'$. Target sequences were obtained from the National Center for Biotechnology Information (NCBI) (McEntyre & Ostell, 2002). For each target mRNA and channel, details on probe set size, HCR amplifier, and fluorophore are summarized in Table S1. For zebrafish embryos, reference expression patterns are available from the Zebrafish Information Network (ZFIN) (Howe *et al.*, 2013). For mouse embryos, reference expression patterns are available from the EMAGE gene expression database (Richardson *et al.*, 2014).

S3.1 Probes for redundant detection studies of Figure 2

For the 2-channel redundant mapping studies of Figures 2 and S12-S23, each target mRNA is detected with two different probe sets, each carrying initiators for a different HCR amplifier.

S3.1.1 *desma*

For redundant mapping of *desma* in WT zebrafish embryos, one probe set contains 8 probes and one probe set contains 7 probes.

Target mRNA: **desmin a (*desma*)**
Amplifier: **HCR B1**
Fluorophore: **Alexa546**

Initiator I1	Spacer	Probe Sequence	Spacer	Initiator I2
gAggAgggCAgCAAACgggAAgAgTCTTCCTTTACg	ATATT	AggCTgAATATTTCgTgCTCATgACTgggCCTgTTgggTTTgTACgCTgT	ATATA	gCATTCTTTCTTgAggAgggCAgCAAACgggAAgAg
gAggAgggCAgCAAACgggAAgAgTCTTCCTTTACg	ATATT	TCTTggTCACCTCgTAAACTCTggAggTCAgTCTTgAggAgCCAgAggAA	ATATA	gCATTCTTTCTTgAggAgggCAgCAAACgggAAgAg
gAggAgggCAgCAAACgggAAgAgTCTTCCTTTACg	ATATT	TCATTgAggTgCTggAgCTCggCCTTCTCATTAgTACgCgTgTTgAggAA	ATATA	gCATTCTTTCTTgAggAgggCAgCAAACgggAAgAg
gAggAgggCAgCAAACgggAAgAgTCTTCCTTTACg	ATATT	CACCTgTCCgCgCAgCTCTCTCATCTCCTCCTCgTACAgCTCTgCAATAC	ATATA	gCATTCTTTCTTgAggAgggCAgCAAACgggAAgAg
gAggAgggCAgCAAACgggAAgAgTCTTCCTTTACg	ATATT	TAggTTgTCCCTCTCgATCTCCACACgggATCTCTgATTggTCAgTgCCT	ATATA	gCATTCTTTCTTgAggAgggCAgCAAACgggAAgAg
gAggAgggCAgCAAACgggAAgAgTCTTCCTTTACg	ATATT	TCTggTggATCTCCTCTTgAAgTCTgAgCTTTAgTTTCTgTAggTCATCg	ATATA	gCATTCTTTCTTgAggAgggCAgCAAACgggAAgAg
gAggAgggCAgCAAACgggAAgAgTCTTCCTTTACg	ATATT	CATCTTCACATTCAgCAgATCCTggTACTCgCggAggTggCgggCCATCT	ATATA	gCATTCTTTCTTgAggAgggCAgCAAACgggAAgAg
gAggAgggCAgCAAACgggAAgAgTCTTCCTTTACg	ATATT	AgCCTgAggCCATCAgTgAAAATgCAAggCATTCTgTgAAACTCgATCTg	ATATA	gCATTCTTTCTTgAggAgggCAgCAAACgggAAgAg

Target mRNA: **desmin a (*desma*)**
Amplifier: **HCR B3**
Fluorophore: **Alexa647**

Initiator I1	Spacer	Probe Sequence	Spacer	Initiator I2
gTCCCTgCCTCTATATCTCCACTCAACTTTAACCCg	TACAA	TTggCTTCTCTgAgAgCCTCgTTATTCTTgTTCACTgCCTggTTCAAATC	TAAAA	AAAgTCTAATCCgTCCCTgCCTCTATATCTCCACTC
gTCCCTgCCTCTATATCTCCACTCAACTTTAACCCg	TACAA	TCTCgCAggTgTAggACTggAgCTggTgACggAACTgCATggTCTCCTgC	TAAAA	AAAgTCTAATCCgTCCCTgCCTCTATATCTCCACTC
gTCCCTgCCTCTATATCTCCACTCAACTTTAACCCg	TACAA	TgAAACCTTAgACTTATACCAgTCCTCggCCTCgCTgATATTCTTggCAg	TAAAA	AAAgTCTAATCCgTCCCTgCCTCTATATCTCCACTC
gTCCCTgCCTCTATATCTCCACTCAACTTTAACCCg	TACAA	CgATAgCCTCgTACTgCAggCgAATgTCTCTgAgggCCgCAgTCAggTCT	TAAAA	AAAgTCTAATCCgTCCCTgCCTCTATATCTCCACTC
gTCCCTgCCTCTATATCTCCACTCAACTTTAACCCg	TACAA	ggTTTggACATgTCCATTTggATCTgCACCTgACTCTCCTgCATCTggTT	TAAAA	AAAgTCTAATCCgTCCCTgCCTCTATATCTCCACTC
gTCCCTgCCTCTATATCTCCACTCAACTTTAACCCg	TACAA	CTgCAgCTCACggATCTCCTCCTCATgAATCTTCCTgAggAATgCAATCT	TAAAA	AAAgTCTAATCCgTCCCTgCCTCTATATCTCCACTC
gTCCCTgCCTCTATATCTCCACTCAACTTTAACCCg	TACAA	CTTCgTgAAgACCCTCgATACgTCTTTCCAggTCCAgCCTggCCAgAgTg	TAAAA	AAAgTCTAATCCgTCCCTgCCTCTATATCTCCACTC

S3.1.2 *citrine*

For redundant mapping of *citrine* in heterozygous transgenic *Gt(desma-citrine)*$^{ct122a/+}$ zebrafish embryos, both probe sets contain 3 probes.

Target mRNA: **citrine fluorescent protein (*citrine*)**
Amplifier: **HCR B2**
Fluorophore: **Alexa546**

Initiator I1	Spacer	Probe Sequence	Spacer	Initiator I2
CCTCgTAAATCCTCATCAATCATCCAgTAAACCgCC	AAAAA	gTTCTTCTgCTTgTCggCCATgATATAgACgTTgTggCTgTTgTAgTTgT	AAAAA	AgCTCAgTCCATCCTCgTAAATCCTCATCAATCATC
CCTCgTAAATCCTCATCAATCATCCAgTAAACCgCC	AAAAA	TTCAgCTCgATgCggTTCACCAgggTgTCgCCCTCgAACTTCACCTCggC	AAAAA	AgCTCAgTCCATCCTCgTAAATCCTCATCAATCATC
CCTCgTAAATCCTCATCAATCATCCAgTAAACCgCC	AAAAA	ACgCTgCCgTCCTCgATgTTgTggCggATCTTgAAgTTCACCTTgATgCC	AAAAA	AgCTCAgTCCATCCTCgTAAATCCTCATCAATCATC

Target mRNA: **citrine fluorescent protein (*citrine*)**
Amplifier: **HCR B3**
Fluorophore: **Alexa647**

Initiator I1	Spacer	Probe Sequence	Spacer	Initiator I2
gTCCCTgCCTCTATATCTCCACTCAACTTTAACCCg	TACAA	gCgggTCTTgTAgTTgCCgTCgTCCTTgAAgAAgATggTgCgCTCCTggA	TAAAA	AAAgTCTAATCCgTCCCTgCCTCTATATCTCCACTC
gTCCCTgCCTCTATATCTCCACTCAACTTTAACCCg	TACAA	CgTAgCCTTCgggCATggCggACTTgAAgAAgTCgTgCTgCTTCATgTgg	TAAAA	AAAgTCTAATCCgTCCCTgCCTCTATATCTCCACTC
gTCCCTgCCTCTATATCTCCACTCAACTTTAACCCg	TACAA	gCggTCACgAACTCCAgCAggACCATgTgATCgCgCTTCTCgTTggggTC	TAAAA	AAAgTCTAATCCgTCCCTgCCTCTATATCTCCACTC

S3.1.3 *elavl3*

For redundant mapping of *elavl3* in WT zebrafish embryos, one probe set contains 5 probes and one probe set contains 4 probes.

Target mRNA: **ELAV like neuron-specific RNA binding protein 3 (*elavl3*)**
Amplifier: **HCR B1**
Fluorophore: **Alexa546**

Initiator I1	Spacer	Probe Sequence	Spacer	Initiator I2
gAggAgggCAgCAAACgggAAgAgTCTTCCTTTACg	ATATT	ggTAgTTgACgATCAggTTAgTTTTgCTgTCATCTgTggCgCCgTTAgTg	ATATA	gCATTCTTTCTTgAggAgggCAgCAAACgggAAgAg
gAggAgggCAgCAAACgggAAgAgTCTTCCTTTACg	ATATT	CTCTggCCTgTgATCTTgTCTCTgACCAATTTgCAggACTCgATTTCCCC	ATATA	gCATTCTTTCTTgAggAgggCAgCAAACgggAAgAg
gAggAgggCAgCAAACgggAAgAgTCTTCCTTTACg	ATATT	CACCTTgATTgTTTTggTCTgCAgTTTgAgACCgTTgAgCgTgTTgATAg	ATATA	gCATTCTTTCTTgAggAgggCAgCAAACgggAAgAg
gAggAgggCAgCAAACgggAAgAgTCTTCCTTTACg	ATATT	AAAACAACTgCTCCATgTCTTTCTgACTCATggTTTTgggCAggCCgCTC	ATATA	gCATTCTTTCTTgAggAgggCAgCAAACgggAAgAg
gAggAgggCAgCAAACgggAAgAgTCTTCCTTTACg	ATATT	gCTTCgTTCCgTTTgTCgAACCgAATgAAACCTACCCCgCgCgATATACC	ATATA	gCATTCTTTCTTgAggAgggCAgCAAACgggAAgAg

Target mRNA: **ELAV like neuron-specific RNA binding protein 3 (*elavl3*)**
Amplifier: **HCR B3**
Fluorophore: **Alexa647**

Initiator I1	Spacer	Probe Sequence	Spacer	Initiator I2
gTCCCTgCCTCTATATCTCCACTCAACTTTAACCCg	TACAA	CTgTCCTgTCTTCTgACTggggTTgTTggCgAACTTTACggTgATgggCT	TAAAA	AAAgTCTAATCCgTCCCTgCCTCTATATCTCCACTC
gTCCCTgCCTCTATATCTCCACTCAACTTTAACCCg	TACAA	TgTCAATggTTATgggggAgAATCTgAAgCgCTgggTCTggTggTgCAgA	TAAAA	AAAgTCTAATCCgTCCCTgCCTCTATATCTCCACTC
gTCCCTgCCTCTATATCTCCACTCAACTTTAACCCg	TACAA	AggACACTTTCgTCAgCTTCCggggACAggTTgTAgACgAAgATgCACCA	TAAAA	AAAgTCTAATCCgTCCCTgCCTCTATATCTCCACTC
gTCCCTgCCTCTATATCTCCACTCAACTTTAACCCg	TACAA	ggTCATggTgACgAAgCCAAAgCCCTTACATTTgTTggTggTgAAgTCAC	TAAAA	AAAgTCTAATCCgTCCCTgCCTCTATATCTCCACTC

S3.1.4 *Acta2*

For redundant mapping of *Acta2* in WT mouse embryos, each probe set contains 2 probes.

Target mRNA: **actin, alpha 2, smooth muscle, aorta (*Acta2*)**
Amplifier: **HCR B2**
Fluorophore: **Alexa546**

Initiator I1	Spacer	Probe Sequence	Spacer	Initiator I2
CCTCgTAAATCCTCATCAATCATCCAgTAAACCgCC	AAAAA	gCCTTAgggTTCAgTggTgCCTCTgTCAgCAgTgTCggATgCTCTTCAgg	AAAAA	AgCTCAgTCCATCCTCgTAAATCCTCATCAATCATC
CCTCgTAAATCCTCATCAATCATCCAgTAAACCgCC	AAAAA	CAACCATTACTCCCTgATgTCTgggACgTCCCACgATggATgggAAAACA	AAAAA	AgCTCAgTCCATCCTCgTAAATCCTCATCAATCATC

Target mRNA: **actin, alpha 2, smooth muscle, aorta (*Acta2*)**
Amplifier: **HCR B1**
Fluorophore: **Alexa647**

Initiator I1	Spacer	Probe Sequence	Spacer	Initiator I2
gAggAgggCAgCAAACgggAAgAgTCTTCCTTTACg	ATATT	CggCCTTACAgAgCCCAgAgCCATTgTCgCACACCAgggCTgTgCTgTCT	ATATA	gCATTCTTTCTTgAggAgggCAgCAAACgggAAgAg
gAggAgggCAgCAAACgggAAgAgTCTTCCTTTACg	ATATT	CTgTTATAggTggTTTCgTggATgCCCgCTgACTCCATCCCAATgAAAgA	ATATA	gCATTCTTTCTTgAggAgggCAgCAAACgggAAgAg

S3.2 Probes for hom/het studies of Figure 3

For 2-channel studies in homozygous transgenic *Gt(desma-citrine)*$^{ct122a/ct122a}$ zebrafish embryos, heterozygous transgenic *Gt(desma-citrine)*$^{ct122a/+}$ zebrafish embryos, and WT zebrafish embryos in Figures 3 and S24–S28, the probe sets for *desma* and *citrine* each contain 5 probes.

S3.2.1 *desma*

Target mRNA: **desmin a (*desma*)**
Amplifier: **HCR B1**
Fluorophore: **Alexa546**

Initiator I1	Spacer	Probe Sequence	Spacer	Initiator I2
gAggAgggCAgCAAACgggAAgAgTCTTCCTTTACg	ATATT	AggCTgAATATTTCgTgCTCATgACTgggCCTgTTgggTTTgTACgCTgT	ATATA	gCATTCTTTCTTgAggAgggCAgCAAACgggAAgAg
gAggAgggCAgCAAACgggAAgAgTCTTCCTTTACg	ATATT	TCTTggTCACCTCgTAAACTCTggAggTCAgTCTTgAggAgCCAgAggAA	ATATA	gCATTCTTTCTTgAggAgggCAgCAAACgggAAgAg
gAggAgggCAgCAAACgggAAgAgTCTTCCTTTACg	ATATT	TCATTgAggTgCTggAgCTCggCCTTCTCATTAgTACgCgTgTTgAggAA	ATATA	gCATTCTTTCTTgAggAgggCAgCAAACgggAAgAg
gAggAgggCAgCAAACgggAAgAgTCTTCCTTTACg	ATATT	CACCTgTCCgCgCAgCTCTCTCATCTCCTCCTCgTACAgCTCTgCAATAC	ATATA	gCATTCTTTCTTgAggAgggCAgCAAACgggAAgAg
gAggAgggCAgCAAACgggAAgAgTCTTCCTTTACg	ATATT	TAggTTgTCCCTCTCgATCTCCACACgggATCTCTgATTggTCAgTgCCT	ATATA	gCATTCTTTCTTgAggAgggCAgCAAACgggAAgAg

S3.2.2 *citrine*

Target mRNA: **citrine fluorescent protein (*citrine*)**
Amplifier: **HCR B2**
Fluorophore: **Alexa647**

Initiator I1	Spacer	Probe Sequence	Spacer	Initiator I2
CCTCgTAAATCCTCATCAATCATCCAgTAAACCgCC	AAAAA	gTTCTTCTgCTTgTCggCCATgATATAgACgTTgTggCTgTTgTAgTTgT	AAAAA	AgCTCAgTCCATCCTCgTAAATCCTCATCAATCATC
CCTCgTAAATCCTCATCAATCATCCAgTAAACCgCC	AAAAA	TTCAgCTCgATgCggTTCACCAgggTgTCgCCCTCgAACTTCACCTCggC	AAAAA	AgCTCAgTCCATCCTCgTAAATCCTCATCAATCATC
CCTCgTAAATCCTCATCAATCATCCAgTAAACCgCC	AAAAA	ACgCTgCCgTCCTCgATgTTgTggCggATCTTgAAgTTCACCTTgATgCC	AAAAA	AgCTCAgTCCATCCTCgTAAATCCTCATCAATCATC
CCTCgTAAATCCTCATCAATCATCCAgTAAACCgCC	AAAAA	gCgggTCTTgTAgTTgCCgTCgTCCTTgAAgAAgATggTgCgCTCCTggA	AAAAA	AgCTCAgTCCATCCTCgTAAATCCTCATCAATCATC
CCTCgTAAATCCTCATCAATCATCCAgTAAACCgCC	AAAAA	CgTAgCCTTCgggCATggCggACTTgAAgAAgTCgTgCTgCTTCATgTgg	AAAAA	AgCTCAgTCCATCCTCgTAAATCCTCATCAATCATC

S3.3 Probes for read-out/read-in studies of Figures 4 and 5

For 4-channel studies in WT zebrafish embryos in Figures 4, 5 and S29–S46, the probe sets for *myoD*, *tpm3*, *her1*, and *her7* contain 5, 2, 5, and 5 probes, respectively.

S3.3.1 *myod1*

Target mRNA: **myogenic differentiation 1 (*myod1*)**
Amplifier: **HCR B4**
Fluorophore: **Alexa647**

Initiator I1	Spacer	Probe Sequence	Spacer	Initiator I2
CCTCAACCTACCTCCAACTCTCACCATATTCGCTTC	TAAAA	ATAgCTgTTCCgTCTTCTCgTCTgACACgTTgggCCCATAAAATCCATCA	ATTTT	CACATTTACAGACCTCAACCTACCTCCAACTCTCAC
CCTCAACCTACCTCCAACTCTCACCATATTCGCTTC	TAAAA	gTgATgCTCgTCgggTTTgAgCAggCTCACgTgAACAAgCCTggggTCCA	ATTTT	CACATTTACAGACCTCAACCTACCTCCAACTCTCAC
CCTCAACCTACCTCCAACTCTCACCATATTCGCTTC	TAAAA	ACgggCTCTCTTCgTgCCCCTCCggTACTgACAgCACgggACATgCAggA	ATTTT	CACATTTACAGACCTCAACCTACCTCCAACTCTCAC
CCTCAACCTACCTCCAACTCTCACCATATTCGCTTC	TAAAA	CTgATgggATggggAAggggATATCCgACAACTCCATCTTTTTTgTgTTA	ATTTT	CACATTTACAGACCTCAACCTACCTCCAACTCTCAC
CCTCAACCTACCTCCAACTCTCACCATATTCGCTTC	TAAAA	AgAAgTgCATgTCgTTggTgTTgAAgCAAgggTCgTCgTAgAAgTCATCA	ATTTT	CACATTTACAGACCTCAACCTACCTCCAACTCTCAC

S3.3.2 *tpm3*

Target mRNA: **tropomyosin 3 (*tpm3*)**
Amplifier: **HCR B1**
Fluorophore: **Alexa488**

Initiator I1	Spacer	Probe Sequence	Spacer	Initiator I2
gAggAgggCAgCAAACgggAAgAgTCTTCCTTTACg	ATATT	AATCACCTTCATCCCTCTCTCgCTCTCATCTgCggCCTTCTCggCTTCCT	ATATA	gCATTCTTTCTTgAggAgggCAgCAAACgggAAgAg
gAggAgggCAgCAAACgggAAgAgTCTTCCTTTACg	ATATT	TggATCTCCTgCAgCTCCATCTTCTCCTCATCCTTCAgAgCCCTgTTCTC	ATATA	gCATTCTTTCTTgAggAgggCAgCAAACgggAAgAg

S3.3.3 *her1*

Target mRNA: **hairy-related 1 (*her1*)**
Amplifier: **HCR B3**
Fluorophore: **Alexa514**

Initiator I1	Spacer	Probe Sequence	Spacer	Initiator I2
GTCCCTGCCTCTATATCTCCACTCAACTTTAACCCG	TACAA	gATTgTggAACAgCgCTCgTCTCAgAgTCCgTggTTgAgAggATTgAACA	TAAAA	AAAGTCTAATCCGTCCCTGCCTCTATATCTCCACTC
GTCCCTGCCTCTATATCTCCACTCAACTTTAACCCG	TACAA	ggACTCAAgTTATACAgCAAAgACCCCAgAACACATgCATgCACTCTgAA	TAAAA	AAAGTCTAATCCGTCCCTGCCTCTATATCTCCACTC
GTCCCTGCCTCTATATCTCCACTCAACTTTAACCCG	TACAA	CTgTAggAgTCgAgATgATggCAgAgACCTTggACgAAgCTgTCTCgCTg	TAAAA	AAAGTCTAATCCGTCCCTGCCTCTATATCTCCACTC
GTCCCTGCCTCTATATCTCCACTCAACTTTAACCCG	TACAA	TgggATCCATggATggTgggTTggATTgCTggAAACTCTgCCgTggggAA	TAAAA	AAAGTCTAATCCGTCCCTGCCTCTATATCTCCACTC
GTCCCTGCCTCTATATCTCCACTCAACTTTAACCCG	TACAA	ATgCggAgAgATgCTgggAgggAACgggAATTggCAgggCACAgAgAgAT	TAAAA	AAAGTCTAATCCGTCCCTGCCTCTATATCTCCACTC

S3.3.4 *her7*

Target mRNA: **hairy and enhancer of split related-7 (*her7*)**
Amplifier: **HCR B2**
Fluorophore: **Alexa546**

Initiator I1	Spacer	Probe Sequence	Spacer	Initiator I2
CCTCgTAAATCCTCATCAATCATCCAgTAAACCgCC	AAAAA	TCTgTgCCAggATTTTCATTgCACgTgTACTCCAATAgTTgATATCAATg	AAAAA	AgCTCAgTCCATCCTCgTAAATCCTCATCAATCATC
CCTCgTAAATCCTCATCAATCATCCAgTAAACCgCC	AAAAA	AgTCTgATggTggggTgAgCAAgACgTTgACACAgCATggATgTgACCgA	AAAAA	AgCTCAgTCCATCCTCgTAAATCCTCATCAATCATC
CCTCgTAAATCCTCATCAATCATCCAgTAAACCgCC	AAAAA	TgCTgTgggTTggATTCTgCgTgCTgCTTTCTggAgTgACCTCTgACAgg	AAAAA	AgCTCAgTCCATCCTCgTAAATCCTCATCAATCATC
CCTCgTAAATCCTCATCAATCATCCAgTAAACCgCC	AAAAA	gggAggTTggTTgAgCTgTCgAATgCTTTgTgTTggAgTCTgTgCTTCTg	AAAAA	AgCTCAgTCCATCCTCgTAAATCCTCATCAATCATC
CCTCgTAAATCCTCATCAATCATCCAgTAAACCgCC	AAAAA	gCAgAAgTTTCAggTTTTCTAgACTCCggTTCATCCTTTCTCTTCTACgT	AAAAA	AgCTCAgTCCATCCTCgTAAATCCTCATCAATCATC

S3.4 Probes for penetration/hybridization controls of Figures S1 and S2

For 2-channel studies in heterozygous transgenic *Gt(desma-citrine)*$^{ct122a/+}$ zebrafish embryos in Figures S1 and S2, the probe sets for *citrine* and *ta* contain 5 and 9 probes, respectively.

S3.4.1 *citrine*

Target mRNA: **citrine fluorescent protein (*citrine*)**
Amplifier: **HCR B2**
Fluorophore: **Alexa647**

Initiator I1	Spacer	Probe Sequence	Spacer	Initiator I2
CCTCgTAAATCCTCATCAATCATCCAgTAAACCgCC	AAAAA	gTTCTTCTgCTTgTCggCCATgATATAgACgTTgTggCTgTTgTAgTTgT	AAAAA	AgCTCAgTCCATCCTCgTAAATCCTCATCAATCATC
CCTCgTAAATCCTCATCAATCATCCAgTAAACCgCC	AAAAA	TTCAgCTCgATgCggTTCACCAgggTgTCgCCCTCgAACTTCACCTCggC	AAAAA	AgCTCAgTCCATCCTCgTAAATCCTCATCAATCATC
CCTCgTAAATCCTCATCAATCATCCAgTAAACCgCC	AAAAA	ACgCTgCCgTCCTCgATgTTgTggCggATCTTgAAgTTCACCTTgATgCC	AAAAA	AgCTCAgTCCATCCTCgTAAATCCTCATCAATCATC
CCTCgTAAATCCTCATCAATCATCCAgTAAACCgCC	AAAAA	gCgggTCTTgTAgTTgCCgTCgTCCTTgAAgAAgATggTgCgCTCCTggA	AAAAA	AgCTCAgTCCATCCTCgTAAATCCTCATCAATCATC
CCTCgTAAATCCTCATCAATCATCCAgTAAACCgCC	AAAAA	CgTAgCCTTCgggCATggCggACTTgAAgAAgTCgTgCTgCTTCATgTgg	AAAAA	AgCTCAgTCCATCCTCgTAAATCCTCATCAATCATC

S3.4.2 *ta*

Target mRNA: **T, brachyury homolog a (*ta*)**
Amplifier: **HCR B1**
Fluorophore: **Alexa546**

Initiator I1	Spacer	Probe Sequence	Spacer	Initiator I2
gAggAgggCAgCAAACgggAAgAgTCTTCCTTTACg	ATATT	TCAAATAAAgCTTgAgATAAgTCCgACgATCCTACTAAATCCCgTTggAT	ATATA	gCATTCTTTCTTgAggAgggCAgCAAACgggAAgAg
gAggAgggCAgCAAACgggAAgAgTCTTCCTTTACg	ATATT	CATTCgTCTCCCAgTCTTggTgACAATCATTTCATTggTgAgCTCTTTAA	ATATA	gCATTCTTTCTTgAggAgggCAgCAAACgggAAgAg
gAggAgggCAgCAAACgggAAgAgTCTTCCTTTACg	ATATT	CgTATTTCCACCgATTATTATCggCCgCCACAAAATCCAgCAggACCgAg	ATATA	gCATTCTTTCTTgAggAgggCAgCAAACgggAAgAg
gAggAgggCAgCAAACgggAAgAgTCTTCCTTTACg	ATATT	gTgTATCCTgggTTCgTATTTgTgCAATgAgTTTAACATAATCTgTCCTC	ATATA	gCATTCTTTCTTgAggAgggCAgCAAACgggAAgAg
gAggAgggCAgCAAACgggAAgAgTCTTCCTTTACg	ATATT	TgTAgTTATTggTggTAgTgCTgCggTgggAgTAATggCTgggATATggA	ATATA	gCATTCTTTCTTgAggAgggCAgCAAACgggAAgAg
gAggAgggCAgCAAACgggAAgAgTCTTCCTTTACg	ATATT	gTgTTTgTggTgTgggCCAgggTTCCCATCCCgCTggAgTTggggATCTg	ATATA	gCATTCTTTCTTgAggAgggCAgCAAACgggAAgAg
gAggAgggCAgCAAACgggAAgAgTCTTCCTTTACg	ATATT	TgTCAggCCACCTgTAATggAgCCCgATgCTgAgCCTgATggggTgAgAg	ATATA	gCATTCTTTCTTgAggAgggCAgCAAACgggAAgAg
gAggAgggCAgCAAACgggAAgAgTCTTCCTTTACg	ATATT	CCTCgCTTAggCCTggATCgTACATTgAggAgggAgAggACACAggCAgC	ATATA	gCATTCTTTCTTgAggAgggCAgCAAACgggAAgAg
gAggAgggCAgCAAACgggAAgAgTCTTCCTTTACg	ATATT	TCCTTAAATgTgAAgCgATCTCAgTAgCTCTgAgCCACAggCgCCCATgA	ATATA	gCATTCTTTCTTgAggAgggCAgCAAACgggAAgAg

S3.5 Probes for crowding controls of Figures S3-S7

For 2-channel studies in WT zebrafish embryos in Figures S3-S7, the probe sets for *tpm3* and *desma* contain 2 and 7 probes, respectively.

S3.5.1 *tpm3*

Target mRNA: **tropomyosin 3 (*tpm3*)**
Amplifier: **HCR B1**
Fluorophore: **Alexa647**

Initiator I1	Spacer	Probe Sequence	Spacer	Initiator I2
gAggAgggCAgCAAACgggAAgAgTCTTCCTTTACg	ATATT	AATCACCTTCATCCCTCTCTCgCTCTCATCTgCggCCTTCTCggCTTCCT	ATATA	gCATTCTTTCTTgAggAgggCAgCAAACgggAAgAg
gAggAgggCAgCAAACgggAAgAgTCTTCCTTTACg	ATATT	TggATCTCCTgCAgCTCCATCTTCTCCTCATCCTTCAgAgCCCTgTTCTC	ATATA	gCATTCTTTCTTgAggAgggCAgCAAACgggAAgAg

S3.5.2 *desma*

Target mRNA: **desmin a (*desma*)**
Amplifier: **HCR B3**
Fluorophore: **Alexa546**

Initiator I1	Spacer	Probe Sequence	Spacer	Initiator I2
gTCCCTgCCTCTATATCTCCACTCAACTTTAACCCg	TACAA	TTggCTTCTCTgAgAgCCTCgTTATTCTTgTTCACTgCCTggTTCAAATC	TAAAA	AAAgTCTAATCCgTCCCTgCCTCTATATCTCCACTC
gTCCCTgCCTCTATATCTCCACTCAACTTTAACCCg	TACAA	TCTCgCAggTgTAggACTggAgCTggTgACggAACTgCATggTCTCCTgC	TAAAA	AAAgTCTAATCCgTCCCTgCCTCTATATCTCCACTC
gTCCCTgCCTCTATATCTCCACTCAACTTTAACCCg	TACAA	TgAAACCTTAgACTTATACCAgTCCTCggCCTCgCTgATATTCTTggCAg	TAAAA	AAAgTCTAATCCgTCCCTgCCTCTATATCTCCACTC
gTCCCTgCCTCTATATCTCCACTCAACTTTAACCCg	TACAA	CgATAgCCTCgTACTgCAggCgAATgTCTCTgAgggCCgCAgTCAggTCT	TAAAA	AAAgTCTAATCCgTCCCTgCCTCTATATCTCCACTC
gTCCCTgCCTCTATATCTCCACTCAACTTTAACCCg	TACAA	ggTTTggACATgTCCATTTggATCTgCACCTgACTCTCCTgCATCTggTT	TAAAA	AAAgTCTAATCCgTCCCTgCCTCTATATCTCCACTC
gTCCCTgCCTCTATATCTCCACTCAACTTTAACCCg	TACAA	CTgCAgCTCACggATCTCCTCCTCATgAATCTTCCTgAggAATgCAATCT	TAAAA	AAAgTCTAATCCgTCCCTgCCTCTATATCTCCACTC
gTCCCTgCCTCTATATCTCCACTCAACTTTAACCCg	TACAA	CTTCgTgAAgACCCTCgATACgTCTTTCCAggTCCAgCCTggCCAgAgTg	TAAAA	AAAgTCTAATCCgTCCCTgCCTCTATATCTCCACTC

References

Choi, H. M. T., Beck, V. A., & Pierce, N. A. (2014). Next-generation in situ hybridization chain reaction: higher gain, lower cost, greater durability. *ACS Nano*, **8**(5), 4284–4294.

Choi, H. M. T., Calvert, C. R., Husain, N., Huss, D., Barsi, J. C., Deverman, B. E., Hunter, R. C., Kato, M., Lee, S. M., Abelin, A. C. T., Rosenthal, A. Z., Akbari, O. S., Li, Y., Hay, B. A., Sternberg, P. W., Patterson, P. H., Davidson, E. H., Mazmanian, S. K., Prober, D. A., van de Rijn, M., Leadbetter, J. R., Newman, D. K., Readhead, C., Bronner, M. E., Wold, B., Lansford, R., Sauka-Spengler, T., Fraser, S. E., & Pierce, N. A. (2016). Mapping a multiplexed zoo of mRNA expression. *Development*, **143**, 3632–3637.

Grimmett, G. R., & Stirzaker, D. R. (2004). *Probability and random processes*. Oxford, UK: Oxford University Press.

Howe, D. G., Bradford, Y. M., Conlin, T., Eagle, A. E., Fashena, D., Frazer, K., Knight, J., Mani, P., Martin, R., Moxon, S. A. T., Paddock, H., Pich, C., Ramachandran, S., Ruef, B. J., Ruzicka, L., Schaper, K., Shao, X., Singer, A., Sprunger, B., Van Slyke, C. E., & Westerfield, M. (2013). ZFIN, the zebrafish model organism database: increased support for mutants and transgenics. *Nucleic Acids Res.*, **41**(D1), D854–D860.

McEntyre, J., & Ostell, J. (2002). *The NCBI handbook [internet]*. Bethesda, MD: National Center for Biotechnology Information (US).

Richardson, L., Venkataraman, S., Stevenson, P., Yang, Y. Y., Moss, J., Graham, L., Burton, N., Hill, B., Rao, J. G., Baldock, R. A., & Armit, C. (2014). EMAGE mouse embryo spatial gene expression database: 2014 update. *Nucleic Acids Res.*, **42**(D1), D835–D844.